Fakultät für Medizin

Institut für Virologie

Apobec3A is a novel restriction factor antagonizing efficient HAdV replication

Christina Carola Weiß

Vollständiger Abdruck der von der Fakultät für Medizin der Technischen Universität München zur Erlangung des akademischen Grades eines

Doktors der Naturwissenschaften (Dr. rer. nat.)

genehmigten Dissertation.

Vorsitzende: Prof. Dr. Gabriele Multhoff

Prüfende der Dissertation:

1. Priv.-Doz. Dr. Sabrina Schreiner
2. Prof. Dr. Percy Knolle

Die Dissertation wurde am 08.07.2019 bei der Technischen Universität München eingereicht und durch die Fakultät für Medizin am 05.11.2019 angenommen.

Table of Contents

Abstract

Human Adenoviruses (HAdV) need to overcome several cellular barriers to infect their target cells. Up to date, many studies have been conducted to investigate the interaction between HAdV and host cells, which revealed a variety of different host restriction factors as well as viral counteraction mechanisms. However, lots of unknown processes involved in the virus-host interplay remain to be discovered. Recent publications found that Apobec3A, a cytidine deaminase involved in antiviral defenses of host cells, restricts several viruses including HIV-1, HPV, HTLV-1, HBV and Parvoviruses. Until now, it was not known if HAdV represent another target of Apobec3A. Since HAdV need to suppress the host DNA damage response (DDR) in order to replicate efficiently, whereas Apobec3A is known to activate the DDR, the initial hypothesis predicted Apobec3A to be not beneficial for HAdV infection. By contrast, Apobec3A expression levels were drastically increased two days after HAdV infection. Thereby, a network of several proteins was identified to be involved, including the early viral proteins E1B-55K and E4orf6, as well as the cellular proteins p53 and RNF4. Furthermore, the present study revealed that Apobec3A represents a novel restriction factor for HAdV infection. The deaminase activity of Apobec3A plays a crucial role, since 3D-PCR analysis could reveal deamination of the adenoviral Hexon amplicon by Apobec3A. In addition, HAdV were assumed to have evolved mechanisms to counteract the restrictive functions of Apobec3A. Indeed, investigation of the adenoviral genomes led to the discovery of a TC dinucleotide depletion, which might have developed during HAdV evolution. However, the depletion of the preferred target of Apobec3A was not conserved among HAdV species or other viruses such as HBV. Finally, Apobec3A was analyzed for its posttrans-lational modifications. Thereby, HAdV infection decreased Apobec3A ubiquitinylation, which is suggested to depend on RNF4 and to contribute to the Apobec3A stabilization during infection. Furthermore, SUMOylation of the Apobec3A protein was revealed for the first time, which is upregulated during HAdV infection. However, mutation analysis of different potential SUMOylation sites of Apobec3A did not reveal a SUMO mutant of Apobec3A, which exhibits decreased or completely abolished SUMOylation. Currently, it is assumed that Apobec3A SUMOylation might be required for Apobec3A dimer formation. Here, we found that HAdV infection increased Apobec3A homodimer formation. Based on this work, the upregulation of Apobec3A expression, as well as its increased SUMOylation and dimer formation during HAdV infection is currently tempting us to speculate that we identified a novel antiviral mechanism of the host cell.

Taken together, this study revealed novel insights into the HAdV-host interplay, being beneficial for the development of novel HAdV therapies as well as vector application in the fields of gene therapy, vaccination trials and cancer treatment.

Zusammenfassung

Humane Adenoviren (HAdV) müssen mehrere zelluläre Barrieren bewältigen, um ihre Zielzellen zu infizieren. Zahlreiche Studien wurden schon durchgeführt, um die Interaktion zwischen HAdV und ihren Wirtszellen zu untersuchen. Dabei sind viele zelluläre Restriktionsfaktoren sowie entsprechende virale Abwehrmechanismen entdeckt worden. Trotzdem sind einige Prozesse in dieser Virus-Wirt Wechselwirkung noch unbekannt und bedürfen weiterer Aufklärung. Aktuelle Studien zeigen, dass Apobec3A, eine zelluläre Desaminase mit antiviraler Aktivität, mehrere Viren wie HIV-1, HPV, HTLV-1, HBV und Parvoviren inhibiert. Bis heute war es unbekannt, ob die HAdV Infektion auch von Apobec3A beeinflusst wird. Da HAdV die zelluläre DNA-Schadensantwort unterdrücken müssen, um sich effizient replizieren zu können, wohingegen Apobec3A die DNA-Schadensantwort aktiviert, lautete die erste Hypothese, dass Apobec3A die HAdV Infektion negativ beeinflusst. Im Gegensatz dazu sind die Expressionslevel von Apobec3A jedoch zwei Tage nach der HAdV Infektion unerwartet stark angestiegen. Dabei wurde ein Netzwerk an involvierten Proteinen identifiziert, welches die frühen viralen Proteine E1B-55K und E4orf6, sowie die zellulären Proteine p53 und RNF4 beinhaltet. Des Weiteren konnte die vorliegende Studie zeigen, dass Apobec3A ein neuer Restriktionsfaktor für die HAdV Infektion ist. Dabei stellte sich heraus, dass die Desaminase Aktivität von Apobec3A eine wichtige Rolle spielt, da in 3D-PCR Analysen eine Desaminierung des adenoviralen Hexon Amplikons durch Apobec3A festgestellt wurde. Es wurde angenommen, dass HAdV Mechanismen entwickelten, um den reprimierenden Funktionen von Apobec3A entgegenzuwirken. In der Tat konnten durch Untersuchungen der adenoviralen Genome TC Dinukleotid Depletionen für die HAdV Spezies A und C entdeckt werden, die sich möglicherweise während der HAdV Evolution entwickelt haben. Allerdings wiesen andere HAdV Spezies sowie andere Viren wie HBV diese Depletionen der bevorzugten Zielsequenz von Apobec3A nicht auf. Schließlich wurde Apobec3A auch hinsichtlich posttranslationaler Modifikationen untersucht. Dabei wurde festgestellt, dass die HAdV Infektion zu einer Reduktion der Ubiquitinylierung von Apobec3A führt, wofür RNF4 vermutlich eine wichtige Rolle spielt. Wahrscheinlich trägt dies auch zu der verstärkten Expression von Apobec3A während der HAdV Infektion bei. Zusätzlich konnte zum ersten Mal eine SUMOylierung von Apobec3A nachgewiesen werden, welche nach HAdV Infektion verstärkt beobachtet wurde. Jedoch konnten Mutationsanalysen potenzieller SUMOylierungsstellen von Apobec3A keine SUMO-Mutanten von Apobec3A aufweisen, welche weniger oder keine SUMOylierung aufzeigen. Im Moment wird angenommen, dass die SUMOylierung von Apobec3A Voraussetzung für die Bildung von Apobec3A Dimeren ist. Hier konnte gezeigt werden, dass die HAdV Infektion die Dimerbildung von Apobec3A verstärkt. Basierend auf dieser Arbeit, lässt uns der Anstieg der Expression von Apobec3A,

sowie die vermehrte SUMOylierung und Dimerbildung während der HAdV Infektion spekulieren, dass wir einen neuen antiviralen Mechanismus der Wirtszelle identifiziert haben.

Zusammenfassend hat diese Studie einige wichtige Erkenntnisse bezüglich der HAdV-Wirts Wechselwirkung erbracht, welche sich nützlich für die Entwicklung neuer Therapien für HAdV Infektionen sowie die adenovirale Vektorapplikation im Bereich der Gentherapie, Impfstoffentwicklung und Krebsbekämpfung erweisen können.

1. Introduction

1.1. Adenoviruses

1.1.1. Virus classification and pathogenesis

Adenoviruses were discovered in 1953 when they were first isolated from human adenoid tissue during attempts of identifying the cause of an epidemic acute respiratory disease [1-3]. They belong to the family of *Adenoviridae*, which infect a broad range of different vertebrates. According to their host specificity, they can be subdivided into the five genera *Aviadenoviruses*, which infect birds, *Atadenoviruses* that contain an unusually high amount of A + T bases and were isolated from mammals, reptiles and birds, *Mastadenoviruses*, which infect mammals, *Siadenoviruses* which infect birds and reptiles and *Ichtadenoviruses* that were isolated from fish [4]. Human Adenoviruses (HAdV) belong to the *Mastadenoviruses* and are clustered into seven species A-G, based on their agglutination properties [5, 6]. Currently, more than 80 different HAdV types are known [7, 8], which were additionally classified by other properties, such as sequence homology [9], similarity to tumor antigens or oncogenicity in rodents [10], resulting in concordant groups, depicted in Table 1.

Table 1: Classification and associated diseases of HAdV (based on reference [11]).
The newly named types were from GenBank (http://www.ncbi.nlm.nih.gov/Taxonomy/). I, complete agglutination of monkey erythrocytes; II, complete agglutination of rat erythrocytes; III, partial agglutination of rat erythrocytes; IV, little or no agglutination.

Species	Hemagglutination group	Types	% GC	Associated disease
A	IV	12, 18, 31, 61	47~49	Cryptic enteric infection
B	I	B1: 3, 7, 16, 21, 50, 66, 68	50~52	Conjunctivitis; acute respiratory disease; hemorrhagic cystitis; central nervous system
		B2: 11, 14, 34, 35, 55, 79	50~52	
C	III	1, 2, 5, 6, 57	57~59	Endemic infection; respiratory symptoms
D	II	8~10, 13, 15, 17, 19, 20, 22~30, 32, 33, 36~39, 42~49, 51, 53, 54, 56, 58~60, 62~65, 67, 69, 70, 71, 73, 74, 75	57~60	Keratoconjunctivitis in immunocompromised and AIDS patients
E	III	4	57	Conjunctivitis; acute respiratory disease
F	III	40, 41	57~59	Infantile diarrhea
G	Unknown	52	58	Gastroenteritis
Unclassified	Unknown	72, 76, 77, 78	Unknown	Unknown

The non-oncogenic HAdV types 2 and 5 of species C are the most investigated HAdV types and serve as prototypes for clinical vector development [12]. Also, HAdV type 2 was the first virus to be fully sequenced in 1984 [13]. Furthermore, HAdV type 12 was the first oncogenic HAdV to be identified to induce sarcomas in newborn hamsters [14]. These observations led to extensive research on HAdV-induced transformation as well as to their classification into the group of DNA tumor viruses.

Due to the high amount of different serotypes and different tissue tropisms, infection with HAdV can lead to a broad spectrum of human diseases, including pneumonia, gastroenteritis, keratoconjunctivities, pharyngitis and hemorrhagic cystis [15-18] (Table 1). In immunocompetent patients, HAdV infections can be asymptomatic or lead to mild, local diseases that are usually self-limiting by the host. However, the disease´s outcome can be severe to life-threatening for immunocompromised patients lacking an effective immune system i.e. transplant recipients or patients suffering from AIDS [19]. Furthermore, newly evolving strains such as HAdV 14p1 are lethal even in otherwise healthy patients [20]. Currently, there is no specific treatment available for HAdV infections [21]. Infections are treated with common antiviral drugs, such as the nucleotide analog cidofovir or the nucleoside analog ribavirin which can lead to strong side effects, especially in pediatric patients [22, 23]. This emphasizes the need for new treatment possibilities against HAdV.

1.1.2. Structure and genome organization

HAdVs are non-enveloped viruses that consist of an icosahedral capsid with approximately 90 nm diameter in size [10, 24]. The linear, double stranded DNA genome with a total size of 26-45 kbp contains inverted terminal repeats (ITRs) at both ends. Moreover, the terminal proteins (TPs), which are essential for the initiation of the viral DNA synthesis, are attached to the 5'ends [25]. The capsid is composed of 240 homotrimeric hexon (viral protein II) proteins that form 20 triangular facets with 12 pentons consisting of penton bases (viral protein III) and projecting fibers (viral protein IV) at each vertex [26, 27] (Figure 1). For most HAdV species, the fiber knob mediates the attachment of the virus to the cell via the coxsackie/adenovirus receptor CAR [28, 29], whereas some HAdV species primarily use different cellular receptors, such as CD46 for species B [30]. The penton base protein then further interacts with cell surface integrins via its Arg-Gly-Asp (RGD) motif to ensure efficient uptake of the virus [31].

The structural proteins can be divided into the major capsid proteins hexon (II), penton base (III) and fiber (IV), the minor capsid proteins pVI, pIIIa, pVIII and pIX and the core proteins TP, Mu, pVII, pV and IVa2 and the viral protease [26, 27, 32]. Initially, the minor capsid proteins were thought to stabilize the capsid due to their cement function, but recent studies could show that these proteins exert additional, essential functions within the cell. The pVI

protein, for example, is crucial for viral escape from the endosome [33]. Furthermore, it has been shown that pVI activates the E1A promoter by the removal of the transcriptional repressor protein Daxx (death domain associated protein) [34]. The viral DNA within the capsid is condensed into a nucleoprotein complex by the core proteins pV, pVII and Mu [35, 36], whereas the core protein pV is thought to function as a linker between core and capsid, since it binds pVI and the penton base [37]. Additionally, the IVa2 protein was shown to play a role in viral DNA packaging [38] while the viral protease is known to be crucial for viral maturation by the cleavage of precursor proteins [39].

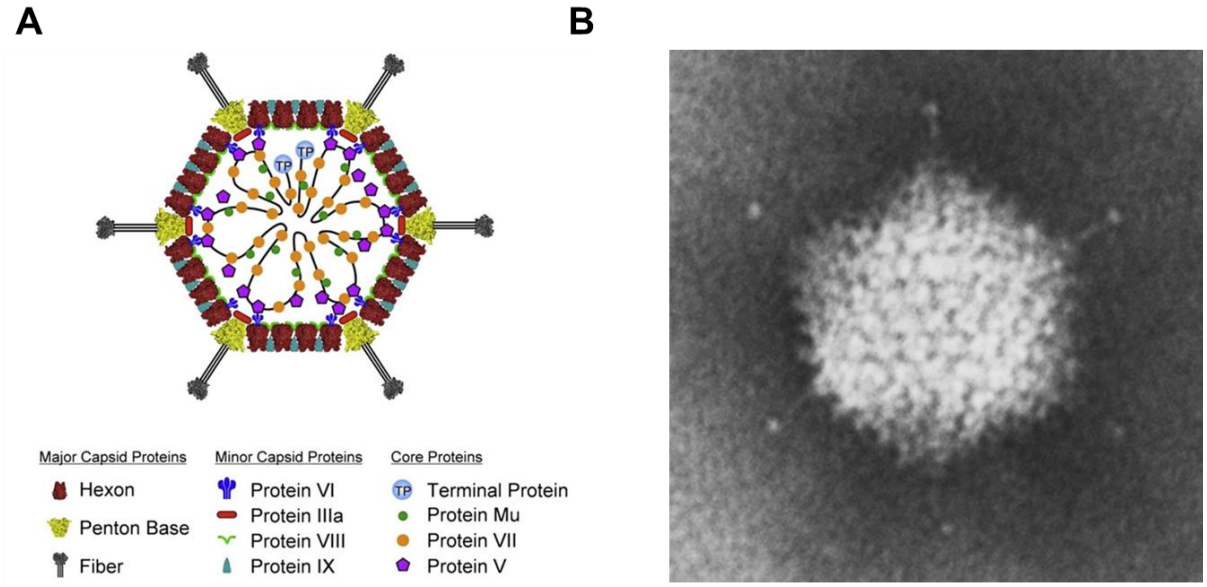

Figure 1: HAdV virion structure.
(A) Schematic overview of HAdV type 5 viral particle with indicated structural proteins. The black line within the capsid represents the viral DNA [26]. (B) Electron microscopy picture of a Mastadenovirus [40].

The HAdV genome is organized by nine transcription units: five early (E1A, E1B, E2, E3, E4), three delayed early (IX, IVa2, E2 late) and one major late transcription unit (MLTU), which is processed to five late mRNA families (L1, L2, L3, L4, L5) (Figure 2). These transcription units encode for a total of 40 structural and regulatory proteins and two VA RNAs (virus-associated RNAs) [12, 25]. Early proteins have different regulatory functions in viral replication (E2), transcriptional and translational regulation (E1A, E4), mRNA export (E1B, E4), cell cycle control (E1A) and immune system modulation (E3) or block of apoptosis (E1B), whereas late proteins exert mainly structural functions [12]. RNA polymerase II synthesizes all HAdV type 5 mRNAs except the VA RNAs, which are transcribed by RNA polymerase III [41].

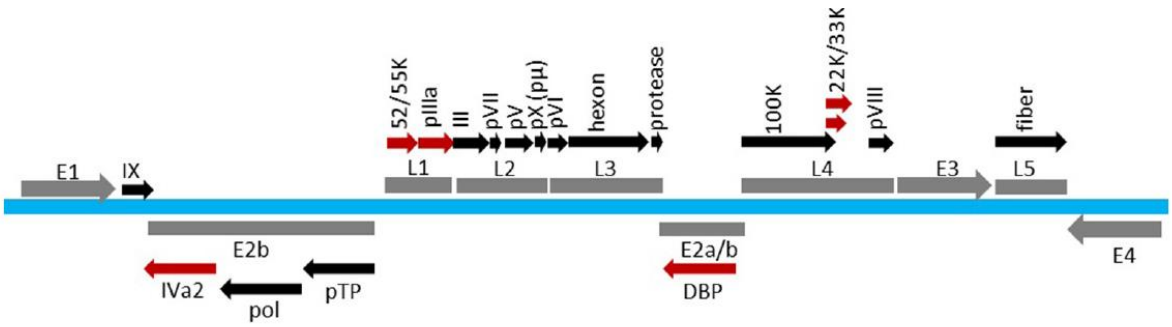

Figure 2: HAdV type 5 genome organization.
Schematic representation of the transcription map of HAdV type 5. The viral DNA is shown in blue, the early and late regions are shown in gray, arrows represent the expressed proteins with indicated orientation, and proteins involved in packaging are marked in red [42].

1.1.3. Adenoviral productive replication cycle

All types of HAdV mainly infect differentiated epithelial cells that are post mitotic resting in the respiratory and gastrointestinal tracts [43]. The lytic infection cycle can be divided into an early and late part, which begins with the onset of viral DNA replication [10]. After attachment of the virus to the cell via binding of the fiber knob to the CAR receptor and following interaction of the penton base with cellular integrins [28, 29, 31], the virus is internalized via clathrin-dependent endocytosis [44]. In the following, the virus escapes the endosome into the cytosol by permeabilization of the endosomal membrane which is mediated by several factors including a shift in the pH values, v beta 5 integrins and pVI [33, 45, 46]. The microtubule cytoskeleton as well as cytoplasmic dynein are then crucial for the subviral particle translocation to the nucleus [47], where it associates with the nuclear pore complex and releases the viral DNA bound to pVII into the nucleus [48]. E1A is the first protein to be expressed, which then activates transcription of the other early genes, E1B to E4, by interacting with many different cellular proteins including i.e. p300, a transcriptional activator protein [10, 49-51]. The early proteins ensure optimal conditions for virus replication. Thereby, E1A and E4 are known to induce cellular S-phase progression and regulate transcription and translation, E1 and E3 proteins counteract antiviral defenses like apoptosis, growth arrest or immune reactions of the host cell and E2 proteins are mainly involved in DNA replication [10, 52-55].

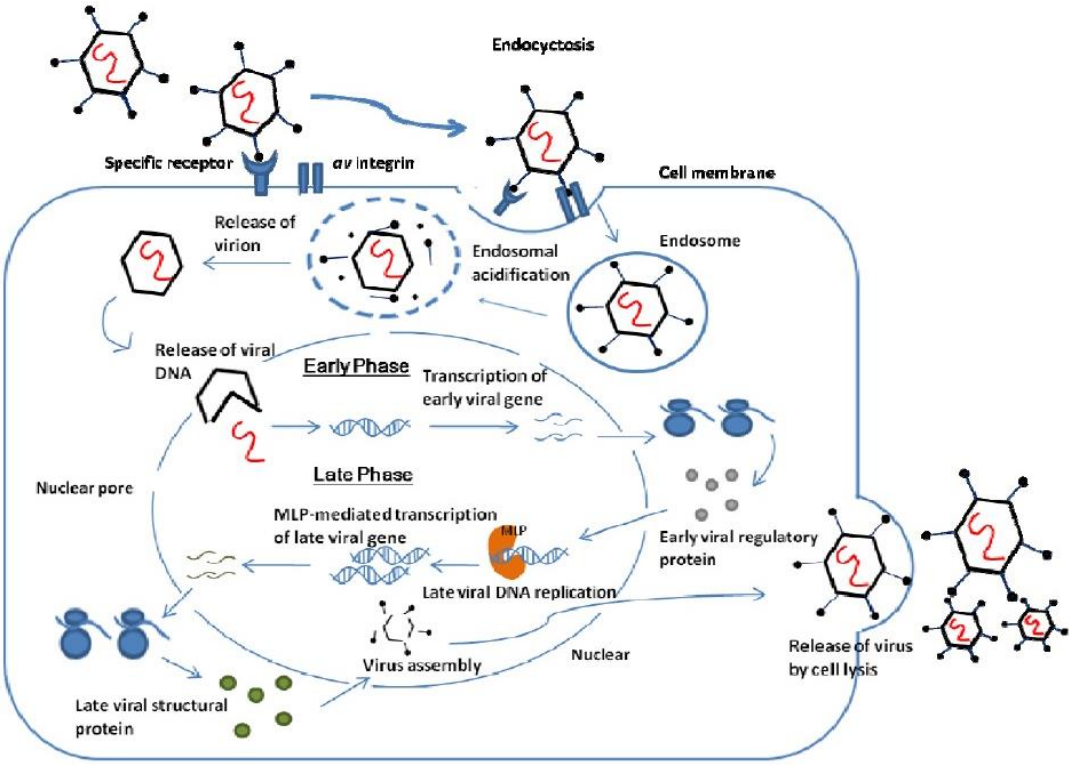

Figure 3: Adenoviral replication cycle.
Schematic representation of the early and late phase of adenoviral infections [56].

The late phase of infection begins with the onset of DNA replication, concomitant with the transcription of the MLTU into one large precursor mRNA that is spliced into at least 20 different mRNAs that can be grouped into five families of late mRNAs [57]. Host cell mRNA transport is shut off during the late phase of infection, whereas viral mRNAs are efficiently transported to the cytoplasm where translation subsequently takes place [58]. The structural proteins are assembled in the cytoplasm. Thereby, trimerization of hexon proteins is mediated by the chaperone L4-100K, whereas penton capsomers seem to self-assemble by associating to pentamers and binding to trimeric fiber proteins [59, 60]. After transport into the nucleus through the nuclear pore complex, new virions are formed in the nucleus supported by L4-33K [61, 62]. In the following, the viral DNA is encapsidated, which depends on several different proteins as well as the packaging sequence within the 200bp left of the ITR [63]. With the release of up to 10^4 progeny virions per cell by cell lysis mediated by the adenoviral death protein (ADP) protein, the HAdV replication cycle is completed after 24 to 36 hours post infection [64] (Figure 3).

1.1.4. Adenovirus suppression of the host DNA damage response

To avoid genome degradation or concatenation, HAdV suppress the DNA damage response (DDR) by several mechanisms, which leads to efficient viral replication [65, 66]. By establishing a viral E3 ubiquitin ligase complex with the early proteins E1B-55K and E4orf6

and the cellular factors Rbx1/Roc1/Hrt1, Cullin2/5 and Elongin B and C, cellular proteins that are not beneficial for virus replication can be ubiquitinylated and are subsequently degraded via the proteasome (Figure 4). Thereby, E1B-55K functions as a substrate recognition factor while E4orf6 assembles all the cellular components by binding Elongin C via the BC-Box motif [67]. Possible targets of the adenoviral E3 ubiquitin ligase complex are for example p53, integrin α3 and several proteins of the DDR like Mre11, DNA ligase IV, bloom helicase and SPOC1 [66, 68-70]. Interestingly, different HAdV serotypes build up different ligase complexes with varying components and targets. Thus, the bloom helicase, for instance, is only targeted by some HAdV serotypes [71].

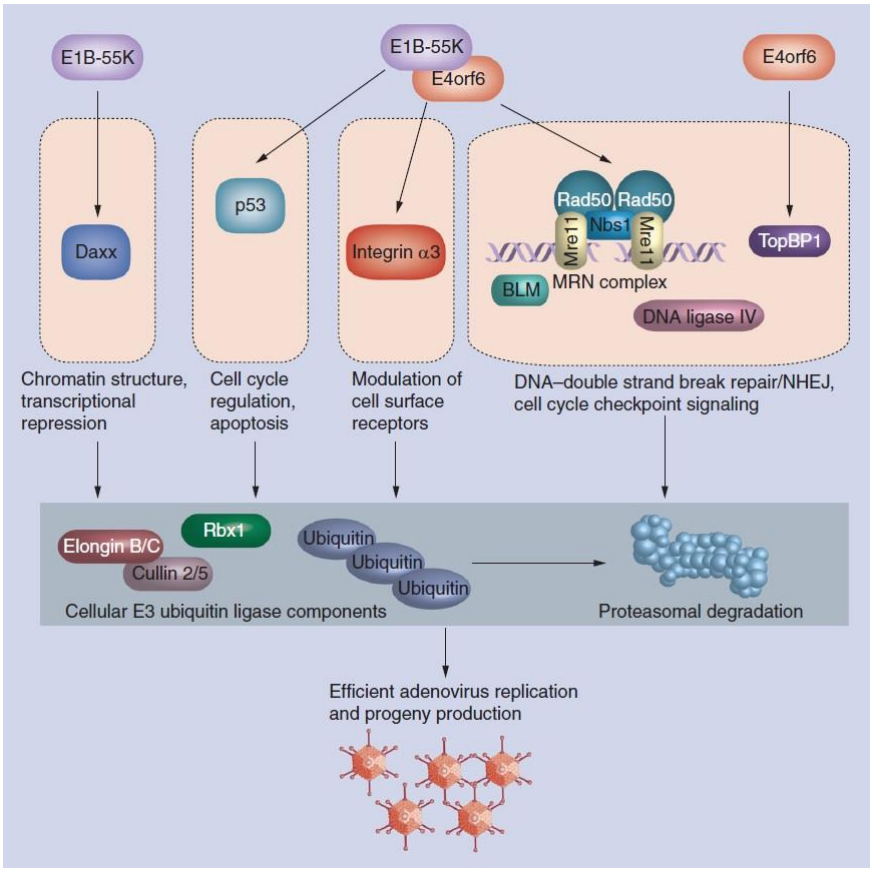

Figure 4: Degradation of cellular proteins by the adenoviral E3 ubiquitin ligase complex.
Cellular proteins that are not beneficial for HAdV, i.e. DDR proteins, are efficiently degraded by the E3 ubiquitin ligase complex established by the early proteins E1B-55K and E4orf6 together with some cellular components [66].

Another way to counteract the host cell DDR is provided by the relocalization of the Mre11-Rad50-NBS1 complex from sites of adenoviral replication to nuclear speckles by the viral E4orf3 protein which was further shown to colocalize with these proteins [72, 73]. Additionally, the E4orf3 protein is known to interact and reorganize promyelocytic nuclear bodies (PML-NBs) from their typical dot-like into so-called track-like structures in the nucleus, which is required for viral replication [74]. In summary, HAdV counteract the cellular DDR to ensure efficient viral replication and progeny virus production.

1.2. Family of Apobec proteins

Several cellular proteins were identified to activate the DDR including members of the Apobec (apolipoprotein B mRNA editing catalytic polypeptide-like) family which are cytidine deaminases that catalyze the reaction from cytidine to uracil. Apobecs can be divided into 11 primary gene products that are alternatively spliced into the variants Apobec1, AID (activation-induced deaminase), Apobec2, Apobec3A-H and Apobec4 proteins [75]. All the variants might be derived from the common ancestor AID [76], a B-cell specific protein that is involved in the diversification of functional immunoglobulin genes by deaminating dC residues that lead to somatic hypermutation, gene conversion and class-switch recombination [77]. Furthermore, interferon α upregulates Apobec protein levels, which are highly expressed in hematopoietic cells including T and B cells and myeloid cells as well as other human tissues [78]. A zinc-dependent deaminase sequence motif is conserved among all 11 Apobecs and forms the cytidine deaminase core catalytic site within a α-β-α secondary structure [75]. In general, Apobec proteins are known to target both foreign and self-DNA or RNA species for cytidine to uridine deamination [75], a process also referred to as DNA or RNA editing. The resulting uracils might be substrates of cellular glycosylases such as the uracil-N-glycosylase 2 (UNG2), which excises the uracils creating nicks (single strand DNA breaks) or DNA double strand breaks (DSBs) that can be recognized by cellular endonucleases leading to the degradation of the deaminated DNA or the activation of cellular repair mechanisms [79-81] (Figure 5).

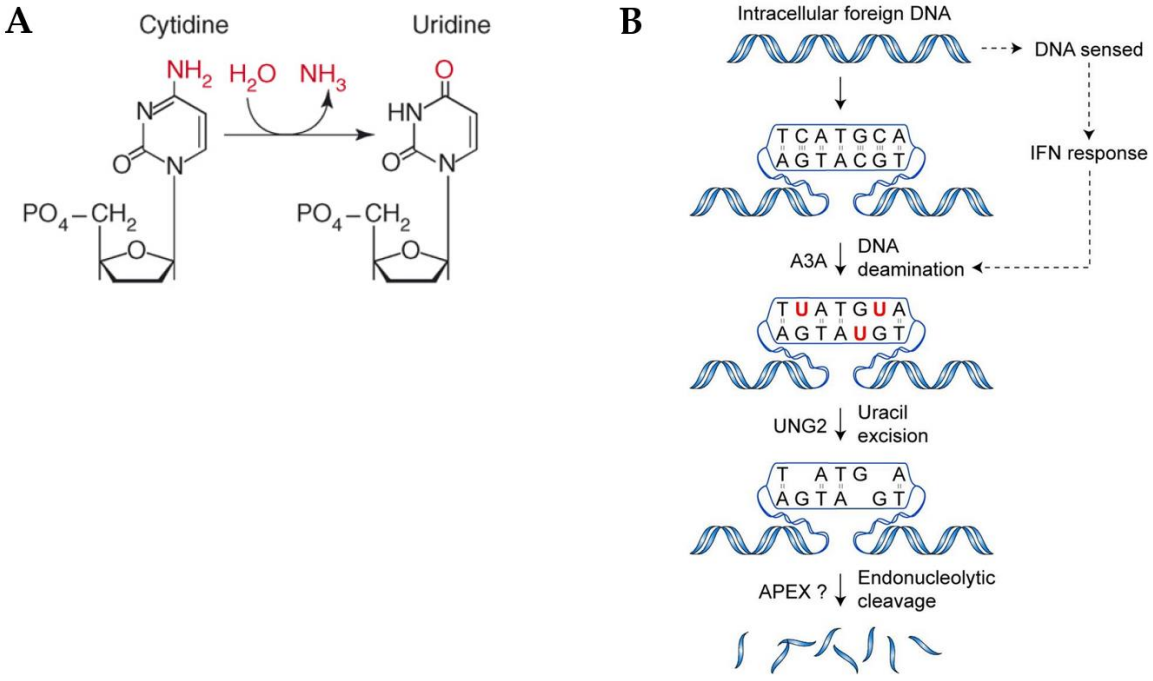

Figure 5: Apobec mediated deamination and consequences.
(A) Hydrolytic deamination of cytidine to uridine leads to ammonia release [82]. (B) Deamination by Apobec proteins leads to uracil excision by cellular gylcosylases like UNG2 which creates abasic sites that are cleaved by endonucleases followed by DNA degradation or DNA repair [79].

Apobec localization is a crucial factor for its regulation in the cell, since ssDNA editing might affect genome integrity. Therefore, nuclear access is strictly regulated for Apobec proteins [75]. AID and Apobec1 are both enzymatically active in the nucleus, however, both proteins remain in the cytoplasm to restrict their functions. Thereby, Apobec1 forms an inactive 60S complex with A1CF in the cytoplasm, whereas AID is retained in the cytoplasm by interactions with several proteins such as HP90 or eEF1A [83, 84]. Furthermore, most of the Apobec3 proteins remain in the cytoplasm, which inhibits editing of genomic DNA by different mechanisms. Apobec3G, for example, is restricted to the cytoplasm by a CRS (cytoplasm retention signal) and thereby remains excluded from chromosomes, even during mitosis [85, 86]. Interestingly, it was found that cancer can be caused by the misregulation of Apobec proteins [75, 87]. Overexpression of Apobec1, for instance, extensively edits and reduces hepatocellular NAT1, which is thought to be a transcriptional repressor, and thereby contributes to potent oncogenesis [88]. Another example is Apobec3B, which was shown to be upregulated in breast cancer, thereby broadly affecting different pathways as well as phenotypes, which plays an important role for tumor heterogeneity [89].

1.2.1. Viral restriction by Apobec proteins

Apobec proteins were shown to restrict foreign DNA, transposons as well as endogenous and exogenous viruses. The retrovirus HIV-1, for example, was shown to be restricted by Apobec3D, -F, -G and -H via a deaminase-dependent mechanism which is counteracted by the viral infectivity factor Vif [90, 91]. In the absence of the Vif protein, Apobec3D, -F, -G and -H assemble cytoplasmic complexes with RNA and the HIV-1 Gag protein, resulting in Apobec encapsidation into virion particles [92]. This leads to an efficient transfer of Apobec proteins to newly infected cells, which target viral cDNA during reverse transcription processes [93] thereby contributing to antiretroviral defenses of the cell. Interestingly, some studies found that HIV-1 restriction by Apobec3F and -G can also occur via a so far unknown deaminase-independent mechanism [94, 95]. HIV-1 counteracts Apobec-mediated restriction via the Vif protein, which establishes an SCF-like complex together with the cellular proteins Cul5, elongins B and C, and Rbx1 and thereby induces Apobec3G ubiquitinylation and final proteasomal degradation [96] (Figure 6).

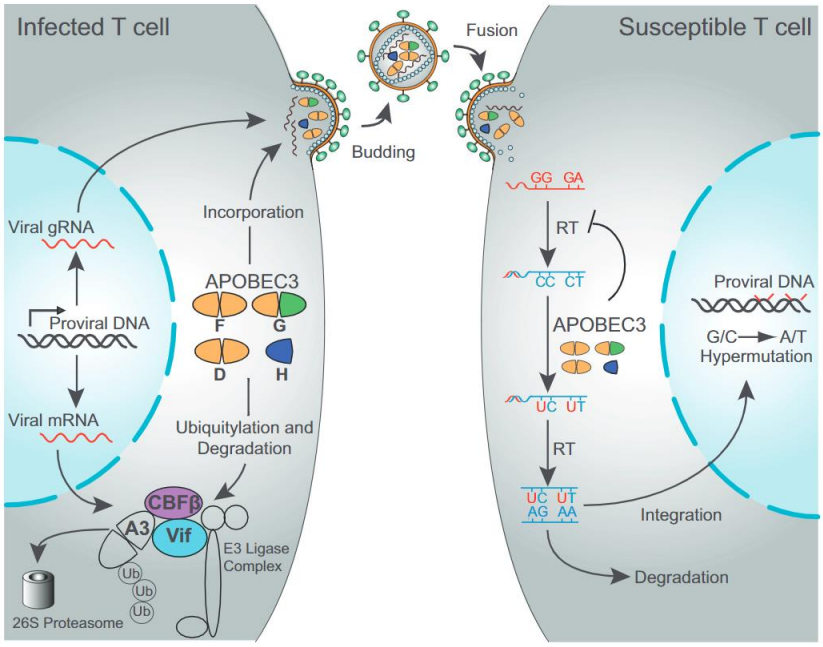

Figure 6: Apobec-mediated restriction of HIV-1 and counteraction by the viral Vif protein.
Apobec3D, -F, -G and -H are incorporated into HIV-1 viral particles and transferred to the other cells in the absence of the viral Vif protein. During viral reverse transcription in the newly infected cell, Apobec proteins can target cDNA for deamination and thereby restrict HIV-1 replication. Counteraction is performed by the viral Vif protein, which forms a SCF-like complex with cellular factors and targets Apobec proteins for ubiquitination and degradation [90].

The human T-cell leukemia virus 1 (HTLV-1) is another RNA virus that was also shown to be restricted by Apobec proteins, but appeared to be more resistant to deamination processes compared to HIV-1, which correlated with a lower amount of Apobec encapsidation [97-99]. Thereby, Apobec proteins were demonstrated to restrict HTLV-1 infection via either deaminase-dependent or -independent mechanisms [97, 100]. Besides, Apobec proteins also target DNA viruses. One of the best studied examples is the Hepatitis B virus (HBV) which has a genome that is partially single-stranded and can be edited by Apobec3 proteins [101]. Apobec3B, -C, -F and -G were observed to extensively edit minus-stranded DNA [102]. Furthermore, interferon α treatment or lymphotoxin ß receptor activation in hepatocyte cells induce Apobec3A and -B levels, which translocate to the nucleus where they get in close contact with the HBV covalently closed circular DNA (cccDNA) via the HBV core protein. Following deamination of the viral cccDNA, the resulting uracils are excised by cellular DNA glycocsylases. Thereby, apurinic/apyrimidinic sites are generated, which are recognized by cellular endonucleases leading to cccDNA degradation [103]. Members of the parvovirus family are also restricted by Apobec proteins, such as the adeno-associated virus (AAV), which is inhibited by Apobec3A expression [104]. In the process, Apobec3A was demonstrated to block the formation of AAV replication centers in the nucleus [104]. However, Parvovirus restriction by Apobec3A seems to be independent of its deaminase activity, but the exact mechanism of inhibition without editing still needs to be elucidated

[105]. Additionally, human papilloma viruses (HPVs) are targeted by Apobec3A, -B and -H, which is dependent on their deaminase activity [106]. Apobec3A, which functions as a restriction factor for HPV, however, was shown to be stabilized by the HPV16 E7 protein via inhibition of Cullin-2 dependent protein degradation [107, 108]. A TC-dinucleotide depletion was observed during HPV evolution, which most presumably represents a counteraction mechanism for Apobec3A restriction, since TC dinucleotides are the main targets of Apobec3A [109]. Since AID is specifically expressed in germinal center B cells, DNA viruses that infect B cells are expected to be targeted by AID [110]. The Epstein-Barr virus (EBV) is a double-stranded DNA virus that replicates in B cells and was shown to inhibit AID restrictive function by the viral protein EBNA2 [111]. Furthermore, Kaposi's sarcoma herpes virus (KSHV) also infects B cells and was shown to antagonize AID via the expression of different miRNAs that are able to bind AID and block its translation [112]. However, not all DNA viruses seem to be restricted by Apobec proteins [90]. The vaccinia virus is one example which is not affected by Apobec-mediated restriction [113].

1.2.2. Activation of the host DNA damage response by Apobec3A

One very potent member of the Apobec family is Apobec3A which was shown to inhibit many different viruses, including HIV-1, HBV, HTLV-1, Parvoviruses and HPVs [98, 103, 105, 108, 114], as well as retrotransposons such as LINE-1 or IAP [104]. In most of the cases, Apobec3A restricts via its deaminase activity. Nevertheless, there are some exceptions such as parvoviruses, which are inhibited via a deaminase-independent, so far unknown mechanism of Apobec3A [105]. Further, it appears that Apobec3A represents the most active Apobec deaminase, and is induced by interferon α [115, 116]. Apobec3A is mainly expressed in cells of the myeloid lineage like PBMCs or macrophages, but also in other human tissue such as lung or spleen tissue [104, 117], where it appears to be non-genotoxic through retention in the cytoplasm [118]. Nevertheless, endogenous Apobec3A is able to translocate to the nucleus for host antiviral defense [103]. Overexpression of Apobec3A leads to its distribution throughout the whole cell and can threaten genome integrity [118], underlining the necessity of strict Apobec regulation in the cell. The Apobec3A gene is arrayed in tandem with the other six Apobec3 pseudogenes on chromosome 22 and is alternatively translated into two isoforms by different translation initiations [76, 116]. Thereby, both isoforms are enzymatically active, but the exact role and function of these two variants still needs to be investigated [116]. One single catalytically active deaminase domain can be found within the sequence of Apobec3A with the motif $HXEX_{28}PCX_4C$, in which the glutamate functions as a proton shuttle, whereas a Zn^{2+} is coordinated by the histidine and cysteines [75, 76]. In contrast to HAdV, which need to suppress the host DDR to replicate efficiently (1.1.4), Apobec3A was shown to activate the DDR by the induction of DNA double strand breaks

through deamination processes [81]. Consistently, Apobec3A is able to block cell-cycle progression leading to a cell-cycle arrest in the early S phase [81].

1.2.3. Role of Apobec3A dimer formation for its deaminase activity

Apobec3A exists in a monomeric and dimeric form, which both display deaminase activity [119]. TC dinucleotides were demonstrated to represent the preferred targets of Apobec3A, which are bound by a potential positively charged DNA-binding groove of Apobec3A that was identified using crystal and NMR structure analysis [119]. Furthermore, a symmetric swap of the N-terminal residues is required for homodimerization of Apobec3A, which is suggested to be the high-affinity DNA binding functional form of the protein [120]. Thereby, the amino acid residues H11, H16, K30 and H56 were observed to play important roles, both for Apobec3A dimerization and substrate affinity (Figure 7). Mutations of these residues led to drastically reduced cooperativity and affinity, except for H56A, which affected dimerization while maintaining substrate affinity [120]. Besides targeting single-stranded DNA, Apobec3A was recently found to additionally bind ssRNA targets [121-123].

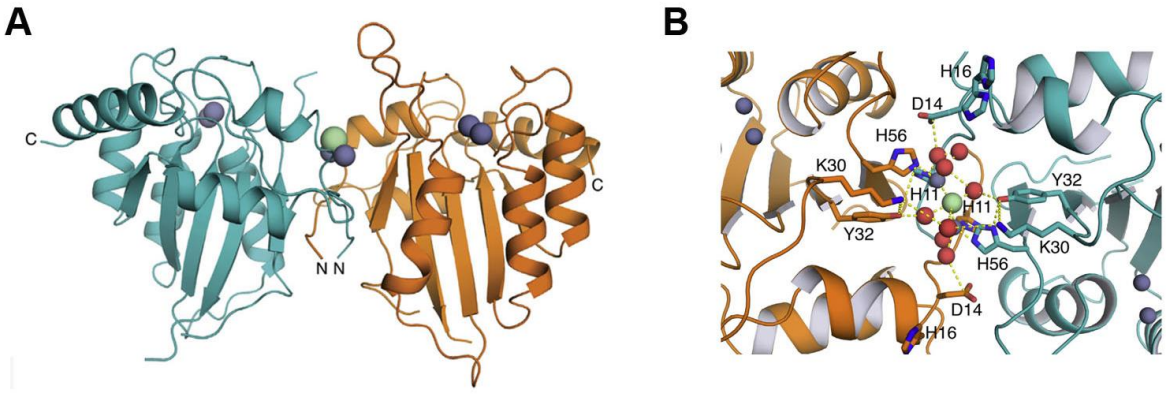

Figure 7: Apobec3A homodimerization with indicated contributing residues.
(A) Apobec3A forms a homodimer via a symmetric swap of the N-terminal residues [120]. (B) Several residues including H11, H16, K30 and H56 are important residues that contribute to Apobec3A dimerization [120].

1.3. The cellular posttranslational modification machinery

1.3.1. Cellular posttranslational modification pathways – SUMO & Ubiquitin

Posttranslational modifications (PTMs) play important roles during many different cellular processes such as cell cycle regulation, cell division, apoptosis, differentiation, immune regulation, signal transduction, transcriptional regulation, protein activity and stability, the DDR, cell growth, viral infections and many more [124-126]. More than 200 different modification types have been identified, including the most common ones like ubiquitinylation, phosphorylation, glycosylation, methylation and acetylation [127, 128]. Hereby, the best-studied example is ubiquitinylation, which is an essential marker for

subsequent protein degradation via the 26S proteasome [124]. Furthermore, ubiquitinylation is known to be implicated in various non-proteolytic cellular processes. Protein-protein interaction, cell signaling, gene transcription control, DNA repair, DNA replication and virus budding are only some examples that involve the ubiquitin system [126]. Another PTM, which is similar to ubiquitin and was identified in 1996, is the small ubiquitin-related modifier (SUMO) [129]. Also SUMOylation appears to play crucial roles during a huge variety of different processes, like cell division, DNA replication, DNA repair, immune response regulation, maintenance of genome integrity and transcriptional regulation [129, 130].

SUMOylation and ubiquitinylation are both reversible protein modifications that are attached via a similar three-step enzymatic cascade. In the beginning, the activating enzyme E1 catalyzes the ATP dependent activation of the C-terminus of ubiquitin/SUMO following formation of a E1 ubiquitin/SUMO complex via a high-energy thioester bond [131, 132]. After transferring the activated ubiquitin/SUMO to a cysteine of the E2 conjugating enzyme leading to an E2 ubiquitin/SUMO thiolester intermediate, the ubiquitin/SUMO is transferred to a substrate via an E3 protein ligase, which conjugates it to a specific lysine residue of the target protein via an isopeptide bond [133-136]. De-ubiquitinating enzymes (DUBs) or SUMO-specific proteases (SENPs) are able to remove these modifications from the substrate by cleavage reactions [137] (Figure 8). Both ubiquitinylation and SUMOylation are covalent protein modifications and involve many different E1, E2 and E3 enzymes. To this day, the ubiquitin carrier protein 9 (Ubc9) is the only known E2 SUMO conjugating enzyme [138]. SUMOylation occurs at the consensus motif ψKxE, in which ψ represents a hydrophobic amino acid and K is the main target lysin for modification [139]. It was shown, that there is functional heterogeneity between SUMO-1 and SUMO-2/3, which share amino acid sequence identities of ~ 50%, whereas SUMO-2 and -3 are almost identical [140]. Furthermore, SUMO-1 functions as a monomer, whereas SUMO-2 and -3 can form polymeric chains, which can be terminated by a single SUMO-1 modification [141]. These SUMO chains are important during replication, mitosis and meiosis as well as the turnover of SUMO targets by the proteasome [142]. Also ubiquitin is able to form chains via lysine 48, which marks the target protein for subsequent proteasomal degradation [143, 144]. Since both modifications are attached in similar ways, SUMO and Ubiquitin are linked by the process of SUMO dependent ubiquitinylation, which involves special ubiquitin ligases that recognize protein SUMO modification [145]. These SUMO-interacting motif (SIM)-containing RING (really interesting new gene)-finger proteins were described to regulate genome stability [146]. Until now, only two human SUMO-targeted ubiquitin ligases (STUbLs) are known, namely the RING finger protein 111 (RNF111) and the RING finger protein 4 (RNF4) [146, 147]. RNF4 dimerizes via its RING domain, which is required for the ubiquitin transfer to SUMOylated target proteins [148]. STUbLs are known to prevent the accumulation of

SUMOylated proteins upon high levels of cellular stress, which can be induced oxidatively, chemically, by DNA damaging or by cancer development [149].

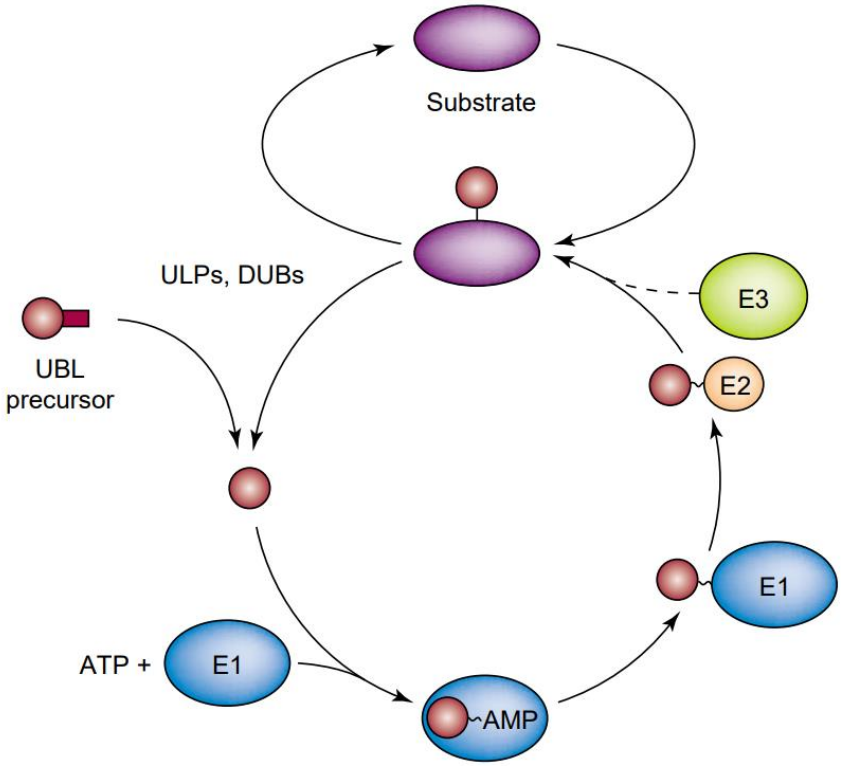

Figure 8: Protein modification by ubiquitin-like proteins.
Ubiquitin-like proteins (ULPs) are activated by an E1 activating enzyme in an ATP-dependent manner and form a complex with E1. After transferring the ULP to an E2 conjugating enzyme, it is conjugated to lysine residues of target proteins via E3 ligase proteins [137].

1.3.2. Role of SUMOylation during productive HAdV infection

Viruses are known to be exposed to PTMs during infection events. Nevertheless, they can also induce PTMs for their own benefit [150]. The lytic infection cycle of HAdV, for example, is supported by several PTMs. Thereby, viral entry might be affected by ubiquitinylation, since adenoviral receptors, like CAR or integrins, have been shown to depend on the ubiquitin-proteasome pathway [151, 152]. Shortly after HAdV entry into the cell, ubiquitinylation of the pVI protein appears to be crucial for microtubule-dependent, intracellular virus trafficking [153]. Furthermore, the E1A protein binds to and relocalizes p300 and CBP, two histone acetyl transferases, to specific promoter regions to facilitate cell cycle progression. Thereby, the E1A protein silences genes involved in antiviral responses or differentiation by the hypo-acetylation of histone H3 lysine 18 (H3K18) in promoter regions, whereas it induces genes to promote cell cycle progression via hyper-acetylation of H3K18 in promoter regions [154]. To additionally benefit the virus, the adenoviral proteinase deubiquitinylates a variety of cellular proteins, which emphasizes the importance of the ubiquitin pathway for adenoviral infection [155].

In addition, the SUMOylation pathway is crucially involved in HAdV infections. Especially early adenoviral proteins extensively use SUMO modifications to ensure efficient viral replication [156]. The early viral protein E1A was shown to bind the E2 enzyme Ubc9, thereby interfering with polySUMOylation [157]. Furthermore, SUMO modification of the retinoblastoma tumor suppressor protein (pRB) is abolished by E1A leading to an inhibition of pRB, which enhances E2F-dependent transcriptional activation [158] (Figure 9). Currently, the only known adenoviral SUMO substrate is the early viral protein E1B-55K, which can be covalently attached to SUMO-1, -2 and -3 at its lysine residue 104 within the typical SUMOylation consensus motif ψKxE [159, 160]. The cellular KAP1 protein was identified as a host restriction factor for HAdV, which is deSUMOylated during viral infection, thereby decreasing epigenetic gene silencing as well as stimulating SUMO conjugation of E1B-55K via a so far unknown mechanism [161]. Additionally, E1B-55K functions as a SUMO E3 ligase, which induces for instance p53 SUMOylation at PML-NBs, thereby contributing to maximal inhibition of p53 followed by its nuclear export to cytoplasmic aggresome complexes (Figure 9). SUMOylation of E1B-55K itself at lysine 104 is crucial for p53 inhibition [162, 163]. Another cellular target is the death-associated protein Daxx, which is proteasomally degraded following its interaction with the SUMOylated version of the viral E1B-55K protein, thereby counteracting its innate antiviral activities [69]. A recent study recognized that the SUMO mutant K104R of E1B-55K is still able to bind Daxx, but not sufficient for Daxx degradation, emphasizing the importance of SUMOylated E1B-55K for the productive viral replication [164]. Further, it has been shown, that the cellular STUBL RNF4 plays an important role in this process. E1B-55K recruits RNF4 into the insoluble matrix fraction, promoting complex formation of RNF4, E1B-55K and Daxx, which leads to the SUMO conjugation of Daxx and thereby inhibits its antiviral functions [165]. Additionally, the viral E4orf3 protein is known to promote SUMOylation of several cellular proteins, including Mre11 and Nbs1 of the Mre11-Rad50-Nbs1 (MRN) complex (Figure 9). Relocalization of Mre11 and Nbs1 into E4orf3 nuclear tracks is required for their SUMO modification, which negatively modulates the cellular DNA damage response [166]. Besides an E3 SUMO ligase function, E4orf3 also has an E4 SUMO elongase activity, leading to increasing poly-SUMO chain formation [167]. Furthermore, the cellular transcription factors TIF1γ as well as TFII-I are SUMOylated by the viral E4orf3 E3 SUMO ligase, which targets them for direct proteasomal degradation, without involving E1B-55K and E4orf6 [168, 169]. Taken together, these examples underline the importance of the SUMO pathway for HAdV infections.

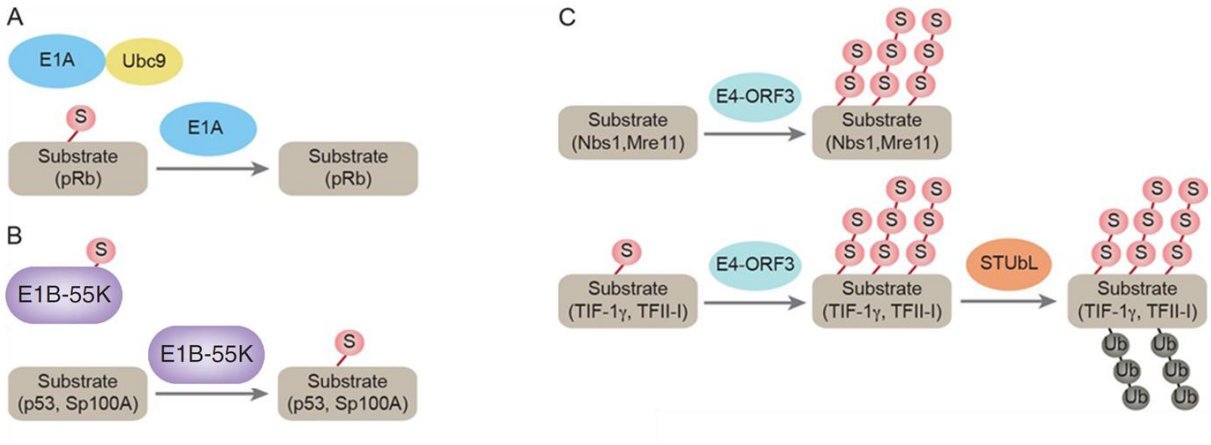

Figure 9: Adenoviral early proteins involved in the SUMOylation pathway.
(A) E1A binds to the E2 enzyme Ubc9 and inhibits SUMOylation of pRb. (B) E1B-55K functions as an E3 SUMO ligase for p53 and SP100A and is a SUMO substrate itself. (C) E4orf3 functions as an E3 SUMO ligase and triggers SUMOylation of various cellular proteins (modified from [156]).

1.4. Aim of the thesis

Apobec3A restricts a variety of different viruses such as HIV-1 or HPV [108, 114]. However, it was not known if HAdV also represent a viral target for Apobec3A. Since HAdV need to suppress the DDR to replicate efficiently while Apobec3A is activating the DDR, the initial hypothesis was that Apobec3A is not beneficial for HAdV infection [66, 81]. Consequently, the work performed in this thesis aimed to reveal, whether Apobec3A represents a novel restriction factor for HAdV infection. In most cases, Apobec3A uses its deaminase activity to restrict viruses, with some exceptions such as parvoviruses, which are inhibited via a so far unknown deaminase-independent mechanism [105]. Therefore, the confirmation of HAdV restriction by Apobec3A raised the question, if the deaminase activity of Apobec3A is necessary for HAdV restriction. Furthermore, Apobec3A expression during HAdV infection was analyzed to detect potential counteraction mechanisms of HAdV. Since it is known, that Apobec3A is ubiquitinylated at K137 and ubiquitinylation as well as SUMOylation play crucial roles during the HAdV infection cycle, potential PTMs of Apobec3A were investigated in this work [156, 170]. Thereby, it was of special interest, if and how HAdV influences Apobec3A PTMs. Finally, the Apobec3A dimer formation was studied during HAdV infection, as it is thought to be the functional form of the protein [120]. Hereby, it was hypothesized that HAdV infection has an impact on Apobec3A dimer formation, which might be another mechanism of HAdV to counteract Apobec3A restrictive functions. In conclusion, the study aimed to get further insights into HAdV-host interplay, which could improve HAdV therapy as well as its vector application in the fields of gene therapy, vaccination and cancer treatment.

2. Material

2.1. Bacteria and Cells

2.1.1. Bacterial strain

Table 2: Used bacterial strain with phenotype and reference.

Strain	Phenotype	Reference
Escherichia coli DH5α	supE44, ΔlacU169, (φ80dlacZΔM15), hsdR17, recA1, endA1, gyrA96, thi-1, relA1	[171]

2.1.2. Mammalian cell lines

Table 3: Used cell lines with database number, genotype and reference.

Database No.	Cell line	Genotype	Reference
1	HepaRG	Primary human hepatocytes, derived from HCV infected Tissue (“pseudo-primary”)	[172]
4	HeLa	Human cervix carcinoma cells with HPV-18 genome integration	[173]
7	HeLa-SUMO2-His	Human cervix carcinoma cells with HPV-18 genome integration, cells stably express 6xHis tagged SUMO2	[174]
12	HepaRG-SUMO2-His	Primary human hepatocytes, stably expressing 6xHis-tagged SUMO2	[175]
15	H1299	Human lung carcinoma cells, derived from metastatic lymph node, lack of p53 expression	[176]
16	HEK293	Human embryonic kidney cell line transformed by HAdV-C5 and stably expressing the HAdV-C5 E1 region	[177]
75	HepaRG-TR-Apobec3A	HepaRG cell line with tetracycline-inducible Apobec3A overexpress-sion	kindly provided by Daniela Stadler [178]
76	HepaRG-TR-UGI	HepaRG cell line with tetracycline-inducible Uracil-N-glycosylase	kindly provided by Daniela Stadler

		inhibitor (UGI) overexpression	(unpublished)
77	HepaRG-TR	Control cell line for the tetracycline-inducible HepaRG cell lines which only expresses the TR	[179]

2.2. Nucleic acids

2.2.1. Recombinant plasmids

Table 4: Used DNA plasmids with database number, description and reference.

Database No.	Plasmid	Description	Reference
12	pcDNA3 empty	Empty pcDNA3 vector	Invitrogen
18	pcDNA3-HA	Empty pcDNA3 vector with CMV promoter and N-terminal HA tag	Group database
21	pEYFP-C1	Empty pEYFP vector	Invitrogen
26	pcDNA3-E4orf6-HA	pcDNA3 vector encoding HAdV E4orf6 with CMV promoter and N-terminal HA tag	Group database
50	pcDNA3 6xHis Ubiquitin	pcDNA3 vector encoding 6xHis Ubiquitin with CMV promoter and N-terminal HA tag	Group database
61	pcDNA3-E1B-55K	pcDNA3 vector encoding HAdV E1B-55K with CMV promoter and N-terminal HA tag	Group database
83	pRenilla-TK	*Renilla*-Luciferase-Assay	Promega
91	pGLbasic3 E1A promoter	HAdV5 E1A promoter reporter gene construct	Group database[70]
94	pGLbasic3 E2E promoter	HAdV5 E2E promoter reporter gene construct	Group database [70]
98	pGLbasic3 MLP promoter	HAdV5 MLP reporter gene construct	Group database [70]
100	pGLbasic3 empty	*Firefly*-Luciferase-Assay	Promega
256	pLenti6.3-V5 empty	Empty pLenti6.3 vector	This study

257	pLenti6.3-Apobec3A-V5	pLenti6.3. vector encoding Apobec3A with CMV promoter and V5 tag	Kindly provided by Daniela Stadler [178]
469	pCMX3b-RNF4-Flag	pCMX3B vector encoding RNF4 with double Flag tag	Group database
582	pCMX3b-empty	Empty pCMX3b vector	Group database
603	pLenti6.3-Apobec3A(K30R)-V5	pLenti6.3 vector encoding the K30 SUMO-site mutated Apobec3A with CMV promoter and V5 tag	This study
604	pLenti6.3-Apobec3A(K47R)-V5	pLenti6.3 vector encoding the K47 SUMO-site mutated Apobec3A with CMV promoter and V5 tag	This study
605	pLenti6.3-Apobec3A(K60R)-V5	pLenti6.3 vector encoding the K60 SUMO-site mutated Apobec3A with CMV promoter and V5 tag	This study
606	pLenti6.3-Apobec3A(K137R)-V5	pLenti6.3 vector encoding the K137 SUMO-site mutated Apobec3A with CMV promoter and V5 tag	This study
607	pLenti6.3-Apobec3A(K159R)-V5	pLenti6.3 vector encoding the K159 SUMO-site mutated Apobec3A with CMV promoter and V5 tag	This study
608	pLenti6.3-Apobec3A(K30R/K47R)-V5	pLenti6.3 vector encoding the K30 and K47 SUMO-site mutated Apobec3A with CMV promoter and V5 tag	This study
609	pLenti6.3-Apobec3A(K30R/K60R)-V5	pLenti6.3 vector encoding the K30 and K60 SUMO-site mutated Apobec3A with CMV promoter and V5 tag	This study
610	pLenti6.3-Apobec3A(K47R/K60R)-V5	pLenti6.3 vector encoding the K47 and K60 SUMO-site mutated Apobec3A with CMV promoter and V5 tag	This study
611	pLenti6.3-Apobec3A(K47R/K159R)-V5	pLenti6.3 vector encoding the K47 and K159 SUMO-site mutated Apobec3A with CMV promoter and V5 tag	This study
631	Apobec3A-YFP in	pEYFP vector encoding Apobec3A with	[103, 180]

	pEYFP-C1/N1 (Clontech)	CMV promoter and C-terminal YFP tag	
674	pHBV1.1 wild type (wt)	HBV bacmid leading to the expression of HBV pgRNA from a CMV promoter, transfection results in HBV infection	[181]

2.2.2. Oligonucleotides

Table 5: Used oligonucleotides (from metabion) with indicated database number, sequence and purpose.

Data-base No.	Primer	Sequence	Purpose
71	366CMVfwd	CCCACTGCTTACTGGC	sequencing
72	675pCMX3Brev	CCAATTATGTCACACCA	sequencing
92	pcDNA3fwd	TAATACGACTCACTATAGGG	sequencing
110	TBP for	TATAATCCCAAGCGGTTTGC	qPCR to investigate Apobec mRNA
111	TBP rev	CTGTTCTTCACTCTTGGCTCCT	qPCR to investigate Apobec mRNA
114	Apobec3B-L	CGCCAGACCTACTTGTGCTA	qPCR to investigate Apobec mRNA
115	Apobec3B-R	GCCACAGAGAAGATTCTTAGCC	qPCR to investigate Apobec mRNA
116	Apobec3C-L	TCAACTGCAAGGACGCTGT	qPCR to investigate Apobec mRNA
117	Apobec3C-R	ATTGCCTTCATCGGGTTTCT	qPCR to investigate Apobec mRNA
118	Apobec3DE-L	ACCCAAACGTCAGTCGAATC	qPCR to investigate Apobec mRNA
119	Apobec3DE-R	CACATTTCTGCGTGGTTCTC	qPCR to investigate Apobec mRNA
120	Apobec3F-L	GCCTATGGTCGGAACGAAA	qPCR to investigate Apobec mRNA
121	Apobec3F-R	TGGGTCTCAGGATCCACCT	qPCR to investigate Apobec mRNA
122	Apobec3G-fw	CCGAGGACCCGAAGGTTAC	qPCR to investigate Apobec

			mRNA
123	Apobec3G-rev	TCCAACAGTGCTGAAATTCG	qPCR to investigate Apobec mRNA
124	Apobec3H-L	AGCTGTGGCCAGAAGCAC	qPCR to investigate Apobec mRNA
125	Apobec3H-R	CGGAATGTTTCGGCTGTT	qPCR to investigate Apobec mRNA
126	Apobec1-L	AGGGACCTTGTTAACAGTGGAG	qPCR to investigate Apobec mRNA
127	Apobec1-R	CCAGGTGGGTAGTTGACAAAA	qPCR to investigate Apobec mRNA
128	Apobec2-L	GGAGAAGTTGGCAGACATCC	qPCR to investigate Apobec mRNA
129	Apobec2-R	TGGCTGTACATGTCATTGCTG	qPCR to investigate Apobec mRNA
130	Apobec4-L	TTCTAACACCTGGAATGTGATCC	qPCR to investigate Apobec mRNA
131	Apobec4-R	TTTACTGTCTTCTAGCTGCAAACC	qPCR to investigate Apobec mRNA
132	AICDA-L	GACTTTGGTTATCTTCGCAATAAGA	qPCR to investigate Apobec mRNA
133	AICDA-R	AGGTCCCAGTCCGAGATGTA	qPCR to investigate Apobec mRNA
134	E4orf6 fwd	GGAGGATCATCCGCTGCTG	viral DNA analysis
135	E4orf6 rev	GCACAACACAGGCACACG	viral DNA analysis
136	pLenti6.3 2473	CCTGGAGACGCCATCC	sequencing
142	pLenti6.3 empty fwd	TCGAGTCTAGAGGGCCCG	clone pLenti6.3 emtpy vector
143	pLenti6.3 empty rev	GTTAAGCCGAATTCCACCAC	clone pLenti6.3 emtpy vector
181	E1A fwd	GTGCCCCATTAACCAGTTG	viral mRNA analysis
182	E1A rev	GGCGTTTACAGCTCAAGTCC	viral mRNA analysis
187	18S fwd	CGGCTACCACATCCAAGGAA	viral mRNA/DNA analysis
188	18S rev	GCTGGAATTACCGCGGCT	viral mRNA/DNA analysis

189	Hexon fwd	CGCTGGACATGACTTTTGAG	viral mRNA analysis
190	Hexon rev	GAACGGTGTGCGCAGGTA	viral mRNA analysis
193	E4orf6 fwd	CCCTCATAAACACGCTGGAC	viral mRNA analysis
194	E4orf6 rev	GCTGGTTTAGGATGGTGGTG	viral mRNA analysis
323	E1B-55K fwd	ATGAGCGACGAAGAAACCCATC TGAGC	viral DNA analysis
324	E1B-55K rev	CGGTGTCTGGTCATTAAGCT	viral DNA analysis
527	pLenti6.3-A3A-SUMO-Mut_30_fwd	GGACCTACCTGTGCTACGAAG	cloning of Apobec3A SUMO mutants
528	pLenti6.3-Apobec3A-SUMO-Mut_30_rev	TATGCCTTCCAATGCCATTG	cloning of Apobec3A SUMO mutants
529	pLenti6.3-Apobec3A-SUMO-Mut_47_fwd	GGATGGACCAGCACAGGGG	cloning of Apobec3A SUMO mutants
530	pLenti6.3-Apobec3A-SUMO-Mut_47_rev	TGACCGAGGTGCCATTGTC	cloning of Apobec3A SUMO mutants
531	pLenti6.3-Apobec3A-SUMO-Mut_60_fwd	GGAATCTTCTCTGTGGCTTTTAC	cloning of Apobec3A SUMO mutants
532	pLenti6.3-Apobec3A-SUMO-Mut_60_rev	TAGCCTGGTTGTGTAGAAAGC	cloning of Apobec3A SUMO mutants
533	pLenti6.3-Apobec3A-SUMO-Mut_137_fwd	GGGAGGCACTGCAAATGCTG	cloning of Apobec3A SUMO mutants
534	pLenti6.3-	TATATAGGGGGTCGTAATCATA	cloning of Apobec3A SUMO

	Apobec3A-SUMO-Mut_137_rev	G	mutants
535	pLenti6.3-Apobec3A-SUMO-Mut_137_fwd	GGCACTGCTGGGACACCTTTG	cloning of Apobec3A SUMO mutants
536	pLenti6.3-Apobec3A-SUMO-Mut_137_rev	TAAATTCATCGTAGGTCATGATG	cloning of Apobec3A SUMO mutants
654	Apobec3A fwd	CTACAGGGTCACTTGGTTCATC	qPCR to investigate Apobec mRNA
655	Apobec3A rev	CAGTCTCACGTGTGTGTTCTC	qPCR to investigate Apobec mRNA
656	Hexon fwd	GCTTCATCCCATTCGCAAGG	3D-PCR analysis
657	Hexon rev	CGCGCCACCGAGACGTAC	3D-PCR analysis
658	cccDNA fwd	ATGGCTGCTARGCTGTGCTGCCAA	3D-PCR analysis
659	cccDNA rev	AAGTGCACACGGTYYGGCAGAT	3D-PCR analysis

2.3. Viruses

Table 6: Used viral strains with database number, genotype and reference.

Database No.	Adenovirus	Characteristics	Reference
2	HAdV-C5 E4orf6-	H5*pm*4154, E4orf6 null mutant, containing a stop codon in the E4orf6 region (AS 66)	[67]
3	HAdV-C5 E1B-55K-	H5*pm*4149, E1B-55K null mutant, containing four stop codons in the E1B-55K region (AS position 3, 8, 86 and 88)	[182]
4	HAdV-C5 wt	H5*pg*4100, containing an 1863 bp deletion in the E3 region (nt 28602-30465)	[182]

2.4. Antibodies

2.4.1. Primary antibodies

Table 7: Used primary antibodies with indicated database number, dilution, properties and company.

Database No.	Antibody	Dilution (for WB if not indicated differently)	Properties	Company [Reference]
1	p53-DO1	1:2000	anti-mouse	Santa Cruz [183]
2	Mre11	1:2000	anti-rabbit	Novus Biologicals
19	Flag-M2	1:1000	anti-mouse	Sigma-Aldrich
33	V5	1:5000 (WB), 1:200 (IF)	anti-mouse	Abcam [184]
34	E4orf6 (RSA3)	1:10	anti-mouse	Kindly provided by E. Kremmer (HMGU monoclonal antibody unit) [185]
39	GFP	1:2000	anti-rabbit	Abcam
41	6-His	1:5000	anti-mouse	Clontech
43	Capsid	1:2000	anti-rabbit	Group database
45	E1A (M73)	1:100	anti-mouse	Group database [186]
49	E2A (B6-8)	1:10	anti-mouse	Group database [187]
52	E2A	1:500 (IF)	anti-rabbit	Kindly provided by R.T. Hay
54	Ubiquitin (P4D1)	1:1000	anti-mouse	Cell Signaling Technology [188]
61	β-actin (AC-15)	1:5000	anti-mouse	Sigma-Aldrich
62	E1B-55K (2A6)	1:10	anti-mouse	Group database [189]
93	pVI	1:1000	anti-rabbit	Group database [153]

2.4.2. Secondary antibodies

Table 8: Used secondary antibodies for western blots with dilution, properties and company.

Antibody	Dilution	Properties	Company
HRP-anti-mouse IgG	1:10000	Peroxidase conjugated AffiniPure F(ab')2 fragment goat anti-mouse IgG	Dianova/Jackson Immunoresearch
HRP-anti-rabbit IgG	1:10000	Peroxidase conjugated AffiniPure F(ab')2 fragment goat anti-rabbit IgG	Dianova/Jackson Immunoresearch
HRP-anti-rat IgG	1:10000	Peroxidase conjugated AffiniPure F(ab')2 fragment goat anti-rat IgG	Dianova/Jackson Immunoresearch

Table 9: Used secondary antibodies for immunofluorescence stainings with dilution, properties and company.

Antibody	Dilution	Properties	Company
647-anti-mouse	1:200	Alexa-647 conjugated goat-anti-mouse-antibody	Thermo Scientific
488-anti-rabbit	1:200	Alexa-488 conjugated goat-anti-rabbit-antibody	Thermo Scientific

2.5. Enzymes and buffers

2.5.1. Commercially available enzymes

Table 10: Used enzymes for DNA preparation.

Enzyme	Company
DpnI (20000 U/ml)	New England BioLabs, Inc., Frankfurt a. M., Germany
NcoI	New England BioLabs, Inc., Frankfurt a. M., Germany
PfuUltra II Fusion HS DNA Polymerase	Agilent Technologies, Santa Clara, US
T4 DNA ligase (400000 U/ml)	New England BioLabs, Inc., Frankfurt a. M., Germany
T4 Polynucleotide Kinase (PNK; 10000 U/ml)	New England BioLabs, Inc., Frankfurt a. M., Germany
Proteinase K	Sigma-Aldrich, Darmstadt, Germany

2.5.2. Commercially available buffers

Table 11: Used reaction buffers for DNA preparation.

Buffer	Company
PfuUltra II Fusion Reaction buffer (10 x)	Agilent Technologies, Santa Clara, US
RNase A	Carl Roth, Karlsruhe, Germany
T4 ligase buffer (10X)	Roche, Basel, Switzerland

2.6. Chemicals and reagents

Table 12: Used chemicals and reagents of the indicated company.

Substance	Company
10x Antarctic phosphatase reaction buffer	New England BioLabs, Frankfurt a.M., Germany
2-Propanol	Carl Roth, Karlsruhe, Germany
30% acrylamide/bisacrylamide mixture	Carl Roth, Karlsruhe, Germany
6x DNA loading dye	New England BioLabs, Frankfurt a.M., Germany
Agarose	Biozym, Hessisch Oldendorf, Germany
Ampicillin	Sigma-Aldrich, Darmstadt, Germany
Antarctic phosphatase	New England BioLabs, Frankfurt a.M., Germany
Aprotinin	Sigma-Aldrich, Darmstadt, Germany
APS	Carl Roth, Karlsruhe, Germany
Boric acid, > 99,8%	Sigma-Aldrich, Darmstadt, Germany
Bovine serum albumin (BSA)	Thermo Scientific, Dreieich, Germany
Bradford reagent	Bio-Rad, München, Germany
Bromphenol blue	Carl Roth, Karlsruhe, Germany
Chloroform	Carl Roth, Karlsruhe, Germany
DAPI	Sigma-Aldrich, Darmstadt, Germany
Developing solution	Tetenal, Norderstedt, Germany
Dimethyl sulfoxide (DMSO) ≥ 99.5%	Carl Roth, Karlsruhe, Germany
DNase I	Carl Roth, Karlsruhe, Germany
dNTP mix (100mM)	New England BioLabs, Frankfurt a.M., Germany
Dulbecco’s modified eagle’s medium (DMEM)	Sigma-Aldrich, Darmstadt, Germany
ECL-A (Luminol sodium salt)	Sigma-Aldrich, Darmstadt, Germany

ECL-B	Sigma-Aldrich, Darmstadt, Germany
EDTA	Carl Roth, Karlsruhe, Germany
Ethanol	Carl Roth, Karlsruhe, Germany
Ethidium bromide	Sigma-Aldrich, Darmstadt, Germany
Fetal Bovine Serum (FBS)	Thermo Fisher Scientific, Dreieich, Germany
Fixation solution	Tetenal, Norderstedt, Germany
Glycerol	AppliChem, Darmstadt, Germany
Glycine	AppliChem, Darmstadt, Germany
Guanidine hydrochloride	AppliChem, Darmstadt, Germany
H_2O_2	Sigma-Aldrich, Darmstadt, Germany
HCl	Carl Roth, Karlsruhe, Germany
Hydrocortisone	AppliChem, Darmstadt, Germany
Insulin	AppliChem, Darmstadt, Germany
Imidazole	AppliChem, Darmstadt, Germany
Iodacetamide	Sigma-Aldrich, Darmstadt, Germany
KCl	Carl Roth, Karlsruhe, Germany
Leupeptin	Sigma-Aldrich, Darmstadt, Germany
Methanol	Carl Roth, Karlsruhe, Germany
$MgCl_2$	Carl Roth, Karlsruhe, Germany
MG132	Sigma-Aldrich, Darmstadt, Germany
Mowiol 4-88	Carl Roth, Karlsruhe, Germany
Na_2HPO_4	AppliChem, Darmstadt, Germany
NaCl	Carl Roth, Karlsruhe, Germany
NaH_2PO_4	AppliChem, Darmstadt, Germany
N-ethylmaleimide	Sigma-Aldrich, Darmstadt, Germany
Ni-NTA resin	Thermo Scientific, Dreieich, Germany
Nonidet-P40	Carl Roth, Karlsruhe, Germany
PageRuler prestained protein ladder plus	Fermentas/Thermo Scientific, Dreieich, Germany
Pansorbin	Calbiochem, Bad Soden, Germany
Penicillin/streptomycin	Sigma-Aldrich, Darmstadt, Germany
Pepstatin	Sigma-Aldrich, Darmstadt, Germany
Phenol/chloroform/isoamyl alcohol (25:24:1)	Sigma-Aldrich, Darmstadt, Germany
Phenylmethylsolfonyl fluoride (PMSF)	Sigma-Aldrich, Darmstadt, Germany
Phosphate buffered saline (PBS)	Biochrom, Berlin, Germany

Polyethylene imine (PEI)	Sigma-Aldrich, Darmstadt, Germany
Proteinase K	Carl Roth, Karlsruhe, Germany
QIAGEN Plasmid DNA Purification Kit	QIAGEN, Hilden, Germany
Quick-Load® 1 kb DNA Ladder	New England BioLabs, Frankfurt a.M., Germany
RNase A	Carl Roth, Karlsruhe, Germany
Sepharose A beads	Sigma-Aldrich, Darmstadt, Germany
Skim milk powder	Sigma-Aldrich, Darmstadt, Germany
Sodium acetate	Carl Roth, Karlsruhe, Germany
Sodium azide	AppliChem, Darmstadt, Germany
Sodium dodecylsulfate (SDS)	Carl Roth, Karlsruhe, Germany
Sodiumacetate	Sigma-Aldrich, Darmstadt, Germany
T4 DNA ligase	Roche, Basel, Switzerland
T4 DNA Ligation buffer, 2 x conc.	Roche, Basel, Switzerland
TEMED	AppliChem, Darmstadt, Germany
Tris(hydroxymethyl)aminomethane (Tris)	Carl Roth, Karlsruhe, Germany
Triton X-100	AppliChem, Darmstadt, Germany
Trizol	Thermo Scientific, Dreieich, Germany
Trypsin/EDTA	Sigma-Aldrich, Darmstadt, Germany
Tween-20	AppliChem, Darmstadt, Germany
Urea	AppliChem, Darmstadt, Germany
β-mercaptoethanol	AppliChem, Darmstadt, Germany

2.7. Laboratory equipment

Table 13: Used laboratory equipment of the indicated company.

Device	**Company**
Agfa Curix 60	AGFA, Mortsel, Belgium
Avanti Je centrifuge	Beckman Coulter, Munich, Germany
Axiovert 200 M microscope	Zeiss, Oberkochen, Germany
BRAND® accu-jet® pro pipette controller	Sigma-Aldrich, Darmstadt, Germany
Branson Ultrasonics Sonifier™ S-450 Digital Ultrasonic Cell Disruptor/Homogenizer	Thermo Fisher Scientific, Dreieich, Germany
Eppendorf® Mastercycler Gradient	Eppendorf, Hamburg, Germany
Eppendorf® Multipipette Plus	Eppendorf, Hamburg, Germany
Eppendorf® Research® plus pipette, 0.1-2.5	Eppendorf, Hamburg, Germany

µl	
Eppendorf® Research® plus pipette, 0.5-10 µl	Eppendorf, Hamburg, Germany
Eppendorf® Research® plus pipette, 2-20 µl	Eppendorf, Hamburg, Germany
Eppendorf® Research® plus pipette, 10-100 µl	Eppendorf, Hamburg, Germany
Eppendorf® Research® plus pipette, 20-200 µl	Eppendorf, Hamburg, Germany
Eppendorf® Research® plus pipette, 100-1000 µl	Eppendorf, Hamburg, Germany
Eppendorf® Thermomixer Comfort 5355	Eppendorf, Hamburg, Germany
Eppendorf®Thermomixer Compact	Eppendorf, Hamburg, Germany
Freezer, -20°C	Liebherr-International Deutschland GmbH, Biberach and der Riß, Germany
Gel Doc™ XR+ Gel Documentation System	Bio-Rad, Munich, Germany
Glass Micro Pipette	Hamilton Company, Reno, US
Heraeus® BB16 Function Line CO_2 incubator	Heraeus Instruments GmbH, Hanaua, Germany
Heraeus™ Biofuge Pico™	Thermo Fisher Scientific, Dreieich, Germany
Heraeus™ Fresco™ 17 Microcentrifuge	Thermo Fisher Scientific, Dreieich, Germany
Heraeus™ Fresco™ 21 Microcentrifuge	Thermo Fisher Scientific, Dreieich, Germany
Heraeus™ Herafreeze HFU 586 Basic, -80°C	Thermo Fisher Scientific, Dreieich, Germany
Heraeus™ Laminair HLB 2448 GS	Thermo Fisher Scientific, Dreieich, Germany
Heraeus™ Megafuge™ 40 centrifuge	Thermo Fisher Scientific, Dreieich, Germany
Heracell™ 150i CO2 incubator	Thermo Fisher Scientific, Dreieich, Germany
Memmert incubator model 200, D 06058	Memmert, Büchenbach, Germany
Microwave 9029GD	Privileg, Stuttgart, Germany
ML-DNY-43 NewClassic	Mettler Toledo, Greifensee, Switzerland
MS 3 basic vortexer	IKA®-Werke GmbH & Co. KG, Staufen, Germany

Multigel electrophoresis chamber	Biometra, Jena, Germany
Multitron incubation shaker	Infors HT, Bottmingen, Switzerland
Nalgene Mr. Frosty™ Cryo 1°C freeze container	Thermo Fisher Scientific, Dreieich, Germany
NanoDrop 2000c UV-Vis Spectrophotometer	Thermo Fisher Scientific, Dreieich, Germany
Neubauer counting chamber (improved)	LO Laboroptik
No frost refrigerator and freezer CUN3523	Liebherr, Biberach an der Riß, Germany
Pipetboy acu	Integra Biosciences GmbH, Biebertal, Germany
Pipetboy acu 2	Integra Biosciences GmbH, Biebertal, Germany
PowerPac™ Basic Power Supply	Bio-Rad, Munich, Germany
PowerPac™ Universal Power Supply	Bio-Rad, Munich, Germany
Primovert light microscope	Zeiss, Oberkochen, Germany
Reciprocating Shaker 3016	GFL Gesellschaft für Labortechnik mbH, Burgwedel, Germany
Rotina 420R centrifuge	Hettich Zentrifugen, Tuttlingen, Germany
Rotixa 50 RS centrifuge	Hettich Zentrifugen, Tuttlingen, Germany
Sartorius portable	Sartorius AG, Göttingen, Germany
SmartSpec™ Plus Spectrophotometer	Bio-Rad, Munich, Germany
Sprout® Mini Centrifuge	Heathrow Scientific
Test Tube Rotating Shaker 3025	GFL, Burgwedel, Germany
Thermocycler peqSTAR 96x universal gradient	VWR International GmbH, Darmstadt, Germany
Trans-Blot® Cell	Bio-Rad, Munich, Germany
Unitwist RT	UniEquip Laborgerätebau- und Vertriebs GmbH, Planegg, Germany
Vacusafe vacuum pump	Integra, Biosciences GmbH, Biebertal, Germany
Vortex-Genie 2	Scientific Industries, Inc., Bohemia, US

2.8. Disposable laboratory equipment

Table 14: Used laboratory equipment of the indicated company.

Equipment	Company
Blotting paper 460x570 mm, 195 g/m^2	A. Harenstein GmbH, Würzburg, Germany
Cell scraper	Sarstedt, Nürnbrecht, Germany
CryoPure Tube 72.379, 1,8 ml white	Sarstedt, Nürnbrecht, Germany
Eppendorf® Combitips advanced® pipette tips	Eppendorf, Hamburg, Germany
Falcon® 2059 polypropylene round-bottom tube	Fisher Scientific Company LLC, Pittsburgh, US
Greiner CELLSTAR® serological pipette, 2 ml	Sigma-Aldrich, Darmstadt, Germany
Greiner CELLSTAR® serological pipette, 5 ml	Sigma-Aldrich, Darmstadt, Germany
Greiner CELLSTAR® serological pipette, 10 ml	Sigma-Aldrich, Darmstadt, Germany
Greiner CELLSTAR® serological pipette, 25 ml	Sigma-Aldrich, Darmstadt, Germany
Kimtech Science* Purple Nitrile*gloves, small	Kimberly-Clark Worldwide, Inc., Koblenz, Germany
Kimtech Science* Purple Nitrile*gloves, medium	Kimberly-Clark Worldwide, Inc., Koblenz, Germany
Kimtech Science* Purple Nitrile*gloves, large	Kimberly-Clark Worldwide, Inc., Koblenz, Germany
Micro tube 1.5 ml	Sarstedt, Nürnbrecht, Germany
Multiply®-Pro tube 0.2 ml	Sarstedt, Nürnbrecht, Germany
Nitril® NextGen® gloves, small	Meditrade GmbH, Kiefersfelden, Germany
Nitril® NextGen® gloves, medium	Meditrade GmbH, Kiefersfelden, Germany
Nitrocellulose membrane 0.45 µm NC, Amersham™ Protran™	GE Healthcare, Solingen, Germany
Parafilm® M All-Purpose Laboratory Film	Bemis Company, Inc., Oshkosh, US
PFA membrane	GE Healthcare, Solingen, Germany
Semi-micro cuvette, acrylic	Sarstedt, Nürnbrecht, Germany
TC dish 100, standard 83.3902	Sarstedt, Nürnbrecht, Germany
TC dish 150, standard 83.3903	Sarstedt, Nürnbrecht, Germany
TC plate 6 well, standard F 83.3920	Sarstedt, Nürnbrecht, Germany
TC plate 12 well, standard F 83.3921	Sarstedt, Nürnbrecht, Germany
Tube 50 ml, 114x23, PP, 62.547.254	Sarstedt, Nürnbrecht, Germany
Tube 15 ml, 120x17, PP, 62.554.502	Sarstedt, Nürnbrecht, Germany
X-ray films	Consumer Electronics Association (CEA), Arlington, US

2.9. Software

Table 15: Used software with indicated publisher and purpose.

Software	Publisher	Purpose
Adobe Photoshop CS5	Adobe	Image and Layout processing
Adobe Reader XI	Adobe	PDF data processing
CLC Sequence Viewer 6	CLC bio	Genome and Sequencing analyses
Endnote X8	Thomson Reuters	Reference organization
Excel 2010	Microsoft	Data and table processing
Filemaker Pro 14	Filemaker, Inc.	Database management
GPS-SUMO	The CUCKOO Workgroup	Prediction of potential SUMOylation and SUMO interacting motifs
GraphPad Prism 5	GraphPad Software	Figure processing and statistical analyses
ImageJ	NIH	Signal intensity calculations
PowerPoint 2010	Microsoft	Presentation processing
Volocity	PerkinElmer Inc.	Microscopic image processing
Word 2010	Microsoft	Text processing

3. Methods

3.1. Bacteria

3.1.1. Storage and culture

For long-term storage, DH5α *E.coli* strains were pelleted, resuspended in a solution containing 50% of sterile LB medium and 50% of 87% glycerol and subsequently stored in *CryoPure Tubes* in a *Heraeus™ Herafreeze* at -80°C. For solid cultures, bacteria were plated on LB-agar plates containing the appropriate amount of antibiotics depending on the resistance of the plasmid (100 µg/ml ampicillin or 25 µg/ml kanamycin) and incubated at 30°C or 37°C overnight. One single colony was inoculated into 5-500 ml sterile LB medium, depending on the prospective technique, with addition of the appropriate antibiotic (100 µg/ml ampicillin or 25 µg/ml kanamycin) and incubated in a *Multitron* incubation shaker at 30°C or 37°C at 150 rpm overnight. Solid and liquid *E.coli* cultures were stored for several days at 4°C.

Table 16: Composition of LB medium.

LB Medium	Tryptone	10 g/l
	Yeast extract	5 g/l
	NaCl	5 g/l
	(Autoclaved)	

3.1.2. Chemically competent bacteria preparation

Chemically competent bacteria (DH5α *E.coli*) were plated on a LB plate without selective antibiotics and incubated at 37°C overnight (*Memmert*). The next day, one single colony was inoculated in 10 ml LB medium without antibiotics and shaked at 220 rpm at 37°C (*Multitron*) overnight. 200 ml LB medium without antibiotics were inoculated with 2 ml overnight culture and incubated at 37°C at 220 rpm until reaching an OD_{600} of 0.3-0.5 (optimum 0.43) which was repeatedly measured using a *SmartSpec™ Plus Spectrophotometer*. After cooling in ice water for 20 min, the *E.coli* bacteria were transferred to 50 ml falcon tubes and centrifuged at 3000 rpm at 4°C for 5 min (*Rotina 420R*). The pellet was resuspended in 15 ml of TFB-I buffer, pelleted again using the same conditions and resuspended in 4 ml of TFB-II buffer. Liquid nitrogen was used to freeze aliquots of 100 µl of the chemical competent bacteria in pre-cooled Eppendorf tubes which were stored at -80°C (*Heraeus™ Herafreeze*).

Table 17: Composition of TFB-I and TFB-II.

TFB-I	Glycerin	15%
	$CaCl_2$	10 mM
	KOAc	30 mM
	$RbCl_2$	100 mM
	$MnCl_2$	50 mM
	pH 5.8	
TFB-II	Glycerin	15%
	MOPS pH 7.0	10 mM
	$CaCl_2$	75 mM
	$RbCl_2$	10 mM

3.1.3. Chemical transformation of E.coli

Chemical competent *E.coli* bacteria were thawed from -80°C on ice. 100 µl of the bacteria were mixed with 10 µl of DNA solution in a pre-cooled *Falcon® 2059 polypropylene round-bottom tube*. The 10 µl of DNA solution contained either 50-100 ng of DNA for retransformation or 10 µl of ligation mixture for transformation during cloning procedures. In the following, a heat shock was performed at 42°C for 30-40 s in a water bath. After cooling the bacteria on ice for 1-2 min, 1 ml of sterile, non-selective LB medium was added to the tube. The *E.coli* were incubated at 30°C or 37°C at 150 rpm for approximately one hour, centrifuged at 4000 rpm for 3 min (*Heraeus™ Fresco™ 21 Microcentrifuge*), resuspended in 100 µl of LB medium and plated on selective agar plates containing the appropriate antibiotic. The plates were incubated at 30°C or 37°C overnight and colonies of transformed bacteria were expected the following day. Single colonies were picked and inoculated into 5-500 ml LB medium, depending on the subsequent method.

3.2. Mammalian cells

3.2.1. Cell cultivation

Mammalian adhesive cell lines were propagated in Dulbecco's Modified Eagle Medium (DMEM) containing 0.11 g/l sodium pyruvate, 10% fecal bovine serum (FBS) and 1% of penicillin/streptomycin solution (1000 U/ml penicillin and 10 mg/ml streptomycin in 0.9% NaCl) as monolayers on polystyrene cell culture dishes (12-well, 6-well, 100 mm, 150 mm tissue culture dishes, Sarstedt). The medium was additionally supplemented with 5 µg/ml of insulin and 0.5 µM hydrocortisone for hepatoma cell lines like HepaRG cells. The cells were incubated at 37°C with 5% of CO_2 atmosphere (*Heraeus® BB16 Function Line*) and all work with cells was performed sterile under a *Heraeus™ Laminair HLB 2448 GS* safety cabinet cleaned with ethanol. For splitting of confluent cells, plates were washed once with

phosphate buffered saline (PBS) and trypsin/EDTA was added to remove the cells from the dishes. After incubation for 3-5 min at 37°C, trypsin activation was blocked by the addition of standard propagation medium. The cells were transferred to a 50 ml *falcon*, centrifuged for 3 min at 2000 rpm (*Heraeus™ Megafuge™* 40) and the pellet resuspended in an appropriate amount of propagation medium. For propagation, cells were splitted 1:2 – 1:20 or counted and seeded in an appropriate amount for following experiments as described in 3.2.3.

Table 18: Composition of PBS.

PBS	NaCl	140 mM
	KCl	3 mM
	Na_2HPO_4	4 mM
	KH_2PO_4	1.5 mM
	(pH 7.3, autoclaved)	

3.2.2. Storage

Confluent mammalian cells were trypsinized and centrifuged as described in 3.2.1. For long-term storage, the pellet was resuspended in FBS supplemented with 10% dimethyl sulfoxide (DMSO) and frozen slowly to -80°C in *CryoPure Tubes* using a *Nalgene Mr.Frosty* freezing device. For thawing, cells were incubated shortly at 37°C in a water bath, added to pre-warmed propagation medium, pelleted at 2000 rpm for 3 min, resuspended in fresh culture medium to remove the DMSO and seeded in appropriate culture dishes.

3.2.3. Cell number determination

As described in 3.2.1., the cells were trypsinized, centrifuged and the pellet resuspended in fresh culture medium. 10 µl of cell suspension were mixed with 10 µl of Trypan Blue solution and pipetted into a *Neubauer* cell counting chamber. After counting the cells using a *Primovert* light microscope, the total cell number was determined with the following formula:

Cell number/ml = counted cells x 2 (dilution factor) x 10^4

Table 19: Composition of Trypan Blue solution.

Trypan Blue solution	Trypan Blue	0.15%
	NaCl	0.85%

4-8 x 10^6 cells or 4-8 x 10^5 were seeded per 100 mm dish or six well, respectively. Seeded cells were incubated at 37°C and 5% CO_2 for approximately 24 h, after which transfection (3.2.4.) or viral infection (3.3.3.) followed.

3.2.4. Transfection with Polyethylenimine

The polymer polyethylenimine (PEI) was used to transfect DNA into mammalian cells. PEI was dissolved in Milli-Q water with a concentration of 1 mg/ml, adapted to pH 7.2 using 0.1 M HCl, sterile filtered and stored in aliquots at -80°C. For transfection, DNA was pipetted into 2 ml *Eppendorf* tubes and 1.8 ml of pre-warmed DMEM without supplements as well as PEI (10 µl per 1 µg DNA) was added. The mixture of DNA, medium and PEI was vortexed thoroughly and incubated for 15-30 min at room temperature (RT). After changing the medium of the cells from culture medium to DMEM without supplements, the transfection mixture was added to the cells and incubated for 4-6 h, after which the medium was changed to culture medium. Harvesting of the transfected cells was performed 24-72 h post transfection (3.2.5.).

3.2.5. Cell harvesting

24-72 h after transfection (3.2.4.), the cells were removed from the plate with cell scrapers and transferred to 15 ml falcon tubes. After centrifugation at 2000 rpm for 3 min (*Rotina 420R*), the supernatant was discarded, and washed once with PBS. The cells were centrifuged, the supernatants discarded and the pellets frozen at -20°C (*Liebherr*) for follow up experiments.

3.3. Adenovirus

3.3.1. Propagation and storage of adenovirus stocks

HEK293 cells cultured in a 150 mm dish with 80-90% confluency were infected with a multiplicity of infection (MOI) of approximately 5 fluorescent forming units (ffu)/cell of an established laboratory adenovirus stock (3.3.3.). The cells were harvested 3-5 days post infection, depending on the visible cytopathic effect, centrifuged at 2000 rpm for 3 min (*Rotina 420R*) and washed once with PBS. After another centrifugation step, the cells were resuspended in 1 ml DMEM without supplements per 150 mm dish. To break the cells up, three subsequent freeze (liquid nitrogen) and thaw (37°C, water bath) cycles were performed followed by a centrifugation step at 3000 rpm for 10 min to pellet the cell debris. The supernatant containing the virus was mixed with 10% glycerol and stored at -80°C for long-term storage.

3.3.2. Virus titration

The virus titer is determined via immunofluorescence staining with the adenoviral early DNA binding protein (DBP or E2A) which enables the calculation of the number of ffu [187]. 8 x 10^5 HEK293 cells per six well were infected (3.3.3.) with dilutions of the virus stock by factors of 10^2-10^6 with DMEM without supplements. 24 h post infection, the medium was removed from the infected cells, which were fixed with ice-cold methanol for 20 min at -20°C. After

removing the methanol, the six wells were dried at RT and further stored at -20°C or directly used for immunofluorescence staining. Therefore, non-specific antibody sites were blocked with TBS-BG buffer, which was incubated for 1 h on an *Unitwist RT* shaker. The six wells were incubated with the primary E2A-specific antibody B6-8 (1:10 in TBS-BG) for at least one hour at RT or 2-3 h at 4°C and washed three times with TBS-BG. Secondary *Alexa Fluor* 488-coupled secondary antibody (1:500 in TBS-BG) was added for 1 h at RT or 2 h – overnight at 4°C, while covered with aluminium foil to protect the samples from light. After washing three times with TBS-BG, stained cells were either stored at 4°C or directly investigated using a fluorescent *Axiovert 200 M* microscope (*Zeiss*). The virus titer or viral progeny production was determined by the number of infectious particles which was calculated by the mean value of several independent countings of the visual field, multiplied with the microscope magnifications and virus dilutions, and finally diluted by the infected cell numbers.

Table 20: Composition of TBS-BG buffer.

TBS-BG	Tris-HCl (pH 7.6)	20 mM
	NaCl	137 mM
	KCl	3 mM
	MgCl2	1.5 mM
	Tween-20	0.05% (v/v)
	Sodium azide	0.05% (v/v)
	Glycine	5% (w/v)
	BSA	5% (w/v)

3.3.3. Adenovirus infection

Mammalian cells were infected at a confluency of 80-90%. The virus was diluted to an appropriate amount with DMEM without supplements and added to the cells. Therefore, the amount of virus needed for the desired MOI was determined using the following calculation:

$$\text{volume}_{\text{virus stock solution}}\ (\mu l) = (\text{MOI} \times \text{total cell number}) / \text{virus titer (ffu/}\mu l)$$

After incubating the virus with the cells for approximately 1 hour, the medium was removed and replaced by fresh culture medium. The infected cells were harvested 24-72 h post infection as described in 3.2.5 and proceeded for further investigation, such as protein lysate preparation and western blot analysis (3.6).

3.4. DNA techniques

3.4.1. Preparation of plasmid DNA from *E.coli*

A single colony was picked from the agar plate, inoculated in 5 ml LB-medium supplemented with the appropriate antibiotics and incubated at 30°C/37°C overnight. 200-500 µl of the pre-culture were inoculated into 500 ml LB-medium containing antibiotics and incubated at 30°C or 37°C at 150 rpm (*Multitron*). After 24-30 h of incubation, the bacteria were centrifuged at 4500 rpm for 20 min (*Rotixa 50 RS*) and the plasmid DNA was extracted using the *QIAGEN Plasmid DNA Purification* Kit according to the manufacturer's protocol.

For a maxi preparation (500 ml culture), each 10 ml of the P1-P3 QIAGEN buffers (resuspension buffer, lysis buffer, neutralization buffer) were added successively, whereas the pellet was split into two parts and only 600 µl of P1-P3 were added for a midi preparation (50 ml culture). For analytical purposes, 300 µl of P1-P3 were added to mini preparations of 1 ml culture. The samples were mixed and centrifuged at 4500 rpm for 30 min (maxi) and 14800 rpm for 10 min (midi/mini). Qiagen columns were prepared with 10 ml/1 ml (maxi/midi) equilibration buffer QBT, the supernatants of the samples were transferred to the columns, let run through and washed twice with washing buffer QC. After eluting the DNA with 15 ml/ 840 µl elution buffer QF, 12.5 ml/700 µl isopropanol were added, mixed thoroughly and followed by a centrifugation step at 4500 rpm for 45 min or 14800 rpm for 10 min for maxi and midi preparation, respectively. For mini preparation, the columns steps were left out and the supernatant was directly added to 1 volume isopropanol containing 0.1 volume 3 M NaAc and centrifuged at 14800 rpm for 5 min to precipitate the DNA. The pelleted DNA was washed once with 75% (v/v) ethanol, centrifuged again at 4500 rpm (maxi) or 14800 rpm (midi/mini) for 5 min and dried at RT or 42°C. After resuspending the DNA in 20 – 500 µl Milli-Q water (ultrapure water), the DNA concentration was measured using a *Nanodrop 2000c UV-Vis* spectrophotometer at a wavelength of 260 nm. The ratio of OD_{260}/OD_{280} indicated the purity of the DNA, with a value of 1.8 for highly pure DNA. The DNA concentration was adapted to 1 µg/µl (maxi/midi) or directly digested and analyzed on an agarose gel without measuring the concentration (mini).

3.4.2. Agarose gel electrophoresis

Agarose was dissolved in TBE buffer at a concentration of 0.6-1% (w/v), depending on the DNA fragment sizes, to prepare analytical or preparative agarose gels. Therefore, the agarose was melted using a microwave to dissolve it in 1 x TBE buffer and 0.5 µg/ml ethidium bromide was added before pouring the agarose onto a gel tray with inserted combs. After hardening of the gel, DNA samples mixed with 6 x loading buffer were loaded into the gel pockets. For the indication of DNA fragment sizes, either a 100 bp or 1 kp DNA ladder was applied. Electrophoresis was carried out at in 1 x TBE running buffer at 140 V for

approximately 1-1.5 h. A *Gel Doc™ XR+* gel documentation system was used to visualize the DNA bands under UV light at 365 nm.

Table 21: Composition of 5 x TBE buffer, 6 x loading dye and DNA ladders.

5 x TBE	Tris (pH 7.8) Boric acid EDTA	0.45 M 0.45 M 10 mM
6 x loading dye	EDTA Glycerol Bromphenol blue Xylen Cyanol	10 mM 50% (v/v) 0.25% (w/v) 0.25% (w/v)
DNA ladder	100 bp or 1 kb ladder 6 x loading dye Milli-Q water	100 µl 100 µl 400 µl

3.4.3. Polymerase chain reaction

The polymerase chain reaction (PCR) was used to amplify DNA templates or to create DNA with point mutations due to primers that contain a different complementary base. Therefore, a PCR mix was prepared in a 0.2 ml PCR reaction tube by the addition of 5 µl 10 x PCR reaction buffer, 1 µl dNTP mixture (dATP, dTTP, dCTP, dGTP), 125 ng forward and reverse primer, 25 – 100 ng DNA template and 1 µl polymerase (PfuUltra II Fusion or Taq) and filled up to 50 µl with Milli-Q water. The PCR program shown in Table 22 was run for 27 cycles in the thermocycler *PeqSTAR 96x universal gradient*. The annealing and elongation step were adapted to the theoretical primer melting temperature and the DNA fragment length, respectively. 5-10 µl of the PCR reaction was analyzed on an agarose gel (3.4.2.) to determine the efficiency of the PCR.

Table 22: PCR setup with indicated time periods, temperatures and number of cycling steps.

pre-denaturation	2 min	95°C	1 x
denaturation	1 min	95°C	27 x
annealing	30 s - 1 min	59°C	
elongation	15 s – 4.5 min	72°C	
final elongation	10 min	68°C	1 x
storage	indefinitely	4°C	indefinitely

3.4.4. 3D-PCR

Cells were transfected and/or infected as described in 3.2.4. and 3.3.3. Genomic DNA was isolated using the manufacturer's protocol of the *Machery-Nagel NucleoSpin® Tissue* Kit and eluted in 100 µl of elution buffer. The PCR mix was set up with 10 µl DNA, 125 ng of forward and reverse primer, 2 µl dNTP mix, 5 µl reaction buffer and 1 µl of Taq polymerase. The following PCR program was run for 45 cycles using the thermocycler *PeqSTAR 96x universal gradient*. Different denaturing temperatures were applied ranging from 79-89°C. 10 µl of the PCR mix was loaded onto a 1% agarose gel to analyze the result. For increasing the product yield, the PCR was repeated once, loaded in total on an agarose gel and target bands cut out of the gel. After centrifugation for 20000 rpm for 1.5 h at 15°C, the DNA was precipitated like described in 3.4.1. and sent for DNA sequencing (3.4.6.).

Table 23: 3D-PCR setup with indicated time periods, temperatures, including eight different linear distributed denaturing temperatures (≡), and number of cycling steps.

pre-denaturation	10 min ≡	87°C +/- 3.5°C	1 x
denaturation	1 min ≡	87°C +/- 3.5°C	45 x
annealing	30 s min	59°C	
elongation	15 s	72°C	
final elongation	10 min	68°C	1 x
storage	indefinitely	4°C	indefinitely

3.4.5. Phosphorylation and Ligation

The amplification product of the PCR was incubated with 1 µl of the restriction enzyme DpnI for 2 h or overnight at 37°C in the incubator (*Memmert*) to remove methylated template DNA. For DNA precipitation, 1 volume of isopropanol and 0.1 volume of 3 M sodium acetate (NaAc, pH 5.2) were added and centrifuged at 14800 rpm for 10 min (*Heraeus™ FrescoTM 21 Microcentrifuge*). The pelleted DNA was washed with 75% ethanol, spun down for 3 min, dried at 42°C and dissolved in 30 µl sterile Milli-Q water. To phosphorylate the DNA for following ligation, 10 µl of the DNA was mixed with 8 µl Milli-Q water, 2 µl of 10 x ligase buffer and 1 µl kinase PKN and incubated at 37°C for 2 h shaking at 330 rpm (*Eppendorf®Thermomixer Compact*). The ligation reaction was carried out by the addition of 18 µl water, 2 µl 10 x ligase buffer and 1 µl T4 ligase at 13°C for 2 h or overnight (*Eppendorf®Thermomixer Compact)*. After transformation of 10 µl of ligation mixture into chemical competent *E.coli* bacteria as described in 3.1.3., single colonies were picked, inoculated in LB medium with supplemented antibiotics, incubated overnight followed by plasmid DNA preparation (3.4.1.) and sequencing analysis (3.4.6.).

3.4.6. Sequencing of DNA

1 µg of DNA was mixed with 30 pmol of the appropriate sequencing primer and added up to 17 µl with Milli-Q water. The samples were sent to Eurofins Genomics (Ebersberg), which performed the DNA sequencing. The received results were analyzed using *BioEdit*, *BLAST* and *Serial Cloner*.

3.5. RNA techniques

3.5.1. Preparation of total cellular RNA

Cells were seeded in 100 mm dishes or six well plates, transfected and/or infected followed by harvesting according to already described protocols. From the beginning of harvesting the cells, all work was performed continuously on ice and with filtered tips. The cell pellet was resuspended in 600 µl of Trizol reagent and stored at -80°C (*Heraeus™ Herafreeze*) or directly further processed by the addition of 200 µl Chloroform. After vortexing each sample for at least 15 s, a centrifugation step at 14800 rpm for 15 min at 4°C (*Heraeus™ Fresco™ 21 Microcentrifuge*) was performed for phase separation. The upper, transparent phase containing the RNA was carefully taken without touching any of the other phases and added to a new *Eppendorf tube* containing 600 µl isopropanol. After mixing thoroughly, the samples were spun down again for 15 min at 14800 rpm at 4°C. The isopropanol was carefully removed before washing once with 75% ethanol. After another centrifugation step with the same conditions, the ethanol was removed, and the pellet air-dried and dissolved in 20-50 µl nuclease-free water. To determine the RNA amount and purity, the samples were measured with a *Nanodrop 2000c UV-Vis* spectrophotometer, which indicates highly pure RNA with a ratio of OD_{260}/OD_{280} of ~2.0. The RNA was either stored at -20°C (*Liebherr*) or directly used for cDNA reverse transcription (3.5.2).

3.5.2. Reverse transcription of RNA into cDNA

The *Reverse Transcription System* (*Promega*) was used to reverse transcribe cDNA from the RNA, which was isolated from cells as described in 3.5.1. Therefore, 1 µg RNA was filled up to 10 µl with nuclease-free water and added to a master mix containing 3 µl nuclease-free water, 4 µl $MgCl_2$ (25 mM), 2 µl 10 x reverse transcription buffer, 2 µl dNTP mixture (10 mM), 1µl $oligo(dT)_{15}$ random primers, 0.5 µl recombinant RNasin® ribonuclease inhibitor and 0.7 µl AMV reverse transcriptase. After incubation at 42°C for 45-60 min (*Eppendorf® Thermomixer Comfort 5355*), the reaction was inactivated by heating to 95°C for 5 min, followed by cooling down on ice for 5 min. The obtained cDNA was stored at -20°C (*Liebherr*).

3.5.3. Quantitative PCR (qPCR)

For qPCR analysis, the cDNA was diluted 1:5 up to 1:100. 4 µl of DNA were mixed with 0.5 µl of each forward and reverse primer with a concentration of 30 pmol and 5 µl of *LightCycler® 480 SYBR Green I Master* (*Roche*). The reaction mix was pipetted into *FrameStar® 480/96* 96 well plates, covered with adhesive seals and a *LightCycler 480 Instrument II* was used to run one of the following programs: 10 min at 95°C, followed by 40 cycles of 30 s at 95°C, 30 s at 62°C, and 30 s at 72°C (for adenoviral mRNAs) or 5 min at 95°C, followed by 45 cycles of 15 s at 95°C, 10 s at 60°C and 25 s at 72°C (for Apobec mRNAs). The CT values (average threshold cycle) were obtained for triplicate reactions, which were set in relation to CT values of a housekeeping gene (TATA-binding protein TBP or 18S). Melting curves were analyzed to confirm the identities of the obtained products.

3.6. Protein techniques

3.6.1. Preparation of whole-cell lysates

The harvested cell pellets (3.2.5) were resuspended in 75-500 µl RIPA buffer, depending on the pellet sizes, supplemented with the protease inhibitors PMSF, Aprotinin, Leupeptin and Pepstatin A. While incubating on ice for half an hour, the samples were vortexed every 10 min (*Vortex-Genie 2*). After sonification for 30 s at 5°C using a *Branson Ultrasonics Sonifier™* (0.8 output impulse/s), the lysates were centrifuged at 11000 rpm for 3 min at 4°C (*Heraeus™ FrescoTM 21 Microcentrifuge*). The supernatant was transferred to pre-cooled *Eppendorf tubes* and protein concentration measured with a spectrophotometry (*SmartSpec™ Plus*) using the Bradford method [190]. Therefore, 800 µl of Milli-Q water were pipetted into semi-micro cuvettes and exactly 1 µl of each protein lysate was added. After the addition of 200 µl Bradford reagent, the cuvettes were sealed using *Parafilm® M All-Purpose Laboratory Film* and the samples mixed thouroughly. The samples were measured at 595 nm in the photometer and protein concentrations were determined in relation to the standard curve of several BSA dilutions. Following dilution of the desired protein concentration in Milli-Q water, 5 x Laemmli buffer containing β-mercaptoethanol was added. The lysates were boiled at 95°C for 3 min (*Eppendorf® Thermomixer Comfort 5355*) for denaturation and subsequently stored at -20°C (*Liebherr*) for further analysis.

Table 24: Composition of RIPA buffer and 5 x Laemmli buffer.

RIPA	Tris/HCL, pH 8.0	50 mM
	NaCl	150 mM
	EDTA	5 mM
	Nonidet P-40	1% (v/v)
	SDS	0.1%
	Sodium deoxycholat	0.5% (v/v)
	PMSF	1 mM
	Aprotinin	10 U/ml
	Leupeptin	1 µg/ml
	Pepstatin A	1 µg/ml
5 x Laemmli buffer	Tris/HCl, pH 6.8	250 mM
	Glycerol	50% (v/v)
	SDS	10% (w/v)
	Bromphenol blue	0.5% (w/v)
	β-mercaptoethanol	5% (w/v)

3.6.2. Treatment with the proteasome inhibitor MG132

The cells were seeded (3.2.3), transfected (3.2.4) and/or infected (3.3.3) like already described. 8 h before harvesting, 5 ml of fresh medium supplemented with MG132 were added to the cells resulting in a total amount of 10 µM MG132 per 100 mm dish. Harvesting (3.2.5) and further experimental steps were performed according to described protocols.

3.6.3. Cycloheximide treatment

The cells were seeded (3.2.3), transfected (3.2.4) and/or infected (3.3.3) like already described. 48 h after HAdV infection, the cells were treated with 100 µg/ml cycloheximide to inhibit translation. Harvesting (3.2.5) was performed 18 h, 24 h and 48 h post treatment and further experimental steps were carried out according to described protocols.

3.6.4. Nickel-nitrilotriacetic acid (Ni-NTA) pull down

Transfection (3.2.4) and infection (3.3.3) of cells was performed as described previously. For harvesting, the cells were scraped, transferred to 15 ml *Falcon tubes* and dishes washed with PBS to ensure harvesting of the total amount of cells. After centrifugation at 2000 rpm for 3 min (*Rotina 420R*), the supernatant was removed, and the pellets resuspended in 5 ml PBS. 1 ml was transferred to *Eppendorf tubes* for total input controls, while the remaining lysates were spun down again and resuspended in 5 ml B1 buffer supplemented with β-mercaptoethanol. The input controls were stored at -20°C (*Liebherr*) and further processed to

whole-cell lysates (3.6.1), and the remaining cells dissolved in 5 ml B1 buffer were either stored at -80°C (*Heraeus™ Herafreeze*) or directly sonicated three times for 10 s at 5°C (*Branson Ultrasonics Sonifier*™). 30 µl Ni-NTA beads per sample were centrifuged at 1000 x g for 3 min at 4°C (*Heraeus™ FrescoTM 21 Microcentrifuge*) and washed three times with B1 buffer. The beads were added to the sonicated samples and incubated rotating overnight at 4°C (*GFL 3025* spinning shaker). Subsequently, the samples were centrifuged at 4000 rpm for 10 min at 4°C the following day (*Rotina 420R*) and successively washed with 1 ml of each B1, B2 and B3 buffer which were supplemented with the protein inhibitors aprotinin (10 U/ml), leupeptin (1 µg/ml) and pepstatin A (1 µg/ml) as well as β-mercaptoethanol (5 mM), centrifuging at 1000 x g for 3 min at 4°C. The samples were eluted in 20 µl elution buffer, denatured at 95°C for 3 min (*Eppendorf® Thermomixer Comfort 5355*) and stored at -20°C.

Table 25: Composition of B1, B2, B3 and elution buffer used for Ni-NTAs.

B1 (guanidinium lysis buffer)	Guanidinium-HCL	6 M
	Na2HPO4	0.1 M
	NaH2PO4	0.1 M
	Tris/HCL, pH 8.0	10 mM
	Imidazol	20 mM
	β-mercaptoethanol	5 mM
B2 (wash buffer, pH 8.0)	Urea	8 mM
	Na2HPO4	0.1 mM
	NaH2PO4	0.1 mM
	Tris/HCL, pH 8.0	10 mM
	Imidazol	20 mM
	β-mercaptoethanol	5 mM
B3 (wash buffer, pH 6.3)	Urea	8 mM
	Na2HPO4	0.1 mM
	NaH2PO4	0.1 mM
	Tris/HCL, pH 6.3	10 mM
	Imidazol	20 mM
	β-mercaptoethanol	5 mM
Elution buffer	Imidazol	200 mM
	SDS	0.1% (w/v)
	Tris/HCL, pH 6.3	150 mM
	Glycerol	30% (v/v)
	β-mercaptoethanol	720 mM
	Bromphenol blue	0.01% (w/v)

3.6.5. Co-immunoprecipitation

For immunoprecipitation (IP), cell lysates were prepared like described in 3.6.1. and a total of 1-3 mg of protein amount were precleared with 30 µl pansorbin per sample, rotating for 1 h on a spinning shaker at 4°C (*GFL 3025*) to block unspecific binding. 3 mg of sepharose A beads per IP sample were swelled at 4°C for 15-20 min with 1 ml RIPA buffer and incubated with the appropriate amount of antibody for 1 h on the spinning shaker at 4°C in the following. The antibody-coupled sepharose beads were washed two times with RIPA buffer containing fresh protease inhibitors by centrifuging at 6000 rpm for 3 min at 4°C (*Heraeus™ FrescoTM 21 Microcentrifuge*) and distributed equally to the supernatant of the pre-cleared cell lysates, which were pipetted into fresh *Eppendorf tubes*. After another incubation step on the spinning shaker at 4°C for 1 h, the IP samples were washed three times with RIPA buffer supplemented with protease inhibitors by centrifuging at 6000 rpm for 3 min at 4°C. Finally, the pellets were resuspended in 20 µl of 2 x Laemmli buffer containing β-mercaptoethanol, boiled to 95°C for 5 min (*Eppendorf® Thermomixer Comfort 5355*) and stored at -20°C (*Liebherr*) for further analysis. To improve co-immunoprecipitation with pEYFP-Apobec3A, the *GFP-Trap® (ChromoTe*k) was used according to the manufacturer's description.

Table 26: Composition of 2 x Laemmli buffer.

2 x Laemmli buffer	Tris/HCL, pH 6.8	100 mM
	SDS	4% (w/v)
	DTT	200 mM
	Bromphenol blue	0.2% (w/v)
	Glycerol	20% (v/ v)

3.6.6. SDS-polyacrylamid gel electrophoresis (SDS-PAGE)

SDS-PAGE was used to separate the protein samples according to their molecular weights. Therefore, *Multigel* chambers (*Biometra*) were fixed like described in the manufacturer's protocol and gels were prepared using a 30% acrylamide/bisacrylamide solution, which was diluted with Milli-Q water and Tris to total concentrations ranging from 8-15%. After the addition of SDS, APS and TEMED, the separating gel was mixed and approximately 7 ml were cast into the gap between the two glass plates. It was covered with isopropanol and let harden. The isopropanol was removed, 3 ml of 5% stacking gel added and clean combs inserted, containing 12 or 24 pockets. The hard gels were fixed in *Multigel* SDS chambers, which were filled up with TGS running buffer. After loading the protein samples into the pockets using a *Hamilton Glass Micro Pipette*, 1 µl of the *PageRulerTM plus prestained protein ladder* was used to indicate molecular sizes and the gels were run at 15-20 mA/gel for approximately 1.5-2 h.

Table 27: Composition of stacking and separating gel as well as TGS buffer.

Stacking gel (5%)	H_2O	69%
	30% Acrylamide solution	17% (v/v)
	1 M Tris/HCL, pH 6.8	12.5% (w/v)
	SDS	0.1% (w/v)
	APS	0.1% (w/v)
	TEMED	0.01% (v/v)
Separating gel (12%)	H_2O	34%
	30% Acrylamide solution	40% (v/v)
	1.5 M Tris/HCL, pH 8.0	25% (w/v)
	SDS	0.1% (w/v)
	APS	0.1% (w/v)
	TEMED	0.4% (v/v)
TGS buffer	Tris	25 mM
	Glycine	200 mM
	SDS	0.1% (w/v)

3.6.7. Western blotting

Proteins were separated using SDS-PAGE (3.6.6.) and blotted onto 0.45 µm nitrocellulose or 0.2 µm polyvinylidene fluoride (PVDF) membranes in a *Trans-Blot® Cell* chamber according to manufacturer's protocol. The gels and membranes were soaked in towbin buffer and placed between four *Whatman* blotting papers and two blotting pads into plastic cassettes. After adding the cassettes into the *TransBlot® Cell* chambers with the correct orientation, the electrophoretic transfer was carried out at 400 mA for 90 min. To block unspecific binding of antibodies, the membranes were incubated with 5% dry milk in PBS at 4°C for 1 h or overnight. The membranes were briefly washed three times with PBS-Tween and primary antibodies diluted in PBS-Tween to appropriate concentrations were added and incubated for 3 h or overnight at 4°C on a reciprocating shaker (*GFL 3016*). Primary antibodies were removed and stored at 4°C or -20°C, to be able to reuse them for several times. After washing thrice with PBS-Tween, the membranes were incubated with secondary antibodies conjugated to horseradish peroxidase (HRP) and diluted 1:5000 – 1:10000 in 3% milk in PBS-Tween. After incubating for at least 2 h on the reciprocating shaker at 4°C, the membranes were washed three times with PBS-Tween. Developing of the membranes onto films was performed under red light in a dark chamber. Therefore, the protein bands were visualized by enhanced chemiluminescence using a mixture of 10 ml substrate ECL-A, 100 µl of substrate ECL-B and 10 µl H_2O_2. The membranes were shortly incubated in the solution

and laid into plastic foils in developing cassettes. X-ray films were placed into the cassettes, which were closed and incubated for different time frames. The *Agfa Curix 60* developing machine was used to develop the films, which were labelled, scanned and cropped and further prepared for figures using *PowerPoint* (*Microsoft*) and *Photoshop* (*Adobe*). The *ImageJ* (*Wayne Rasband*) program was used for the quantification of protein signals if necessary.

Table 28: Composition of Towbin buffer, PBS-Tween and ECL-A and ECL-B solutions.

Towbin buffer	Tris/HCl Glycine SDS Methanol	25 mM 200 mM 0.05% (w/v) 20% (v/v)
PBS-Tween	Tween-20 in 1x PBS	0.1% (v/v)
ECL-A	Tris/HCl, pH 6.8 Luminol sodium	100 mM 250 µg/ml
ECL-B	p-Coumaric acid in DMSO	1.25 mg/ml

3.6.8. Indirect immunofluorescence

Cells were grown on glass coverslips and transfected or infected like described previously (3.2.4./3.3.3.) for immunofluorescence (IF) analysis. Fixation of the cells was performed with 4% paraformaldehyde (PFA) for 10 min at RT followed by one wash with PBS. The cells were either stored in PBS at 4°C (not exceeding two weeks) or directly permeabilized with PBS containing 0.5% (v/v) Triton-X-100 for 5 min at RT before blocking unspecific antibody binding with 1 x TBS-BG for 1 h on a *Unitwist RT* shaker. Antibody dilutions were prepared in PBS according to descriptions in the company's datasheets and 20 µl incubated with each glass plate for 1 h at RT in a dark and wet environment. After three washing steps with 1 x TBS-BG, the secondary antibodies diluted in PBS were incubated with the glass plates for 1 h at RT in a dark and wet environment. The washing steps were repeated, the cover slips dried and mounted on glass slides with 10 µl Mowiol glowing solution. The IF stainings were dried overnight at RT in the dark and stored for further analysis at 4°C. A confocal microscope (*Axiovert 200 M microscope*) was used to acquire digital images, which were further processed and analyzed using the *Volocity* program (*PerkinElmer*).

Table 29: Composition of TBS-BG and Mowiol.

TBS-BG	Tris/HCl, pH 7.6	20 mM
	NaCl	137 mM
	KCl	3 mM
	MgCl2	1.5 mM
	Tween-20	0.05% (v/v)
	Sodium azide	0.05% (w/v)
	Glycine	5% (w/v)
	BSA	5% (w/v)
Mowiol	Glycerin	6 g
	Mowiol	2.4 g
	0.2 M Tris/HCl, pH 8.5	12 ml, 0.2 M
	DABCO	0.1% (v/v)

3.6.9. Reporter gene assay

The *Dual-Luciferase® Reporter Assay System* (Promega) was used according to manufacturer's description to investigate viral promoter activity. Therefore, the *Firefly* luciferase was expressed under the control of a promoter of interest and normalized to *Renilla* luciferase. Cells were transfected in a 12 well dish like described previously (3.2.4.) and harvested 24 h post transfection by applying 100 µl *Passive Lysis Buffer* (Promega) per dish, which was incubated for 15 min at RT on an orbital shaker. 20 µl of lysate were mixed with 30 µl of *Luciferase Assay Substrate* and luciferase luminescence was measured with a *Tecan Reader*, before adding 30 µl of *Stop & Glo®* solution and measuring the apparent luminescence.

4. Results

4.1. Apobec3A expression during HAdV infection

4.1.1. Apobec mRNA levels are differentially regulated during HAdV infection

Apobec proteins possess restrictive functions for many different viruses, for example HIV or HBV [103, 191]. So far, there is only limited data on Apobec expression and function during productive HAdV infection, stating that HAdV replication is not restricted by any of the Apobec3 proteins, which are suggested to require ssDNA for inhibiton [104]. However, this study does not present any proof for the assumption, which further has already been withdrawn by the fact that DNA viruses (such as HPVs) represent targets for Apobec3 inhibition [104]. Consequently, the effect of adenoviral infection on the different Apobec mRNA levels was investigated in the beginning of our study by performing qPCR analysis.

HepaRG cells were infected with HAdV-C5 wild type (wt) with a MOI of 50 and the cells were harvested 24 and 48 h post infection. After the isolation of mRNA and reverse transcription to cDNA, the samples were analyzed by qPCR, using primers for all eleven different Apobec mRNAs, which were set in relation to the housekeeping mRNA for TBP. The mRNA levels for E1A were used as an infection control, which arose 24 h post infection and increased significantly 48 h post infection as expected. The eleven Apobec mRNAs were regulated differently during HAdV infection (Figure 10). Some Apobec mRNAs were not changed significantly upon adenoviral infection, such as Apobec3F and -G, as well as Apobec2 and AICDA. Expression levels for Apobec1 and Apobec4 were not detected in HepaRG cells. Furthermore, mRNA levels for Apobec3C, -DE and -H were downregulated approximately two-fold during HAdV infection. Only two mRNAs were increased by adenoviral infection, namely Apobec3A and -B (Figure 10). Recently, a publication showed Apobec3B upregulation during adenoviral infection, which is in accordance with the obtained data in the present study [192]. Apobec3A levels were drastically increased, more than 40 times during adenoviral infection in comparison to the mock control. As in conclusion, the strongest effect of HAdV infection was observed for the Apobec3A mRNA, the focus of the following studies was laid on the investigation of Apobec3A expression and function during adenoviral infection.

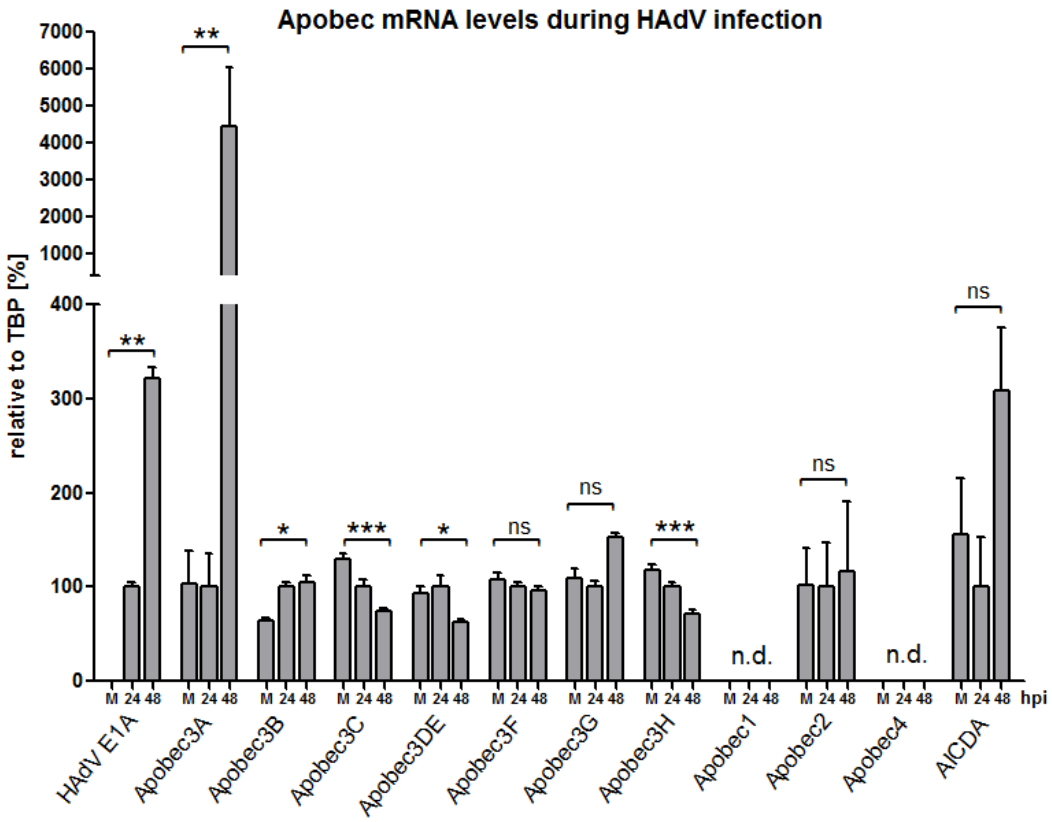

Figure 10: Apobec mRNA levels are differentially modulated during HAdV infection.
HepaRG cells were infected with HAdV (MOI 50) and harvested after 24 h and 48 h. mRNA was isolated and cDNA reverse transcribed, followed by qPCR analysis. The viral protein E1A was used as an infection control. The mRNA levels were set in relation to the housekeeping TBP mRNA levels. Statistical significances were calculated using an unpaired t-test. (ns not significant, n.d. not detected, hpi hours post infection).

4.1.2. Apobec3A is not targeted by the adenoviral E3 ubiquitin ligase complex

Since Apobec3A is known to restrict a variety of different viruses, including HIV-1, HBV, HTLV, HPV and parvoviruses, its function during HAdV infection was studied in this work [98, 103, 105, 108, 114]. Due to the fact, that HAdVs need to suppress the DDR in order to replicate efficiently, whereas Apobec3A was shown to upregulate the DDR, the initial hypothesis was, that Apobec3A protein expression is not beneficial for HAdV [66, 81]. Since first experiments demonstrated highly elevated Apobec3A mRNA levels during HAdV infection (4.1.1), it was assumed that Apobec3A protein function might be counteracted by HAdV via its proteasomal degradation.

To verify the hypothesis, Apobec3A was co-expressed in human lung carcinoma cells (H1299) with the two adenoviral proteins E1B-55K and E4orf6. Both factors that are necessary to establish the viral E3 ubiquitin ligase complex together with several cellular components [66]. Cell lysates were generated, and proteins separated by SDS-PAGE followed by western blot transfer and immunodetection. Apobec3A protein levels were not reduced upon E1B-55K and E4orf6 co-expression, concluding that Apobec3A is not targeted

by the viral E3 ubiquitin ligase complex (Figure 11A, lane 7). This was confirmed using the HepaRG-TR-Apobec3A cell line, inducing Apobec3A expression via tetracycline and transfecting E1B-55K as well as E4orf6 24h later (Figure 11B). Apobec3A levels were reduced in the presence of E1B-55K alone (Figure 11B, lanes 6 and 8), but not dependent on E1B-55K and E4orf6 co-expression, verifying that Apobec3A seems to be no target of the viral E3 ubiquitin ligase. Interestingly, E4orf6 protein levels were reduced to approximately 40% (calculated with ImageJ) by Apobec3A expression in both experiments, which was counteracted by the presence of E1B-55K (Figure 11A, lanes 4 and 6 and Figure 11B, lanes 3 and 7). In order to exclude, that tetracycline-induced expression of Apobec3A is toxic for the cells, cell viability assays as well as an MTT assays were conducted for the three days' time frame, in which all the following experiments including tetracycline induction were performed. A comparison of induced versus non-induced HepaRG-TR-Apobec3A cells did not show significant differences and lead to the conclusion that tetracycline induction does not harm the cells in the applied time frame (Figure 11C).

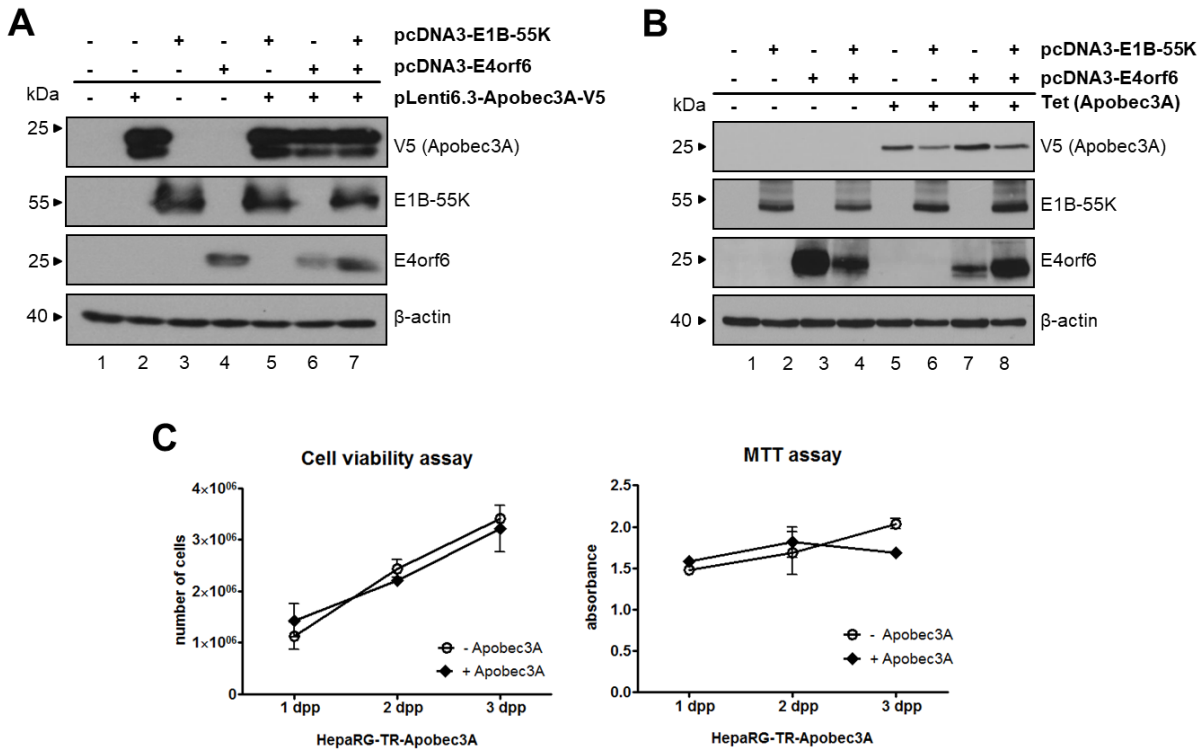

Figure 11: Apobec3A is not targeted by the adenoviral E3 ubiquitin ligase complex.
(A) 5 µg of pLenti6.3-Apobec3A, pcDNA3-E1B-55K and pcDNA3-E4orf6 were transfected into H1299 cells and harvested 24 h after transfection. After performing whole-cell lysates, proteins were separated with SDS-PAGE and subjected to western blot analysis, followed by immunodetection using antibodies for E1B-55K, E4orf6 and V5 (for Apobec3A), as well as β-actin as a loading control. Stained proteins are indicated on the right, molecular weights in kDA on the left. (B) HepaRG-TR-Apobec3A cells were induced with 5 µg/ml tetracycline to express Apobec3A, transfected with E1B-55K and E4orf6 24 h later, and harvested 24 h post transfection. After performing whole-cell lysates, proteins were separated with SDS-PAGE and subjected to western blot analysis, followed by immunodetection using antibodies for E1B-55K, E4orf6 and V5 (for Apobec3A), as well as β-actin as a loading control. Stained proteins are indicated on the right, molecular weights in kDA on the left. The depicted blots represent the result of several repetitions. (C) Cell viability as well as an MTT assays were performed for the first three days, comparing induced versus non-induced HepaRG-TR-Apobec3A cells (dpp - days post plating).

4.1.3. Apobec3A protein levels are upregulated during HAdV infection

After investigating mRNA levels of Apobec3A, which were increased during HAdV infection (4.1.1) as well as showing no degradation of Apobec3A by the adenoviral E3 ubiquitin ligase complex (4.1.2), the question arose, whether HAdV infection affects Apobec3A protein expression. Therefore, HepaRG cells were transfected with the pLenti6.3-Apobec3A-V5 plasmid followed by an infection with HAdV wt at a MOI of 50 and harvested at different time points. Cell lysates were generated and proteins separated by SDS-PAGE followed by western blot transfer and immunodetection. Stainings for E1B-55K, E2A and E4orf6 confirmed viral infection, as well as Mre11 and p53 stainings, which are known to be degraded during HAdV infection at later timepoints [66]. 48 h post transfection and infection, Apobec3A levels normally decreased in the mock samples, which was not the case after infection with HAdV, concluding that HAdV stabilizes Apobec3A protein expression (Figure 12A, lanes 4 and 7). These results could be confirmed by performing a cycloheximide treatment, which is known to inhibit eukaryotic translation [193]. Therefore, HepaRG cells were transfected with pLenti6.3-Apobec3A-V5 and infected with HAdV wt using a MOI of 50. The cells were treated with 100 µg/ml cycloheximide and harvested at different time points post treatment (Figure 12B). E4orf6 was used as a viral control, as well as Mre11, which confirmed the degradation of cellular proteins by HAdV [66]. Although Apobec3A protein levels were reduced by cycloheximide treatment, HAdV infection still was able to increase Apobec3A protein levels 48 h post infection (Figure 12B, lanes 7 and 8). Moreover, upcoming bands for Apobec3A were upregulated by adenoviral infection, indicating an effect of HAdV infection on Apobec3A PTMs or oligomerization (Figure 12B, lanes 2, 4, 6 and 8).

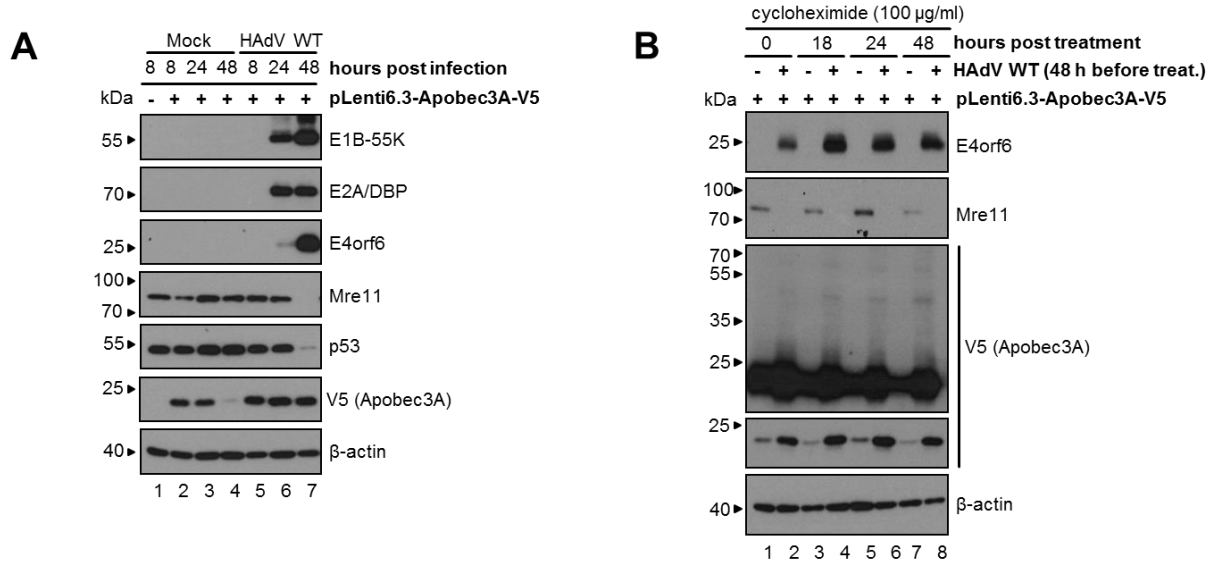

Figure 12: Apobec3A protein expression levels are stabilized during HAdV infection.
(A) HepaRG cells were transfected with 5 µg pLenti6.3-Apobec3A-V5 and infected with HAdV at a MOI of 50. After harvesting the cells 8 h, 24 h and 48 h post infection, cell lysates were performed, proteins separated via SDS-PAGE and subjected to western blot transfer as well as immunodetection. E1B-55K, E2A, E4orf6, Mre11 and p53 served as controls for functional HAdV infection, whereas β-actin served as a loading control. Stained

proteins are indicated on the right, molecular weights in kDA on the left. (B) HepaRG cells were transfected with 5 µg pLenti6.3-Apobec3A-V5 and infected with HAdV at a MOI of 50. 48 h post infection, the cells were treated with 100 µg/ml cycloheximide following harvesting 0 h, 18 h, 24 h and 48 h post treatment. Cell lysates were carried out, proteins separated via SDS-PAGE and subjected to western blot transfer as well as immunodetection. E4orf6 and Mre11 served as controls for viral infection, whereas β-actin was used as a loading control. Stained proteins are indicated on the right, molecular weights in kDA on the left. The depicted blots represent the result of several repetitions.

To investigate, if Apobec3A is upregulated in different human cell lines, 5 µg of pLenti6.3-Apobec3A-V5 were transfected into several cell lines following HAdV infection (MOI 50). The cells were harvested 24 h and 48 h post infection and subjected to immunoblotting. E2A stainings served as a viral control, whereas the His control was used to confirm cell lines. Apobec3A protein expression was increased by adenoviral infection in all the used cell lines, but not to the same extent (Figure 13A – C, lanes 3 and 6). Calculation of the Apobec3A signal intensities normalized to the loading control β-actin with the *ImageJ* program (Figure 13D) demonstrated a strong upregulation of Apobec3A during HAdV infection especially in HeLa and HepaRG cells (Figure 13A, B, D), whereas H1299 cells did not show such a strong effect (Figure 13C, D). Furthermore, SUMO2-overexpressing cell lines (HeLa-S2 and HepaRG-S2) did not show the high increase of Apobec3A protein levels that was observed in normal HeLa and HepaRG cells (Figure 13A, B, D). Taken together, Apobec3A upregulation during HAdV infection was found in all investigated cell lines.

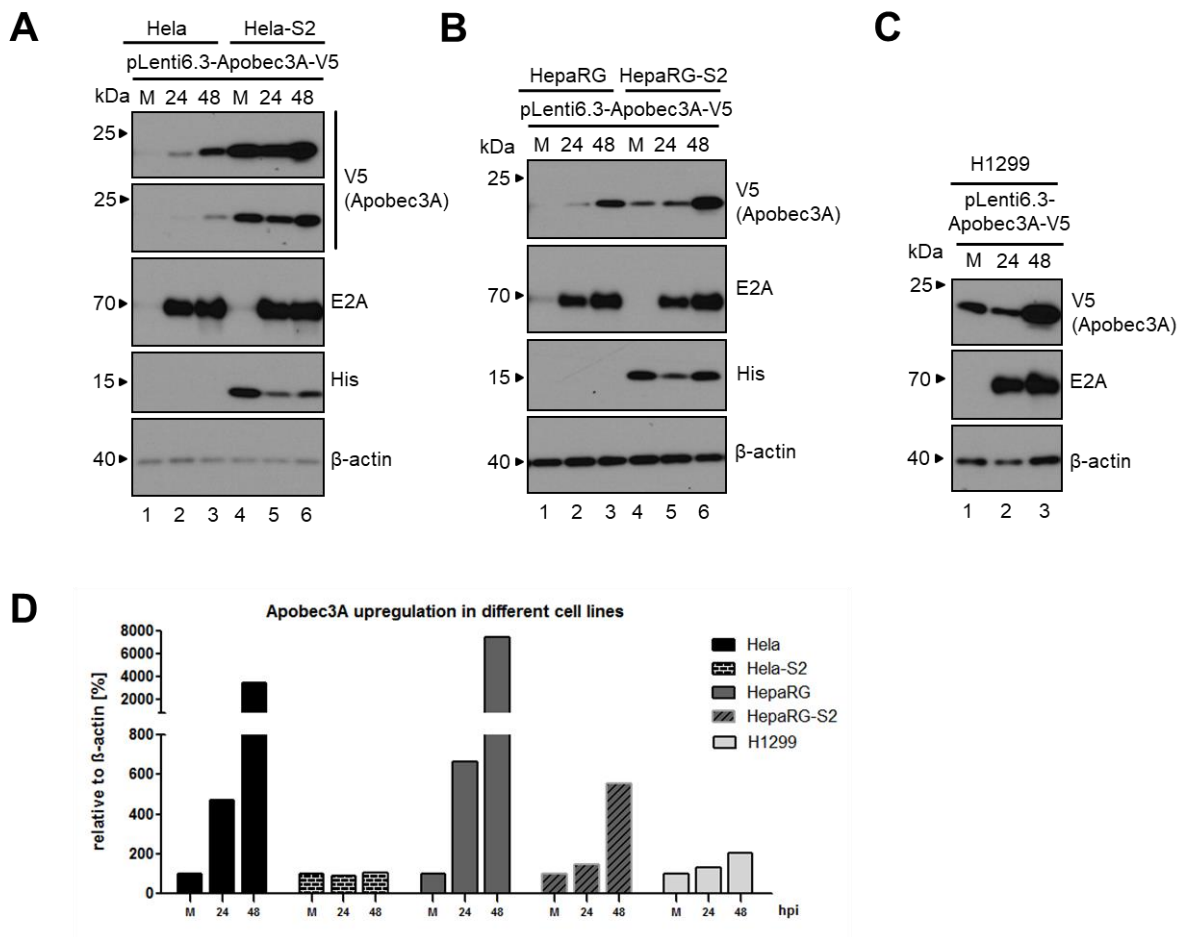

Figure 13: Apobec3A protein expression is increased during HAdV infection in different human cell lines. (A) HeLa and HeLa-S2 cells, (B) HepaRG and HepaRG-S2 cells, as well as (C) H1299 cells were transfected with 5 µg pLenti6.3-Apobec3A-V5 and infected with HAdV (MOI 50). Cells were harvested 24 h and 48 h post infection, cell lysates performed which were subjected to SDS-PAGE, western blot transfer and immunostainings. E2A served as a viral control, whereas the 6xHis control was used to confirm cell lines. β-actin was used as a loading control. Stained proteins are indicated on the right, molecular weights in kDa on the left. The depicted blots represent the result of several repetitions. (D) Signal intensities for Apobec3A were calculated in relation to the β-actin loading controls using the *ImageJ* program.

4.1.4. E1A is not involved in Apobec3A stabilization during HAdV infection

To investigate which viral factor is responsible for Apobec3A upregulation during HAdV infection, co-expression experiments with adenoviral early proteins and Apobec3A were performed. Human papillomaviruses, which are known to be restricted by Apobec3A [108], also increase Apobec3A protein expression levels. The HPV16 E7 protein thereby inhibits cullin 2-dependent protein degradation, which stabilizes Apobec3A that is still catalytically active and promotes cancer mutagenesis [107]. HPV16 E7 and HAdV E1A, both viral oncogenes that induce cellular transformation, are known to share several characteristics and functions like binding to the same cellular proteins including pRB to release E2F transcriptional activators [194]. Due to that, the initial hypothesis was that E1A is involved in Apobec3A upregulation during HAdV infection. Co-expression experiments of viral HA-tagged E1A protein and pLenti6.3-Apobec3A-V5 showed that increasing amounts of E1A do

not result in Apobec3A upregulation (Figure 14, lanes 4-6). Hence, these data refuted the initial hypothesis, concluding that E1A is not responsible for Apobec3A stabilization during HAdV infection.

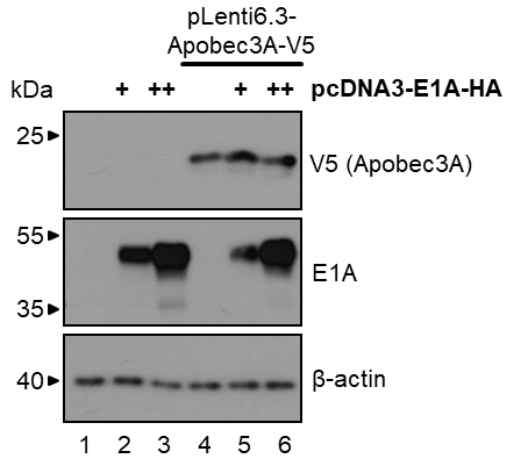

Figure 14: Apobec3A protein levels are not upregulated by E1A expression.
H1299 cells were transfected with 5 µg pLenti6.3-Apobec3A-V5 and 5 µg or 15 µg pcDNA3-E1A-HA and harvested after 48h. Cell lysates were performed, proteins were separated using SDS-PAGE and subjected to western blot transfer and immunodetection using antibodies for V5 (Apobec3A) and E1A. β-actin was used as a loading control. Stained proteins are indicated on the right, molecular weights in kDa on the left.

4.1.5. Apobec3A protein expression is negatively regulated by p53

In 2017, Menendez and colleagues found that Apobec3A expression is transcriptionally regulated by p53. CHIP analysis revealed binding of p53 to transcriptional regulatory regions of Apobec3 genes, which was shown to affect Apobec3 mRNA levels, leading to increasing amounts in the case of Apobec3A [195]. However, protein expression was not analyzed in this study. To investigate, if p53 is the responsible factor for the increase of Apobec3A protein levels during HAdV infection, co-expression experiments were performed in H1299 cells, which lack endogenous p53 expression [176]. However, p53 protein expression did not increase Apobec3A protein levels. Apobec3A protein levels were even drastically reduced by p53 to 3%, as well as vice versa Apobec3A reduced p53 protein levels to 73% (Figure 15A lane 4). To investigate, if Apobec3A reduction by p53 is dependent on the amount of p53 in the cells, another experiment was performed, including different amounts of transfected p53 (0.5 - 2 µg). Increasing amounts of p53 correlated with decreasing Apobec3A protein levels, which demonstrated a dose-dependency of Apobec3A protein reduction by p53 (Figure 15B, lanes 4-8).

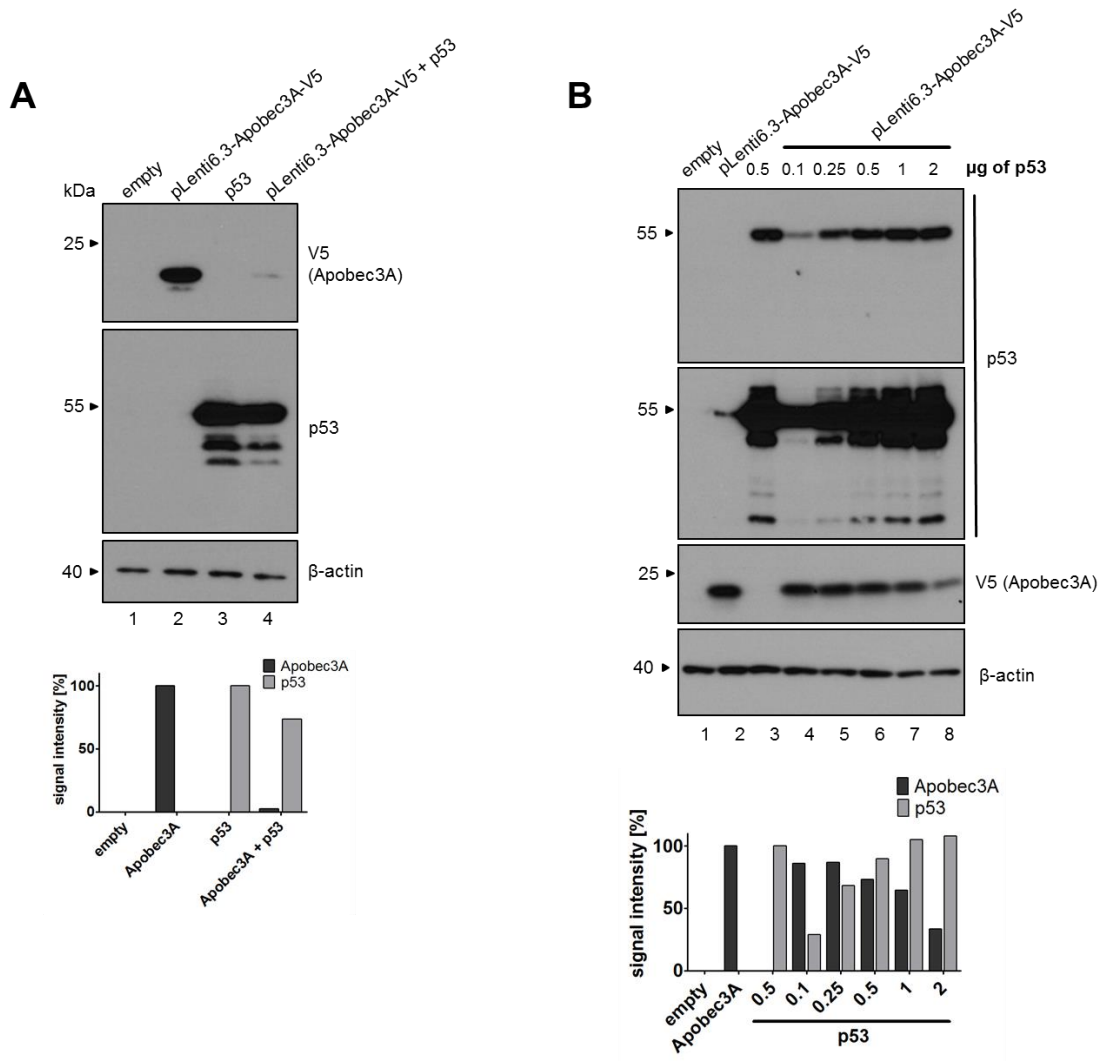

Figure 15: p53 protein expression leads to decreased Apobec3A protein levels.
(A) H1299 cells were transfected with 5 µg pLenti6.3-Apobec3A-V5 and 0.5 µg p53. Cells were harvested 24 h post transfection and whole-cell lysates were performed. Proteins were separated via SDS-PAGE and subjected to western blot analysis as well as immunodetection using antibodies for V5 (Apobec3A), p53 and β-actin as a loading control. Stained proteins are indicated on the right, molecular weights in kDa on the left. (B) H1299 cells were transfected with 5 µg pLenti6.3-Apobec3A-V5 and increasing amounts of p53 (0.5 - 2 µg). Cells were harvested 24 h post transfection and whole-cell lysates were performed. Proteins were separated via SDS-PAGE and subjected to western blot analysis as well as immunodetection using antibodies for V5 (Apobec3A), p53 and β-actin as a loading control. Stained proteins are indicated on the right, molecular weights in kDa on the left. The depicted blots represent the result of several repetitions.

4.1.6. E1B-55K reduces Apobec3A protein levels in a SUMO-dependent manner

In the next step, the E1B-55K protein was investigated concerning its role in Apobec3A upregulation during HAdV infection. E1B-55K is known to cooperate with E4orf6 in the adenoviral E3 ubiquitin ligase complex to degrade a variety of cellular proteins [66]. Nevertheless, E1B-55K was shown to bind to the cellular RNA-binding protein E1B-AP5, which is upregulated during HAdV infection, concluding that E1B-55K also plays a role for the stabilization of cellular proteins [196, 197]. Consequently, we performed co-expression experiments for E1B-55K and Apobec3A in H1299 cells to examine if E1B-55K might be the responsible factor for Apobec3A stabilization during HAdV infection. Additionally, Apobec3B

was included in this experiment, since Apobec3B mRNA levels were increased during HAdV infection during initial experiments (4.1.1). E1B-55K did not promote Apobec3A upregulation. By contrast, Apobec3A levels were reduced by E1B-55K to 43% (Figure 16A, lanes 3 and 5). Apobec3B, which also showed elevated mRNA levels upon HAdV infection (Figure 10), was unaffected by E1B-55K on protein levels (Figure 16A, lanes 4 and 6).

Since SUMOylation of E1B-55K is known to be a prerequisite for its function and degradation of cellular proteins like p53 [159], it was investigated if Apobec3A downregulation by E1B-55K is SUMO-dependent. Therefore, HepaRG cells were transfected with pLenti6.3-Apobec3A and E1B-55K wt as well as two E1B-55K mutants. E1B-55K is known to be SUMO-1 modified at position K104, which dramatically abolishes E1B-55K SUMOylation upon mutation [159]. This SUMO-mutant of E1B-55K as well as the nuclear export signal (NES)-mutant of E1B-55K were included in the following experiment. The NES signal is known to regulate E1B-55K shuttle between the cytoplasm and the nucleus and increases SUMOylation when mutated [182]. Western blot analysis confirmed Apobec3A downregulation by E1B-55K wt in HepaRG cells (Figure 16B, lanes 1 and 2), with a stronger effect in comparison to H1299 cells (Figure 16A, lanes 3 and 5). Moreover, the SUMO-mutant of E1B-55K (E1B-55K K104R) even decreased Apobec3A protein levels to a stronger extent than the E1B-55K wt, whereas the heavily SUMOylated version of E1B-55K (NES mutant) was shown to increase Apobec3A levels (Figure 16B, lanes 3 and 4). The current summary of results is shown in Figure 16C with the findings that the SUMO mutant of E1B-55K is not able to SUMOylate and inactivate p53, but efficiently degrades Apobec3A protein levels; whereas the NES mutant of E1B-55K, which is highly SUMOylated and localizes only to the nucleus, is SUMOylating and thereby inhibiting p53, and cannot degrade Apobec3A protein levels.

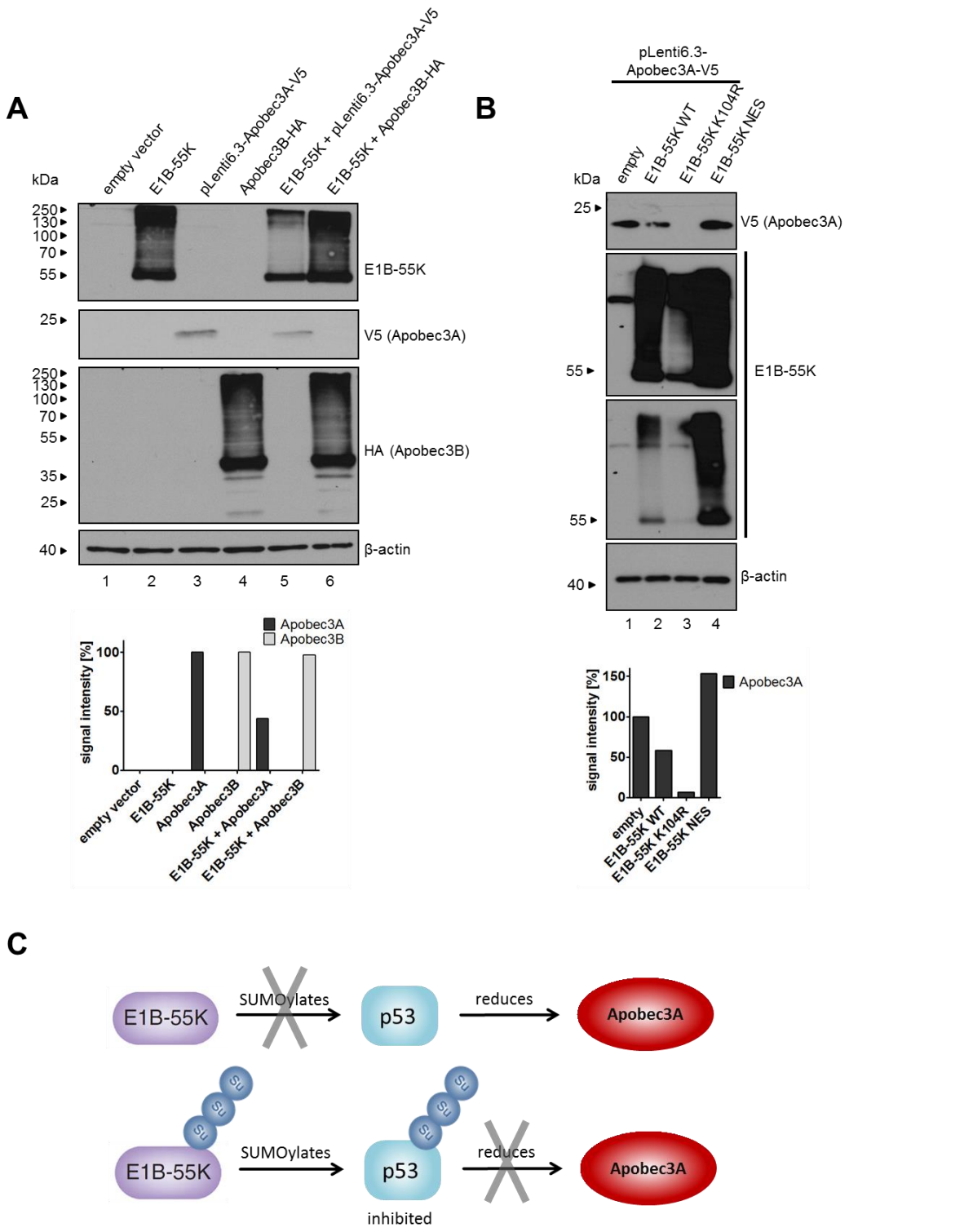

Figure 16: E1B-55K reduces Apobec3A protein levels in a SUMO-dependent manner.
(A) H1299 cells were transfected with 5 µg pLenti6.3-Apobec3A-V5, E1B-55K and pcDNA3-Apobec3B-HA. Following harvesting of the cells 24 post transfection, cell lysates were performed, proteins separated via SDS-PAGE, and subjected to western blot and immunodetection using antibodies for V5 (Apobec3A), E1B-55K as well as HA (Apobec3B). β-actin was used as a loading control. Stained proteins are indicated on the right, molecular weights in kDa on the left. (B) HepaRG cells were transfected with 5 µg pLenti6.3-Apobec3A-V5, E1B-55K wt, E1B-55K K104R and E1B-55K NES. Following harvesting of the cells 24 post transfection, cell lysates were performed, proteins separated via SDS-PAGE, and subjected to western blot and immunodetection using antibodies for V5 (Apobec3A) and E1B-55K. β-actin was used as a loading control. Stained proteins are indicated on the right, molecular weights in kDa on the left. The depicted blots represent the result of several repetitions. (C) Schematic representation of the hypothesis on Apobec3A protein reduction by E1B-55K dependent on the SUMOylation pathway.

4.1.7. E4orf6 expression promotes Apobec3A protein upregulation

The viral E4orf6 protein was shown to affect cellular protein levels mostly by establishing an E3 ubiquitin ligase complex together with the viral protein E1B-55K and several cellular proteins to degrade cellular factors that are not beneficial for HAdV infection [66, 68]. However, some cellular proteins are only targeted by E4orf6, not by E1B-55K, including the p53-related protein p73 or topoisomerase-IIβ–binding protein 1 (TOPBP1) [198, 199]. p73 exhibits sequence homology to p53 and therefore possesses similar functions like transcriptional activation as well as induction of apoptosis [200]. By targeting the ATR activator protein TOPBP1, E4orf6 interferes with ATR signaling pathways in response to cellular stress [199]. Since Apobec3A activates the DDR pathway [81], it was reasonable to investigate the effect of E4orf6 on Apobec3A expression levels. Therefore, HepaRG cells were transfected with pLenti6.3-Apobec3A-V5 and infected with HAdV wt, HAdV E1B-55K- and HAdV E4orf6- virus. Antibody stainings with E1B-55K and E4orf6 confirmed the presence of the virus mutants, whereas E2A served as a control for equal amounts of the different viruses. 48 h after HAdV wt infection, a strong upregulation of Apobec3A protein levels was observed, which confirmed the results of earlier experiments (4.1.3). Interestingly, the mutant viruses lacking functional E1B-55K or E4orf6 were not able to increase Apobec3A protein levels to the same extent as the wt virus (Figure 17A, lanes 3 and 4). The E1B-55K- virus is known to exhibit lower E4orf6 protein levels, which indicated E4orf6 to be the important factor for Apobec3A upregulation during HAdV wt infection. To analyze this hypothesis, HepaRG cells were co-transfected with pLenti6.3-Apobec3A-V5, as well as E1B-55K and E4orf6. 48 h after transfection, E1B-55K was shown to reduce Apobec3A protein levels like expected from earlier results (4.1.6), whereas E4orf6 increased Apobec3A protein levels (Figure 17B, lanes 4 and 5). Consistently with obtained data (Figure 11A and B), E4orf6 protein levels were decreased upon Apobec3A expression. Apobec3A upregulation by E4orf6 was not found in earlier experiments (Figure 11A and B), most likely due to the application of different cell lines and time points in these experiments. Another co-transfection experiment confirmed that E4orf6 induced increase of Apobec3A protein levels and could show that this upregulation depends on the amount of transfected E4orf6 levels (Figure 17C, lanes 4-6). Increasing amounts of E4orf6 correlated with increasing Apobec3A protein levels, which downregulated E4orf6. In conclusion, E4orf6 plays a crucial role for Apobec3A stabilization during HAdV infection.

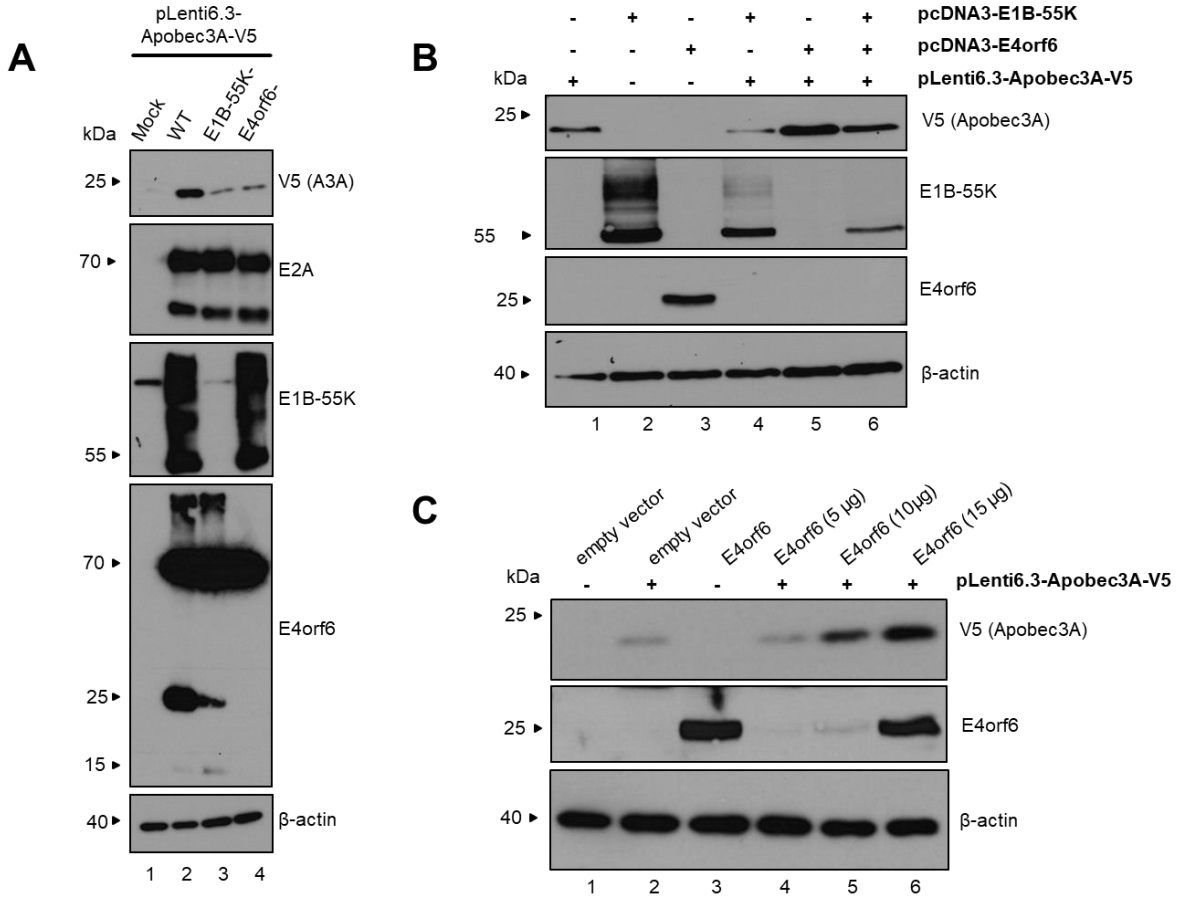

Figure 17: The adenoviral E4orf6 protein plays an important role for Apobec3A upregulation.
(A) HepaRG cells were transfected with 5 µg pLenti6.3-Apobec3A-V5 and infected with HAdV wt, HAdV E1B-55K- and HAdV E4orf6- at MOIs of 50. 48 h after infection, cells were harvested, lysates performed, proteins separated via SDS-PAGE and subjected to western blot analysis using antibodies for V5 (Apobec3A), E2A, E1B-55K and E4orf6. β-actin was used as a loading control. Stained proteins are indicated on the right, molecular weights in kDa on the left. (B) HepaRG cells were co-transfected with 5 µg pLenti6.3-Apobec3A-V5, E1B-55K and E4orf6. 48 h after transfection, cells were harvested, lysates performed, proteins separated via SDS-PAGE and subjected to western blot analysis using antibodies for V5 (Apobec3A), E1B-55K and E4orf6. β-actin was used as a loading control. Stained proteins are indicated on the right, molecular weights in kDa on the left. (C) HepaRG cells were co-transfected with 5 µg pLenti6.3-Apobec3A-V5 and increasing amounts of E4orf6 (5-15 µg). 48 h after transfection, cells were harvested, lysates performed, proteins separated via SDS-PAGE and subjected to western blot analysis using antibodies for V5 (Apobec3A) and E4orf6. β-actin was used as a loading control. Stained proteins are indicated on the right, molecular weights in kDa on the left. The depicted blots represent the result of several repetitions.

4.1.8. Apobec3A stabilization by E4orf6 is conserved among different HAdV types

The E4orf6 protein of HAdV type C5 was shown to increase Apobec3A protein levels (Figure 17B and C). The next experimental setup was designed to examine, whether the observed upregulation is specific for HAdV type 5 or conserved among different HAdV types. Hence, E4orf6 proteins of different HAdV types were co-transfected with pLenti6.3-Apobec3A-V5 into HepaRG cells. Despite the strongest upregulation of Apobec3A was observed for HAdV type 5 E4orf6, the HAdV types 26, 35, 41 and 48 were also observed to increase Apobec3A

protein expression in comparison to Apobec3A expressed alone (Figure 18, lanes 2 and 8-12). However, E4orf6 protein levels for HAdV types 35 and 41 could not be detected and only faint bands were observed for the HAdV types 26 and 48 (Figure 18, red arrows). Nevertheless, Apobec3A was still upregulated by the E4orf6 protein expression of HAdV types 35 and 41, so it was assumed that these proteins are expressed, but cannot be detected due to unknown reasons. In accordance with earlier performed experiments (Figure 11A, B and Figure 17B, C), Apobec3A decreased E4orf6 protein levels (Figure 18, lanes 8-12). Taken together, Apobec3A upregulation by E4orf6 seems to be a conserved mechanism among different HAdV types.

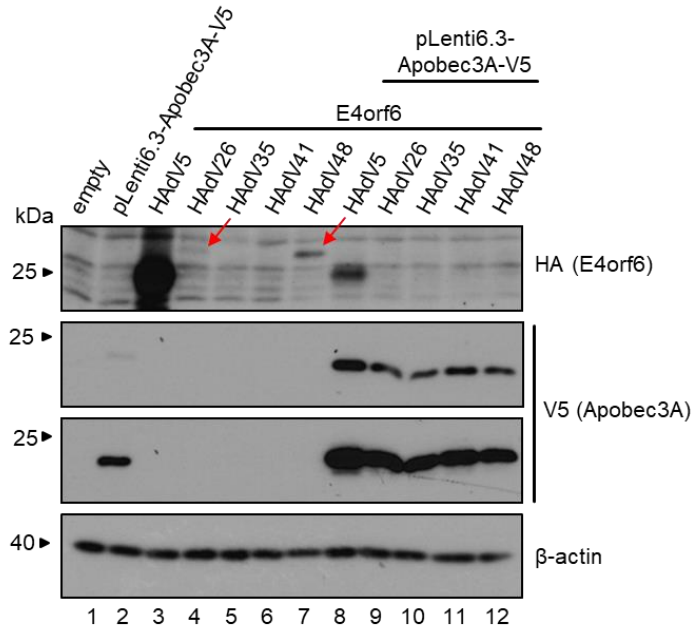

Figure 18: Apobec3A upregulation by E4orf6 is conserved among different HAdV types.
HepaRG cells were transfected with 5 µg pLenti6.3-Apobec3A-V5 and E4orf6 of the HAdV types 5, 26, 35, 41 and 48. 48 h after transfection, the cells were harvested, lysates performed, proteins separated via SDS-PAGE and subjected to western blot analysis using antibodies for V5 (Apobec3A) and HA (E4orf6). β-actin was used as a loading control. Stained proteins are indicated on the right, molecular weights in kDa on the left. The depicted blots represent the result of several repetitions.

4.1.9. E4orf6 protein is no binding partner of cellular Apobec3A

E4orf6 plays an important role during Apobec3A stabilization during HAdV infection (Figure 17), which led to the assumption that both proteins might interact with each other. To investigate this, immunoprecipitations (IPs) were performed in H1299 cells. Consistently with earlier obtained results (Figure 11A, B and Figure 17B, C), E4orf6 protein levels were reduced upon Apobec3A expression (Figure 19A, lanes 3 and 4, Figure 19B, lanes 3 and 4), whereas upregulation of Apobec3A by E4orf6 could not be detected due to another time point (24 h). For both IPs, either pulling down Apobec3A via its V5 tag and staining for E4orf6

(Figure 19A) or pulling down E4orf6 and staining for Apobec3A-V5 (Figure 19B), no signal was detected, indicating that E4orf6 and Apobec3A do not interact.

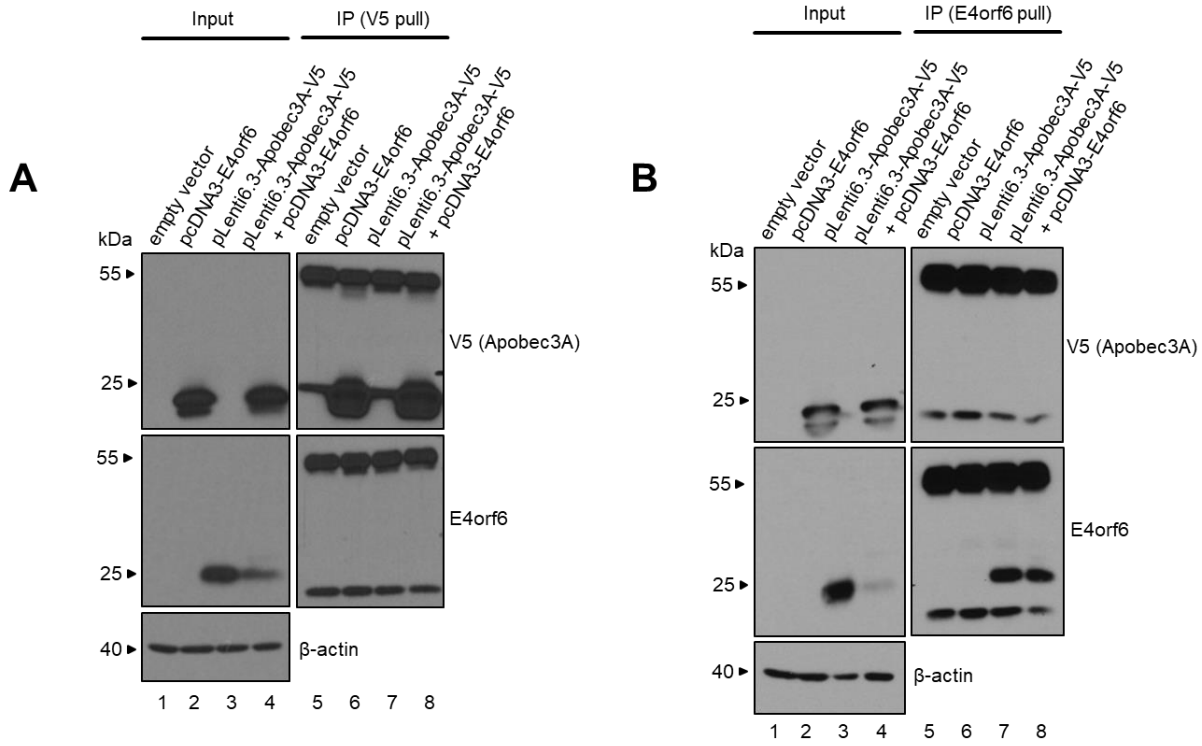

Figure 19: E4orf6 and Apobec3A do not interact.
(A) H1299 cells were transfected with 5 µg pLenti6.3-Apobec3A-V5 and E4orf6 and harvested after 24 h. After performing cell lysates as well as co-immunoprecipitation pulling down Apobec3A via its V5 tag, proteins were separated via SDS-PAGE and subjected to western blot analysis using the antibodies V5 (Apobec3A), E4orf6 and β-actin as a loading control. Stained proteins are indicated on the right, molecular weights in kDa on the left. (B) H1299 cells were transfected with 5 µg pLenti6.3-Apobec3A-V5 and E4orf6 and harvested after 24 h. After performing cell lysates as well as co-immunoprecipitation pulling down E4orf6, proteins were separated via SDS-PAGE and subjected to western blot analysis using the antibodies V5 (Apobec3A), E4orf6 and actin as a loading control. Stained proteins are indicated on the right, molecular weights in kDa on the left. The depicted blots represent the result of several repetitions.

4.1.10. Apobec3A upregulation during HAdV infection is independent of the host proteasome

Human papillomaviruses are known to be restricted by Apobec3A [108]. However, like HAdV, high-risk HPVs induce Apobec3A expression levels, which is mediated by the HPV E7 protein that inhibits cullin 2-dependent degradation processes [107]. Consequently, the question arose, if the proteasome is involved in HAdV-mediated stabilization of Apobec3A. To address this question, the chemical compound MG132 was applied, which is a known inhibitor of the 26S proteasome [152]. HepaRG cells as well as H1299 cells were transfected with pLenti6.3-Apobec3A-V5 followed by infection with HAdV wt (MOI 50). The cells were treated with 10 µM MG132 8 h before harvesting followed by western blot analysis. HepaRG cells, which express endogenous p53 levels, still upregulate Apobec3A during HAdV infection upon MG132 treatment. E2A staining was used for infection control, whereas p53

served as a control for MG132 inhibition of the proteasome (Figure 20A). The slight decrease of Apobec3A expression levels with and without adenoviral infection upon MG132 treatment (Figure 20A, lane 2 and 4), however, can be explained by the already observed reduction of Apobec3A protein levels by p53 (Figure 15), which is stabilized upon proteasome inhibition. This decrease was not observed for H1299 cells, treated with the same conditions (Figure 20B, lanes 2 and 4), which lack endogenous p53 levels and thereby cannot degrade Apobec3A protein levels [176]. In conclusion, Apobec3A upregulation during HAdV infection does not involve the proteasome, since Apobec3A upregulation during HAdV infection was not altered upon MG132 treatment of H1299 cells (Figure 20B).

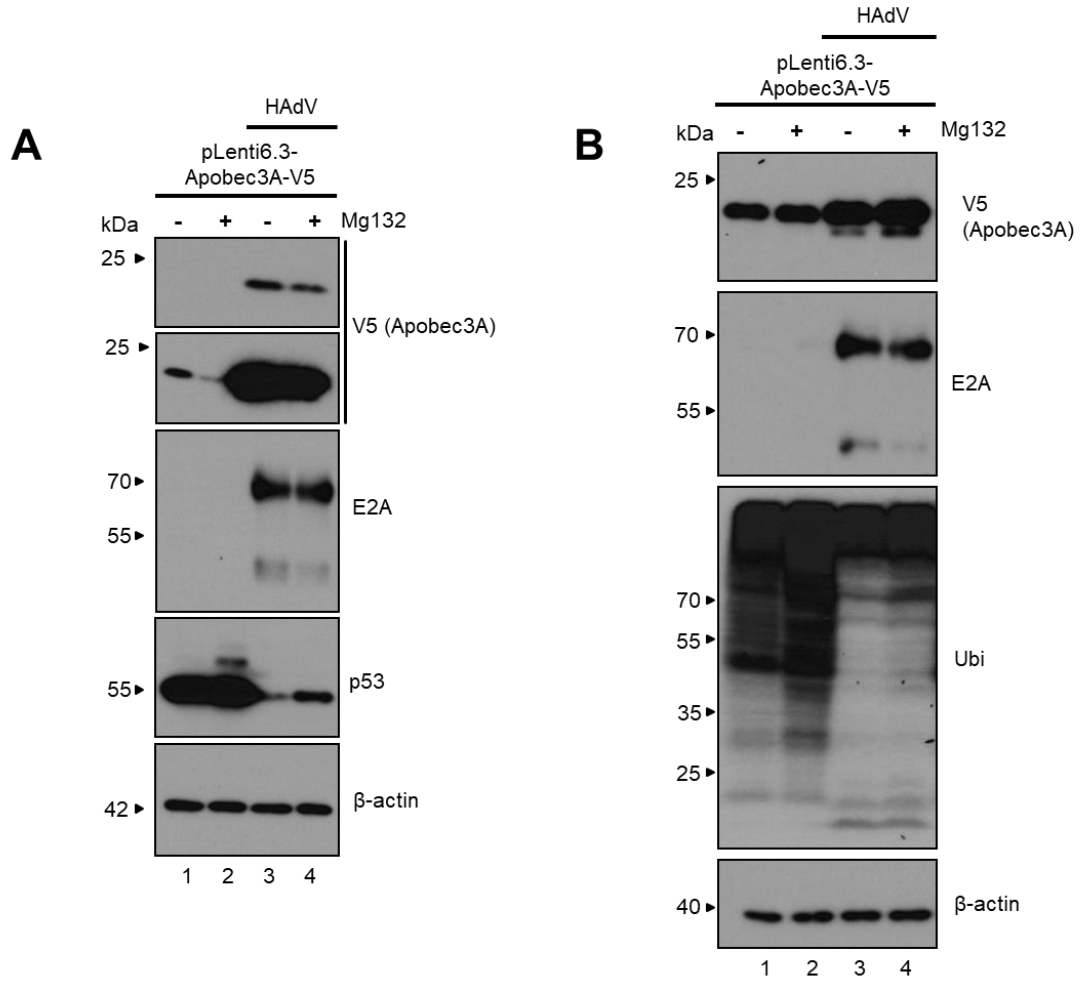

Figure 20: The proteasome is not involved in Apobec3A upregulation during HAdV infection.
(A) HepaRG cells were transfected with 5 µg pLenti6.3-Apobec3A-V5 and infected with HAdV wt using a MOI of 50. 8 h before harvesting (48 h post infection), the cells were treated with 10 µM MG132. Following preparation of whole-cell lysates, the proteins were separated by SDS-PAGE and subjected to western blot analysis using antibodies for V5 (Apobec3A), E2A as an infection control, p53 as MG132 treatment control and β-actin as a loading control. Stained proteins are indicated on the right, molecular weights in kDa on the left. (B) H1299 cells were transfected with 5 µg pLenti6.3-Apobec3A-V5 and infected with HAdV wt using a MOI of 50. 8 h before harvesting (48 h post infection), the cells were treated with 10 µM MG132. Following preparation of whole-cell lysates, the proteins were separated by SDS-PAGE and subjected to western blot analysis using antibodies for V5 (Apobec3A), E2A as an infection control, Ubiquitin as MG132 treatment control and β-actin as a loading control. Stained proteins are indicated on the right, molecular weights in kDa on the left. The depicted blots represent the result of several repetitions.

Taken together, the results of this study suggest that Apobec3A mRNA levels as well as protein levels are increased during HAdV infection (4.1.1, 4.1.3). Furthermore, Apobec3A is not targeted by the viral E3 ubiquitin ligase complex and several factors seem to be involved in Apobec3A upregulation during HAdV infection (4.1.2). E1A was shown to be not involved, whereas E1B-55K, p53 as well as E4orf6 seem to influence Apobec3A stabilization (4.1.4, 4.1.5, 4.1.6, 4.1.7).

4.2. HAdV infection is restricted by Apobec3A

Apobec3A was shown to restrict a variety of different viruses including HIV-1, HBV, HTLV-1, parvoviruses and HPV [98, 103, 105, 108, 114]. In most of these cases, Apobec3A is known to inhibit via its deaminase activity. However, some viruses, such as parvoviruses, are restricted by Apobec3A in a deaminase-independent manner via a so far unknown mechanism [105]. Until now, it was not known if HAdV are restricted by Apobec3A. One study suggested HAdV to be not targeted by any Apobec3 protein, without showing the corresponding data [104]. Hence, Chen and colleagues assumed a requirement for single stranded DNA, which can be targeted by Apobec proteins [104]. However, double stranded DNA viruses like HPVs, are also restricted by Apobec3A, shown in later studies, which could be explained by Apobec3A deamination during replication processes [108, 201]. Since it was shown that HAdV affects Apobec3A expression (4.1), the influence of Apobec3A expression on HAdV infection was investigated in the next experiments.

4.2.1. Apobec3A decreases HAdV DNA levels

To analyze, whether Apobec3A influences HAdV infection, its effect on adenoviral DNA levels was examined in initial experiments. Therefore, HepaRG-TR-Apobec3A cells were induced with tetracycline to express Apobec3A, followed by infection with HAdV wt using a MOI of 50. Apobec3A expression decreased adenoviral DNA levels, which were reduced to approximately one half for E1B-55K and E4orf6 (Figure 21, lanes 3 and 4). As expected, no differences were observed for the 18S DNA, which was used as a control (Figure 21).

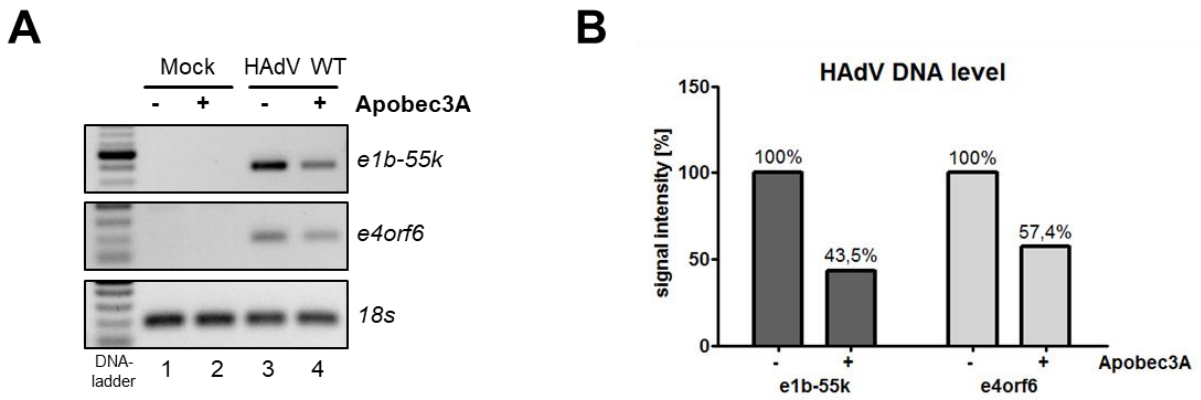

Figure 21: Apobec3A decreases adenoviral DNA levels.
(A) HepaRG-TR-Apobec3A cells were induced with 5 µg/ml tetracycline for Apobec3A expression and infected 24 h later with HAdV wt at a MOI of 50. 24 h post infection, the cells were harvested and lysates were performed of which 10 µg were digested with 10 µl proteinase K. PCR analysis was carried out, using primers for E1B-55K and E4orf6. The DNA for 18s was used as a control. The obtained PCR results were analyzed on an agarose gel. The depicted agarose gels represent the result of several repetitions. (B) Signal intensities of the agarose gel results were calculated using the *ImageJ* program.

4.2.2. HAdV RNA levels are reduced by Apobec3A expression

Since adenoviral DNA was decreased by Apobec3A expression (4.2.1), the next step was, to analyze the influence of Apobec3A on adenoviral mRNA levels. HepaRG-TR-Apobec3A cells were induced with tetracycline for Apobec3A expression and infected with HAdV wt (MOI 50). After the isolation of mRNA and reverse transcription of cDNA, the samples were analyzed by qPCR. Apobec3A mRNA served as a control for tetracycline induction, which was induced upon tetracycline treatment. Furthermore, the early adenoviral mRNAs E1A and E4orf6, as well as the late adenoviral mRNA Hexon were investigated using appropriate primers (see Table 5). Apobec3A expression decreased these viral mRNAs, which were calculated in relation to the 18S mRNA control (Figure 22).

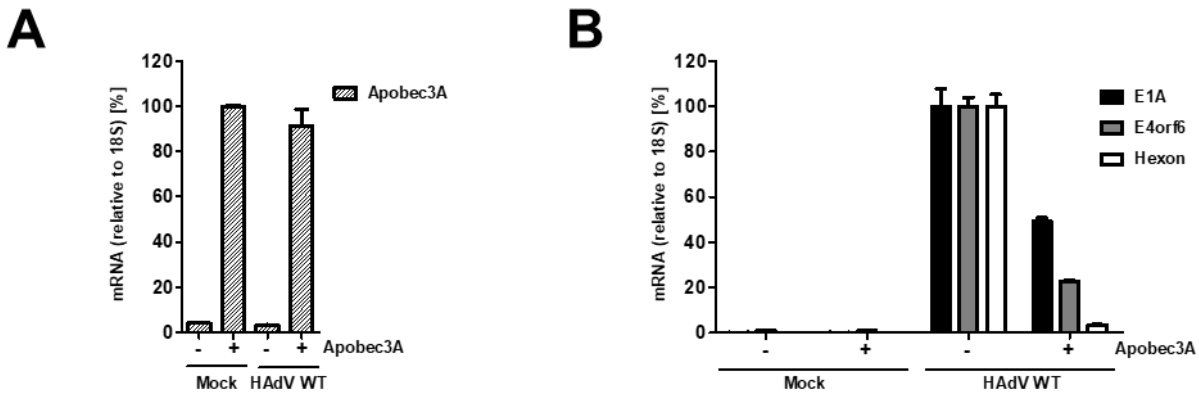

Figure 22: Apobec3A expression reduces adenoviral mRNA levels.
HepaRG-TR-Apobec3A cells were induced with 5 µg/ml tetracycline to express Apobec3A and infected after 24 h with HAdV (MOI 50). 24 h post infection, the cells were harvested, mRNA was isolated and cDNA reverse transcribed, followed by qPCR analysis. (A) Primers to investigate Apobec3A mRNA were used, which served as a tetracycline induction control. 18S mRNA was used as a control and signals calculated in relation to it. (B) Primers for the early adenoviral mRNAs E1A and E4orf6 as well as the late mRNA Hexon were used. 18S mRNA was used as a control and signals calculated in relation to it.

To investigate, if these changes in adenoviral mRNA levels by Apobec3A are due to altered adenoviral promoter activities, luciferase assays were carried out. Therefore, H1299 cells were co-transfected with pLenti6.3-Apobec3A-V5 and the viral promoters E1A, E2E and MLP with a luciferase gene. After harvesting the cells, a luciferase assay was performed, which was measured using a *tecan* reader. Apobec3A expression decreased the activity of the adenoviral promoters approximately two-fold (Figure 23A). Furthermore, HepaRG-TR-Apobec3A cells that were induced with tetracycline for Apobec3A expression and transfected with the adenoviral promoters E1A, E2E and MLP, also showed decreased adenoviral promoter levels up to a two-fold reduction by Apobec3A expression in the luciferase assay (Figure 23B).

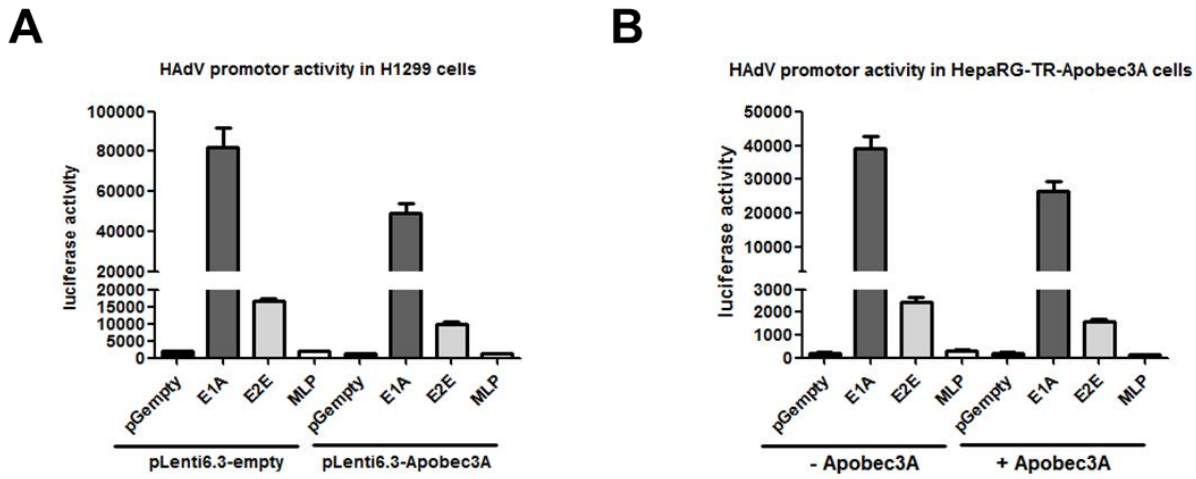

Figure 23: The adenoviral promoters E1A, E2E and MLP are reduced by Apobec3A expression.
(A) H1299 cells were co-transfected with 0.5 µg pLenti6.3-Apobec3A-V5 and 0.5 µg renilla, as well as 1 µg of the adenoviral promoters E1A, E2E and MLP. 24 h post transfection, the cells were harvested following a luciferase assay which was measured in a *tecan* reader. It was not calculated in relation to the renilla control in this experiment, due to Apobec3A influence on renilla levels. (B) HepaRG-TR-Apobec3A-V5 cells were induced with 5 µg/ml tetracycline to express Apobec3A. Following transfection of 0.5 µg renilla and 1 µg of the adenoviral promoters E1A, E2E and MLP, the cells were harvested 24 h post transfection and a luciferase assay was performed which was measured in a *tecan* reader. It was not calculated in relation to the renilla control in this experiment, due to Apobec3A influence on renilla levels.

4.2.3. Apobec3A expression decreases HAdV protein levels

Since Apobec3A was able to decrease adenoviral DNA and RNA levels (4.2.1, 4.2.2), an effect of Apobec3A on adenoviral protein levels was supposed. HepaRG-TR-Apobec3A cells were induced with tetracycline for Apobec3A expression and infected with HAdV wt using a MOI of 50. Western blot analysis showed that Apobec3A expression leads to a reduction of adenoviral protein levels (Figure 24). For E1A and E2A, only minor reductions in protein levels were detected (Figure 24A, lanes 5 and 6), whereas E1B-55K and E4orf6 showed a stronger decrease in protein expression (Figure 24A, lanes 5 and 6). Interestingly, late viral proteins were most predominantly affected, such as capsid, pVI and pVII (Figure 24A, lanes 5 and 6), showing reductions in protein levels to 20% and below (Figure 24B). HepaRG-TR

cells were used as a control to ensure that tetracycline induction does not influence adenoviral protein levels. The *ImageJ* program was used to calculate the signal intensities obtained in western blot analysis (Figure 24B).

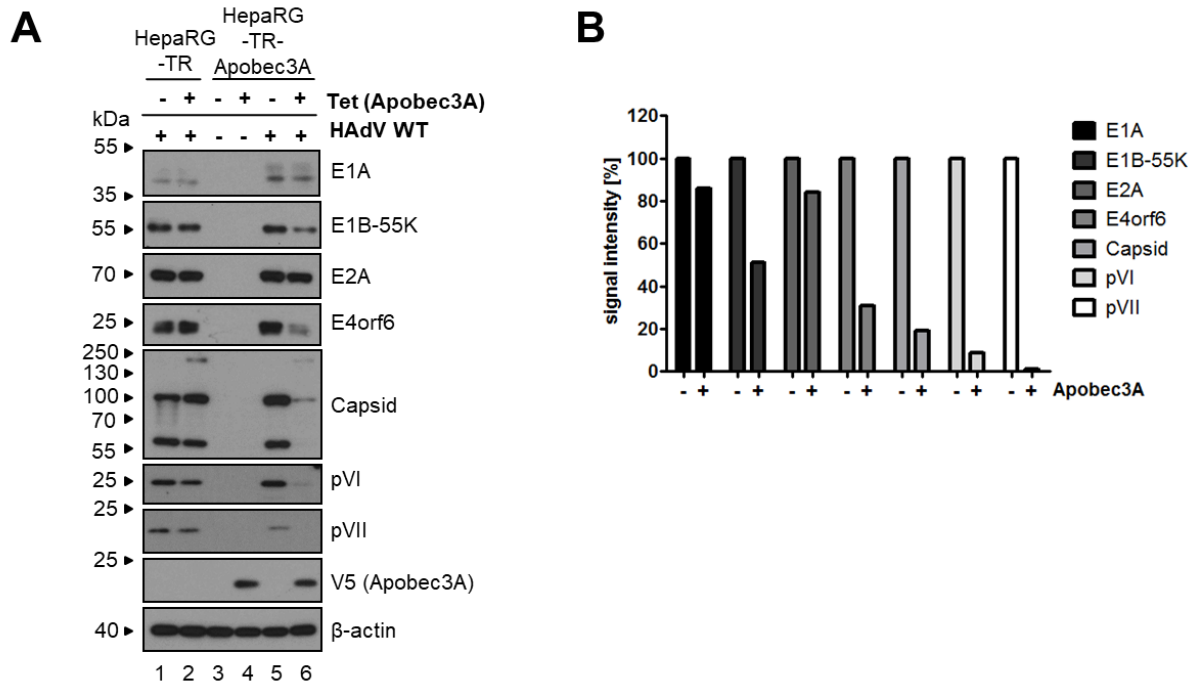

Figure 24: Apobec3A decreases adenoviral protein levels.
(A) HepaRG-TR and HepaRG-TR-Apobec3A cells were induced with 5 µg/ml tetracycline. 24 h later, it was infected with HAdV wt using a MOI of 50. Cells were harvested 24 h post infection, cell lysates prepared, proteins separated via SDS-PAGE and subjected to western blot analysis using antibodies for E1A, E1B-55K, E2A, E4orf6, Capsid, pVI, pVII, V5 (Apobec3A) serving as a tetracycline-induction control and β-actin as a loading control. Stained proteins are indicated on the right, molecular weights in kDa on the left. The depicted blots represent the result of several repetitions. (B) Signal intensities were calculated with the *ImageJ* program.

4.2.4. Adenoviral progeny production is reduced by Apobec3A

Further experiments were performed, to examine the influence of Apobec3A expression on adenoviral progeny production. Therefore, HepaRG-TR-Apobec3A cells were induced with tetracycline to express Apobec3A and infected with HAdV wt at a MOI of 50. The cells were harvested, resuspended in DMEM without supplements and the virus isolated by performing three freeze and thaw steps. Following reinfection of HEK293 cells with different virus dilutions, the cells were fixed with methanol after 24 h and stained with the E2A antibody B6-8. The cells were analyzed with an *Axiovert 200 M* microscope (Zeiss) and infected, luminous cells counted several times. The mean of these counts as well as the dilution factors and microscopic magnifications were used to calculate viral progeny production. Apobec3A significantly reduced adenoviral progeny production approximately 9-fold (Figure 25C), which could be already observed by eye, looking through the microscope (Figure 25A).

Tetracycline-induced Apobec3A expression was proven by western blot analysis (Figure 25B, lanes 2, 4 and 6).

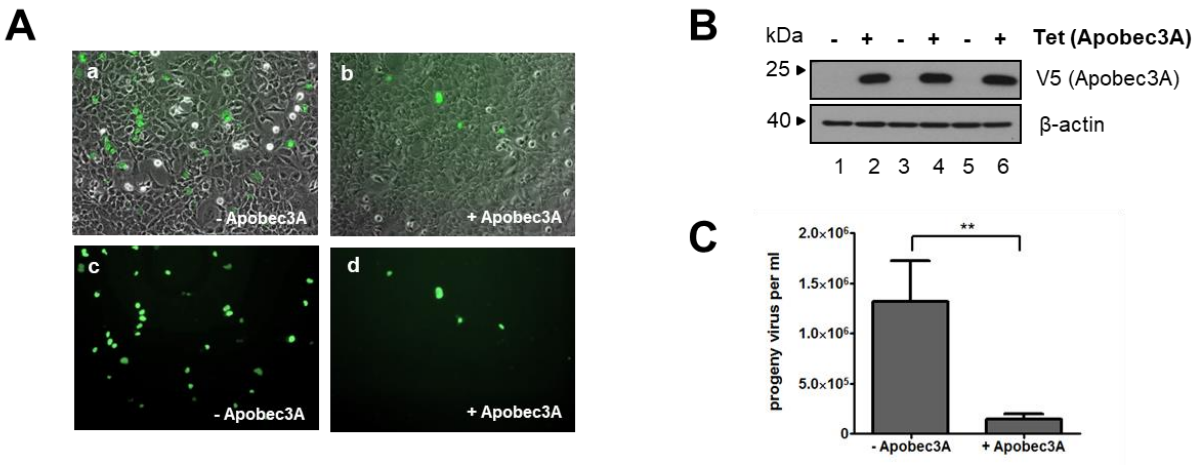

Figure 25: Apobec3A decreases adenoviral progeny production.
HepaRG-TR-Apobec3A cells were induced with 5 µg/ml tetracycline for Apobec3A expression and infected 24 h later with HAdV wt (MOI 50). 24 h post infection, the cells were harvested, resuspended in DMEM without supplements and the virus was isolated by three freeze (liquid nitrogen) and thaw (37°C, water bath) cycles. 293 cells were reinfected with different virus dilutions and fixed with methanol after 24 h. Immunostainings with E2A were performed and viral progeny production analyzed with an *Axiovert 200 M* microscope. (A) Microscopic images (10 x magnification) of cells without Apobec3A expression (a, c) and cells with Apobec3A expression (b, d). (B) One part of the cells was separated for western blot analysis, to confirm tetracycline-induction of Apobec3A. The antibodies V5 (Apobec3A) as well as β-actin as a loading control were used. (C) Adenoviral progeny virus production was calculated by the mean of several counts of different visual fields, considering the dilution factor and microscope magnifications. Statistical analysis was performed using an unpaired t-test.

Taken together, Apobec3A expression was shown to reduce adenoviral DNA-, RNA and protein levels as well as progeny virus production (4.2.1 - 4.2.4). Hence, Apobec3A represents a novel restriction factor antagonizing efficient HAdV replication.

4.2.5. HAdV replication center formation is impaired by Apobec3A expression

Endogenous Apobec3A localizes to the cytoplasm, where it does not exhibit cytotoxic functions [118]. However, endogenous Apobec3A translocates to the nucleus for antiviral defense of the cell, and overexpressed Apobec3A localizes throughout the whole cell [103, 118]. Apobec3A function seems to be strictly regulated by its localization to prevent deamination of genomic DNA [118]. Since it was shown that upregulated Apobec3A restricts HAdV during infection (4.1, 4.2), it was expected that cellular localization of Apobec3A might be influenced by adenoviral infection. Therefore, Apobec3A expression was induced in HepaRG-TR-Apobec3A cells, which were additionally infected with HAdV wt (MOI 50) (Figure 26A). Furthermore, HepaRG cells were transfected with pLenti6.3-Apobec3A-V5 and infected with HAdV wt (MOI 50) (Figure 26B) and subjected to immunofluorescence analysis. Confirming published data, Apobec3A localized throughout the whole cell [118] and E2A marked the adenoviral replication centers [70], which were decreased in number as well as in size upon Apobec3A expression (Figure 26A, C). To validate the visual results statistically, a

substantial number of cells was calculated concerning replication center numbers and sizes. Thereby, Apobec3A significantly reduced adenoviral replication center number and sizes in both experiments (Figure 26B, D). In conclusion, Apobec3A impairs the proper establishment of adenoviral replication centers marked by the viral protein E2A.

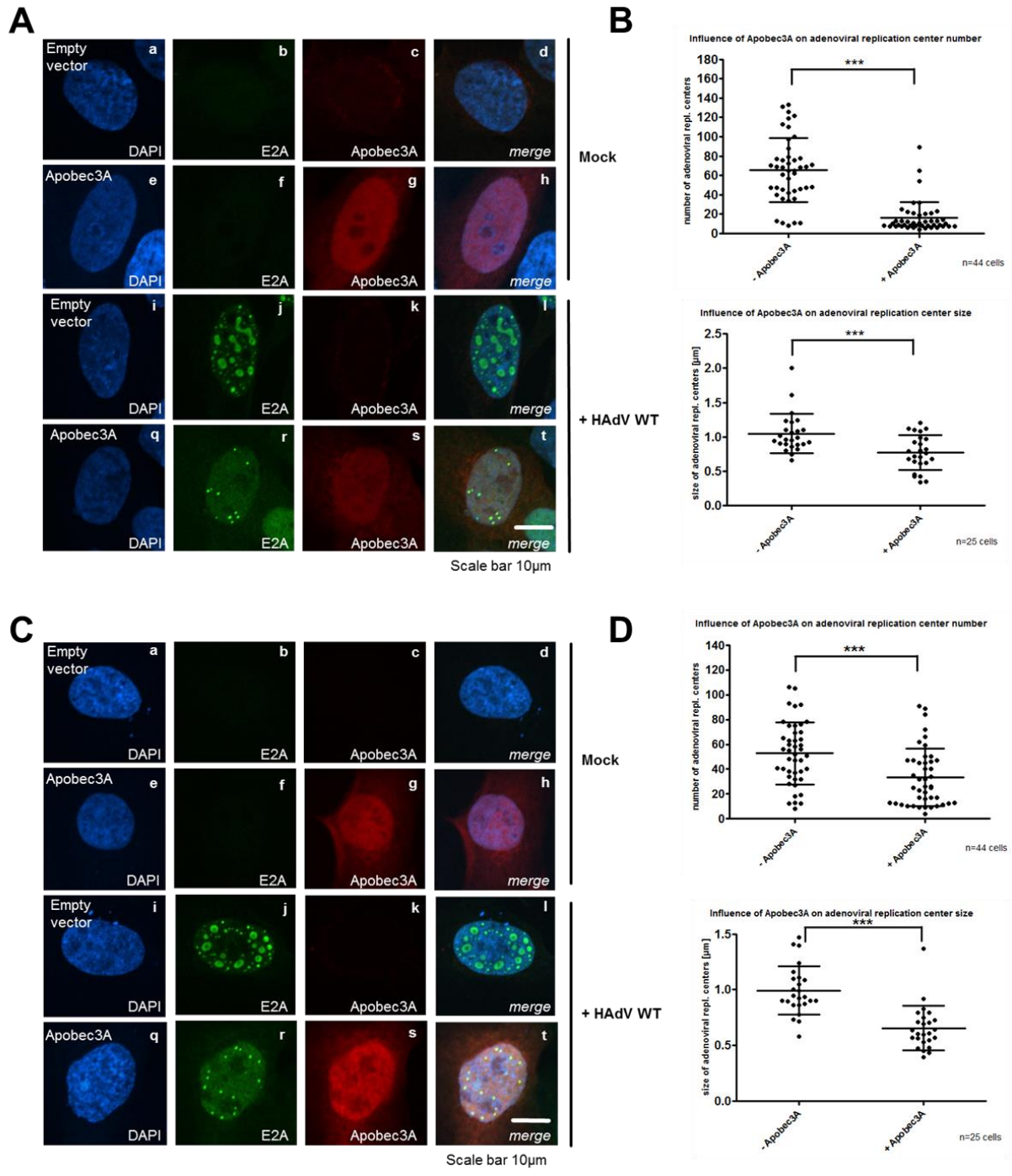

Figure 26: Apobec3A interferes with the proper establishment of adenoviral replication centers.
(A) HepaRG-TR-Apobec3A cells were induced with 5 µg/ml tetracycline for Apobec3A expression and infected with HAdV wt (MOI 50). The cells were harvested 24 h post infection and subjected to immunofluorescence analysis, using DAPI shown in blue (405 nm) and antibodies for V5 (Apobec3A) shown in red (647 nm), as well as E2A shown in green (488 nm). (B) For 44 and 25 cells, the number and sizes of adenoviral replication centers were investigated respectively, and statistical significances calculated using an unpaired t-test ($p < 0.001$).

(C) HepaRG cells were transfected with 5 µg pLenti6.3-Apobec3A-V5 and infected with HAdV wt (MOI 50). The cells were harvested 24 h post infection and subjected to immunofluorescence analysis, using DAPI shown in blue (405 nm) and antibodies for V5 (Apobec3A) shown in red (647 nm), as well as E2A shown in green (488 nm). (D) For 44 and 25 cells, the number and sizes of adenoviral replication centers were determined respectively, and statistical significances calculated using an unpaired t-test ($p < 0.001$).

4.2.6. E2A SUMOylation is reduced by Apobec3A expression

Unpublished data of our working group indicate that E2A is SUMO modified, being essential for several functions of E2A ([202], manuscript submitted). Hence, it was interesting, whether SUMOylation of E2A is affected by Apobec3A, which could lead to the impaired establishment of adenoviral replication centers upon Apobec3A expression observed in earlier experiments (4.2.5). To address this, experiments were performed to investigate E2A SUMOylation as well as ubiquitinylation upon Apobec3A expression. Therefore, HeLa-SUMO2 cells were co-transfected with pLenti6.3-Apobec3A-V5 and E2A-GFP and a Ni-NTA assay was performed (Figure 27A). The obtained results showed that Apobec3A expression leads to a reduction of E2A SUMOylation (Figure 27A, lanes 6 and 8). Additionally, HepaRG-SUMO2 cells were transfected with pLenti6.3-Apobec3A-V5 and infected with HAdV wt (MOI 50) (Figure 27B). E2A SUMOylation was decreased by Apobec3A (Figure 27B, lanes 7 and 8), confirming the results of the experiment shown in A (Figure 27A). Finally, to investigate if E2A ubiquitinylation is also affected by Apobec3A expression, H1299 cells were transfected with the plasmids pLenti6.3-Apobec3A-V5 and 6xHis-ubiquitin, followed by HAdV wt infection using a MOI of 50 (Figure 27C). The Ni-NTA assay showed, however, that ubiquitin modification of E2A is not influenced by Apobec3A expression (Figure 27C, lanes 7 and 8). Taken together, Apobec3A expression decreased E2A SUMOylation, but did not affect E2A ubiquitinylation.

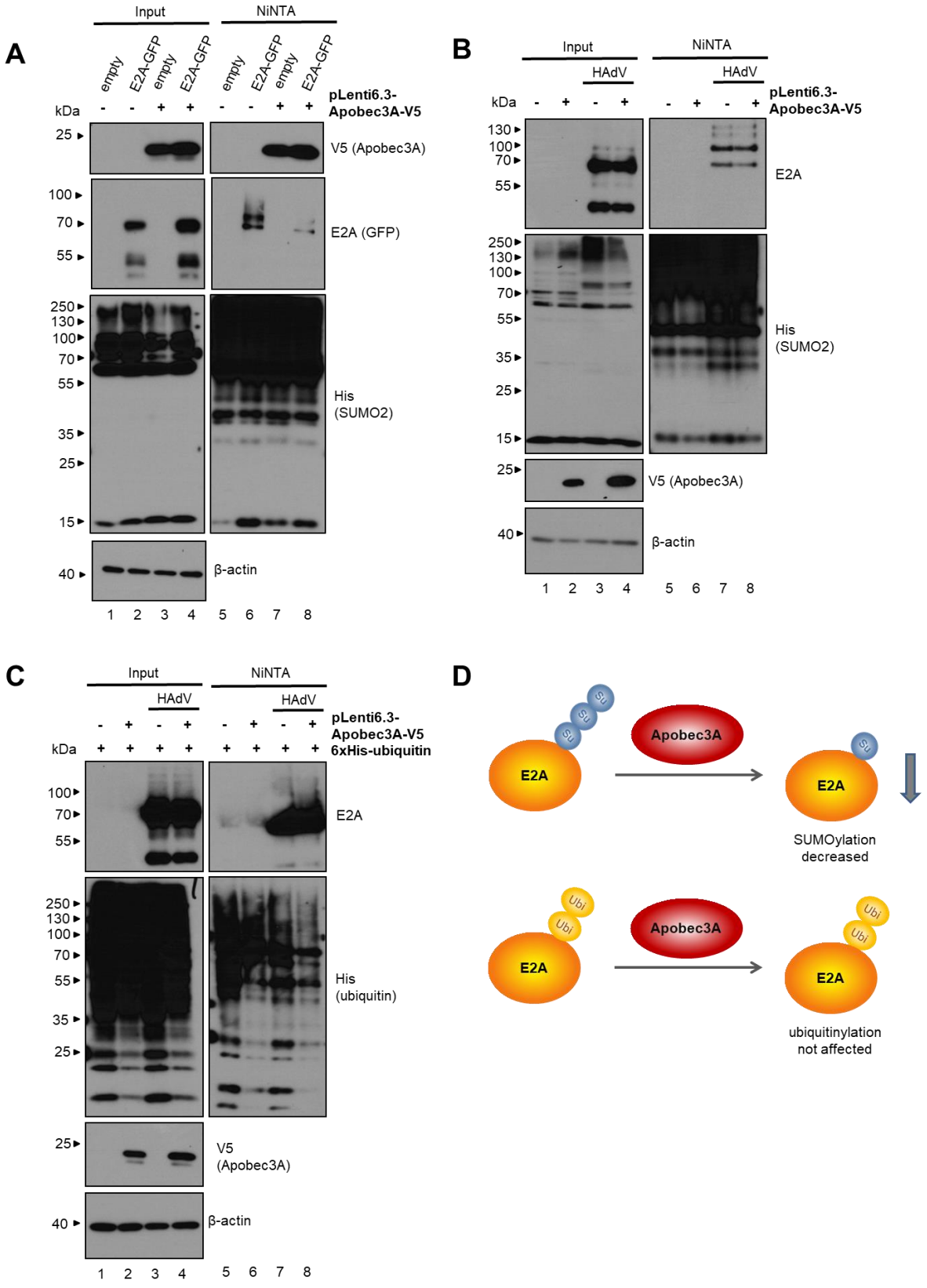

Figure 27: Apobec3A reduces E2A SUMOylation but does not affect E2A ubiquitinylation.
(A) HeLa-S2 cells were transfected with 5 µg of pLenti6.3-Apobec3A-V5 and E2A-GFP. 24 h post transfection, the cells were harvested and a Ni-NTA assay as well as cell lysates were performed. The proteins were separated via SDS-PAGE and subjected to western blot analysis using antibodies for V5 (Apobec3A), E2A, 6xHis (SUMO2) and β-actin as a loading control. Stained proteins are indicated on the right, molecular weights in kDa on the left.

(B) HepaRG-S2 cells were transfected with 5 µg of pLenti6.3-Apobec3A-V5 and infected with HAdV wt (MOI 50). 48 h post infection, the cells were harvested and a Ni-NTA assay as well as cell lysates were performed. The proteins were separated via SDS-PAGE and subjected to western blot analysis using antibodies for V5 (Apobec3A), E2A, 6xHis (SUMO2) and β-actin as a loading control. Stained proteins are indicated on the right, molecular weights in kDa on the left. (C) H1299 cells were transfected with 5 µg of pLenti6.3-Apobec3A-V5 and 10 µg 6xHis-ubiquitin, followed by an infection with HAdV wt (MOI 50). 48 h post infection, the cells were harvested and a Ni-NTA assay as well as cell lysates were performed. The proteins were separated via SDS-PAGE and subjected to western blot analysis using antibodies for V5 (Apobec3A), E2A, 6xHis (ubiquitin) and β-actin as a loading control. Stained proteins are indicated on the right, molecular weights in kDa on the left. The depicted blots represent the result of several repetitions. (D) Schematic representation of Apobec3A influence on E2A SUMO and ubiquitin modification.

4.2.7. The deaminase activity of Apobec3A is crucial for HAdV restriction

For the restriction of many viruses, including HBV and HPV, the deaminase activity of Apobec3A is required [103, 108]. Since it was found that Apobec3A is also able to restrict via a so far unknown deaminase-independent mechanism, like it was shown for parvoviruses, it was interesting to investigate the involvement of the deaminase activity for HAdV restriction by Apobec3A [105]. Therefore, potential deamination processes were investigated by performing a differential DNA denaturation PCR (3D-PCR) [203]. Deamination results in DNA fragments containing a higher amount of A-T basepairing, which only share two hydrogen bonds and are therefore already denatured at lower temperatures. Consequently, appearing bands in lower denaturing temperatures, which are not present in the controls, confirm deamination processes. For 3D-PCR analyses, HepaRG-TR-UGI cells were induced via tetracycline to express the Uracil-N-glycosylase inhibitor (UGI), which impedes already explained downstream processes following deamination (1.2), thereby stabilizing deamination processes. Additionally, the cells were transfected with pLenti6.3-Apobec3A-V5 and infected with HAdV wt (MOI 50). 72 h post infection, the cells were harvested and subjected to PCR analysis, investigating Apobec3A deamination of a favoured target region in the Hexon amplicon. Upcoming bands during lower denaturing temperatures for the sample induced for UGI and transfected with pLenti6.3-Apobec3A-V5 as well as infected with HAdV, indicated deamination of the Hexon amplicon by Apobec3A (Figure 28A). Western blot analysis confirmed Apobec3A induction as well as adenoviral infection (Figure 28B). The indicated amplicons in Figure 28A (lanes 3, 4 and 8) were isolated, sequenced and the results aligned and compared with the Hexon wild type sequence. A lot of G to A transitions were observed in the Hexon amplicons deaminated by Apobec3A, suggesting minus-strand deamination (Figure 28C). In conclusion, it was found that Apobec3A restricts HAdV via a deaminase-dependent mechanism, assuming preferential deamination of the minus-strand DNA.

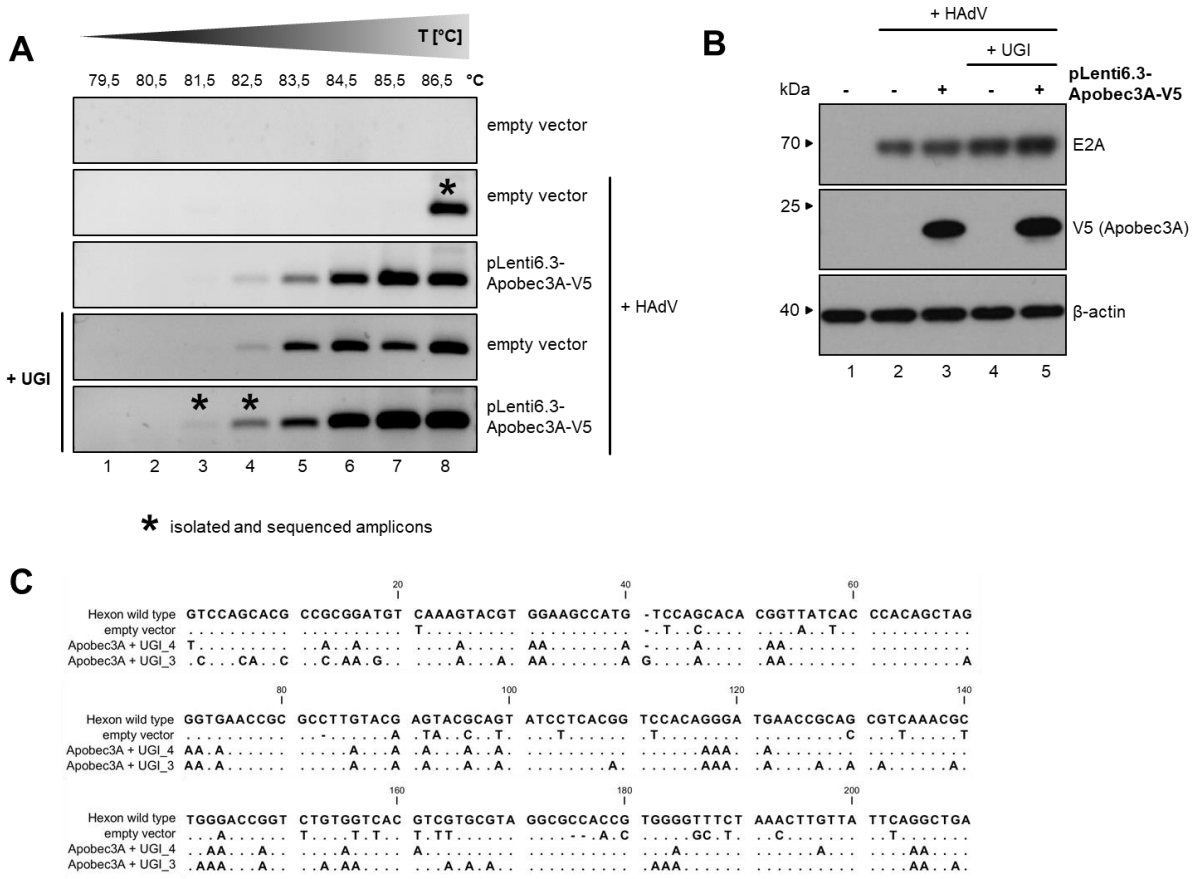

Figure 28: Apobec3A uses its deaminase activity to restrict HAdV.
HepaRG-TR-UGI cells were induced with 5 µg/ml tetracycline for UGI expression and transfected with 5 µg pLenti6.3-Apobec3A-V5, followed by an infection with HAdV wt (MOI 50). 72 h post infection, the cells were harvested using the *NucleoSpin® Tissue Kit* (Machery Nagel) and subjected to 3D-PCR analysis, using primers for an Apobec3A favoured region in the Hexon amplicon as well as denaturing temperatures ranging from 79.5 – 86.5°C. (A) 3D-PCR results were analyzed on a 1% agarose gel. (B) One part of the samples was subjected to western blot analysis using the antibodies for E2A as an infection control, V5 (Apobec3A) as an induction control, as well as β-actin as a loading control. Stained proteins are indicated on the right, molecular weights in kDa on the left. (C) The indicated amplicons in A were isolated, sequenced and aligned and compared to the wild type sequence of Hexon using the *CLC workbench* (QIAGEN).

As a control for adequate assay functionality, 3D-PCR analysis was performed for the HBV cccDNA, a known target for Apobec3A deamination [103]. HepaRG-TR-UGI cells were induced with tetracycline for UGI expression and co-transfected with pLenti6.3-Apobec3A-V5 and the pHBV1.1 plasmid, encoding the viral pgRNA, which establishes HBV infection. After harvesting and DNA extraction, 3D-PCR analysis was performed using primers for the cccDNA amplicon, as well as different denaturing temperatures, ranging from 83-89°C. The results were analyzed on an agarose gel, and confirmed cccDNA deamination by Apobec3A (Figure 29A). Isolation and sequencing of the indicated amplicons in Figure 29A (lanes 2, 3 and 8) and following alignment as well as comparison to the cccDNA wild type sequence confirmed C to T as well as G to A transitions (Figure 29B).

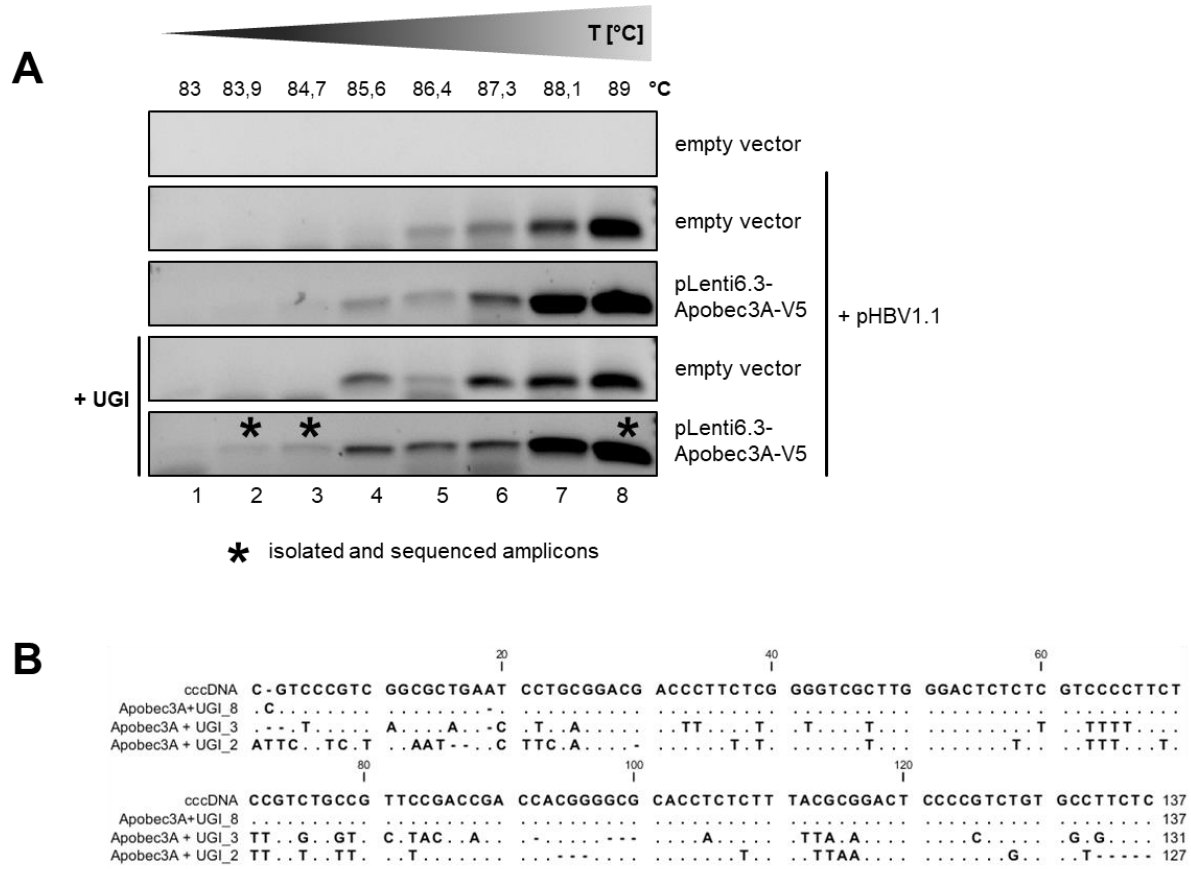

Figure 29: Apobec3A deaminates the HBV cccDNA, thereby leading to its degradation.
HepaRG-TR-UGI cells were induced with 5 µg/ml tetracycline for UGI expression and co-transfected with 5 µg pLenti6.3-Apobec3A-V5 as well as 10 µg of the pHBV1.1 plasmid, which establishes HBV infection. 72 h post transfection, the cells were harvested with the *NucleoSpin® Tissue* Kit (Machery-Nagel) and subjected to 3D-PCR analysis, using cccDNA primers as well as different denaturing temperatures ranging from 83-89°C. (A) 3D-PCR results were analyzed on a 1% agarose gel. (B) The indicated amplicons in A were isolated, sequenced, and aligned and compared to the wild type sequence of HBV cccDNA using the *CLC workbench* (QIAGEN).

4.2.8. Influence of E1B-55K and E4orf6 on deamination processes

Since earlier experiments could show that E1B-55K as well as E4orf6 influence Apobec3A expression levels (4.1.6, 4.1.7), it was interesting for us, if these adenoviral early proteins are able to influence deamination of the Hexon amplicon. To address this question, HepaRG cells were infected with HAdV wt, HAdV E1B-55K- and HAdV E4orf6- using a MOI of 50. After harvesting the cells, 3D-PCR analyses were performed using primers for the Hexon amplicon. As shown in Figure 30A, a mutant virus lacking functional E1B-55K was observed to increase deamination, whereas a mutant virus lacking functional E4orf6 decreased deamination in comparison to the wild type. Western blot analysis confirmed infections with mutant viruses. As expected, no E1B-55K signal was detected for the HAdV E1B-55K- virus, and no E4orf6 signal was detected for the HAdV E4orf6- virus (Figure 30B, lanes 3 and 4). From these results, it was concluded that E1B-55K counteracts, whereas E4orf6 promotes editing processes of the virus.

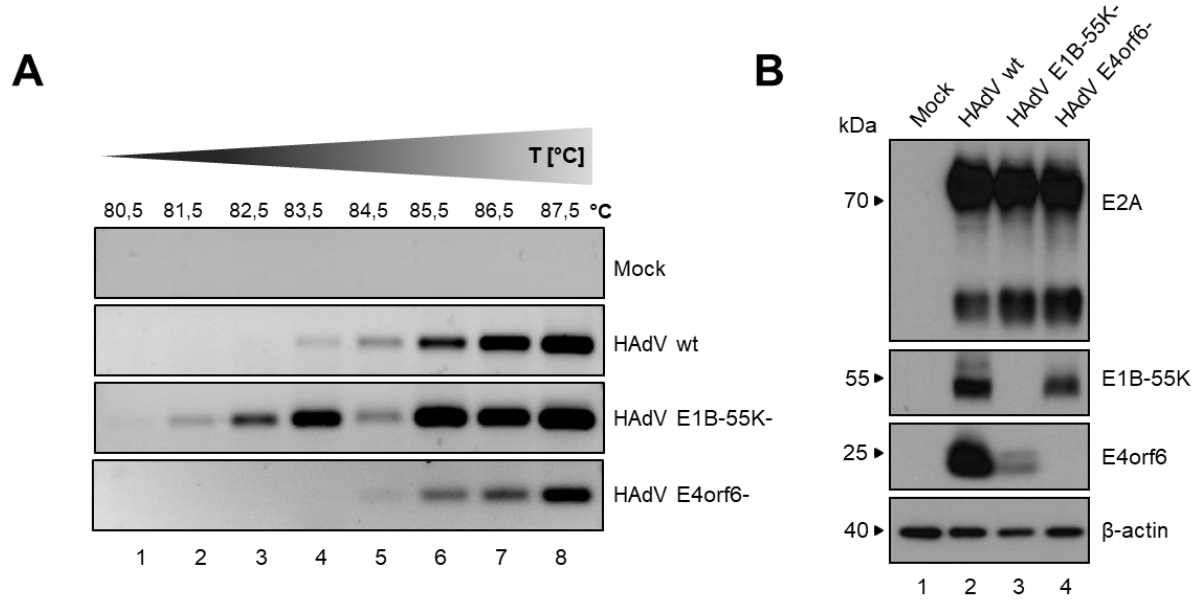

Figure 30: The adenoviral early proteins E1B-55K as well as E4orf6 affect deamination processes.
(A) HepaRG cells were infected with HAdV wt, HAdV E1B-55K- and HAdV E4orf6- at a MOI of 50. 72 h post infection, the cells were harvested using the *NucleoSpin® Tissue* Kit (Machery-Nagel) and subjected to 3D-PCR analysis using primers for Hexon and different denaturing temperatures ranging from 80.5-87.5°C. (B) One part of the cells was harvested for western blot analysis to confirm the infection with HAdV mutants. Antibodies for E2A, as a titration and MOI control, E1B-55K and E4orf6 as viral mutant controls, as well as β-actin as a loading control, were applied. Stained proteins are indicated on the right, molecular weights in kDa on the left. The depicted agarose gels and blots represent the result of several repetitions.

4.3. HAdV counteraction of Apobec3A restrictive function

4.3.1. HAdV species C evolution resulted in depletion of TC dinucleotides

Several viruses, which are inhibited by Apobec cytidine deaminases, have evolved different strategies to counteract Apobec restrictive functions. HIV, for example, counteracts Apobec deamination via the viral Vif protein, which was shown to interact with the cellular proteins Cul5, elongin B and C as well as Rbx1 to establish a SCF complex, which leads to the ubiquitinylation and degradation of Apobec3G [96]. Furthermore, HTLV-1 was relatively resistant to Apobec3G editing, due to lower levels of Apobec3G packaging into nascent virions. This novel strategy of Apobec3 resistance by exclusion was shown to depend on a unique C-terminal extension of its nucleocapsid protein [204]. Another example are human papillomaviruses, which exhibited highly depleted TC dinucleotides, the main target sequence of several Apobec3 deaminases, in their genomes during HPV evolution [109]. Since HAdVs are restricted by Apobec3A, they also might have evolved towards Apobec3A counteraction mechanisms. The online tool *compseq* (Emboss) was used to investigate the frequency of the different dinucleotides in the adenoviral genome. Thereby, the program calculates the observed versus the expected dinucleotide frequency in a given sequence, while considering the amount of A, T, C and G nucleotides in the sequence. Investigating the genomes of the HAdV species C types 1, 2 and 5 led to the observation that the TC

dinucleotide is indeed less frequent than expected (Figure 31A). Furthermore, the TC dinucleotide is depleted in the mean of all open reading frames (ORFs) of HAdV species C type 5 (Figure 31B). In conclusion, HAdV species C has evolved towards TC dinucleotide depletion, which might counteract Apobec3A restrictive functions.

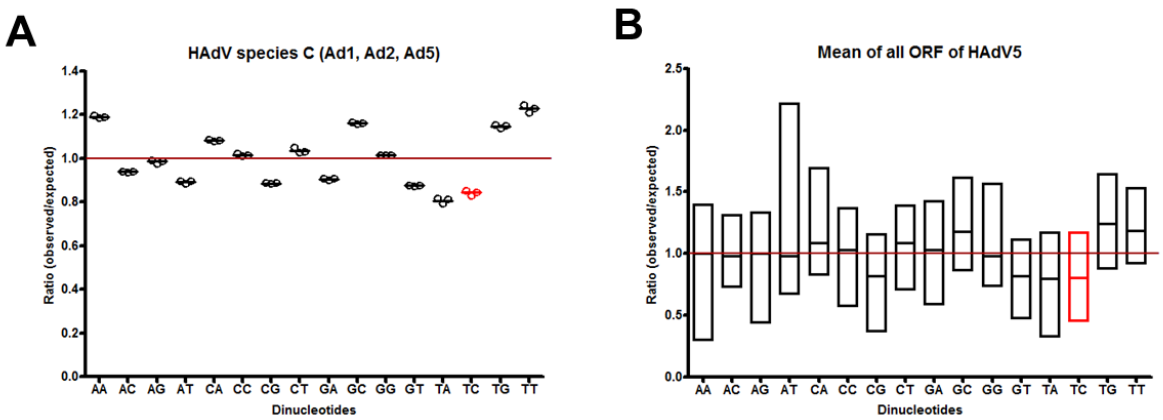

Figure 31: TC dinucleotide depletion during HAdV evolution.
The online tool *compseq* (Emboss) was used to determine the dinucleotide frequencies in the HAdV genome. The program calculates the observed versus the expected frequencies of dinucleotides in a given sequence, taken in account the amount of A, T, C and G nucleotides in the sequence. The sequences were obtained from the nucleotide database of NCBI. (A) The genomes of HAdV species C types 1, 2 and 5 were analyzed. (B) The mean of all ORFs of HAdV type 5 were investigated for their dinucleotide frequencies. The red line indicates, where the observed frequency is exactly like the expected one. Results for the TC dinucleotide, the main target of Apobec3A, are labelled in red.

4.3.2. TC depletion is not conserved among different HAdV species

To investigate, if the TC depletion is specific for HAdV species C or conserved among different HAdV species, the online tool *compseq* (Emboss) was used to determine dinucleotide frequencies in the other HAdV species A, B, D, E, F and G. As depicted in Figure 32, TC dinucleotide depletion was only observed for the HAdV species A, C and F, whereas TC dinucleotides appeared to an expected extent in the genome sequences of HAdV species B, D, E and G. In conclusion, TC dinucleotide depletion is not conserved among different HAdV species.

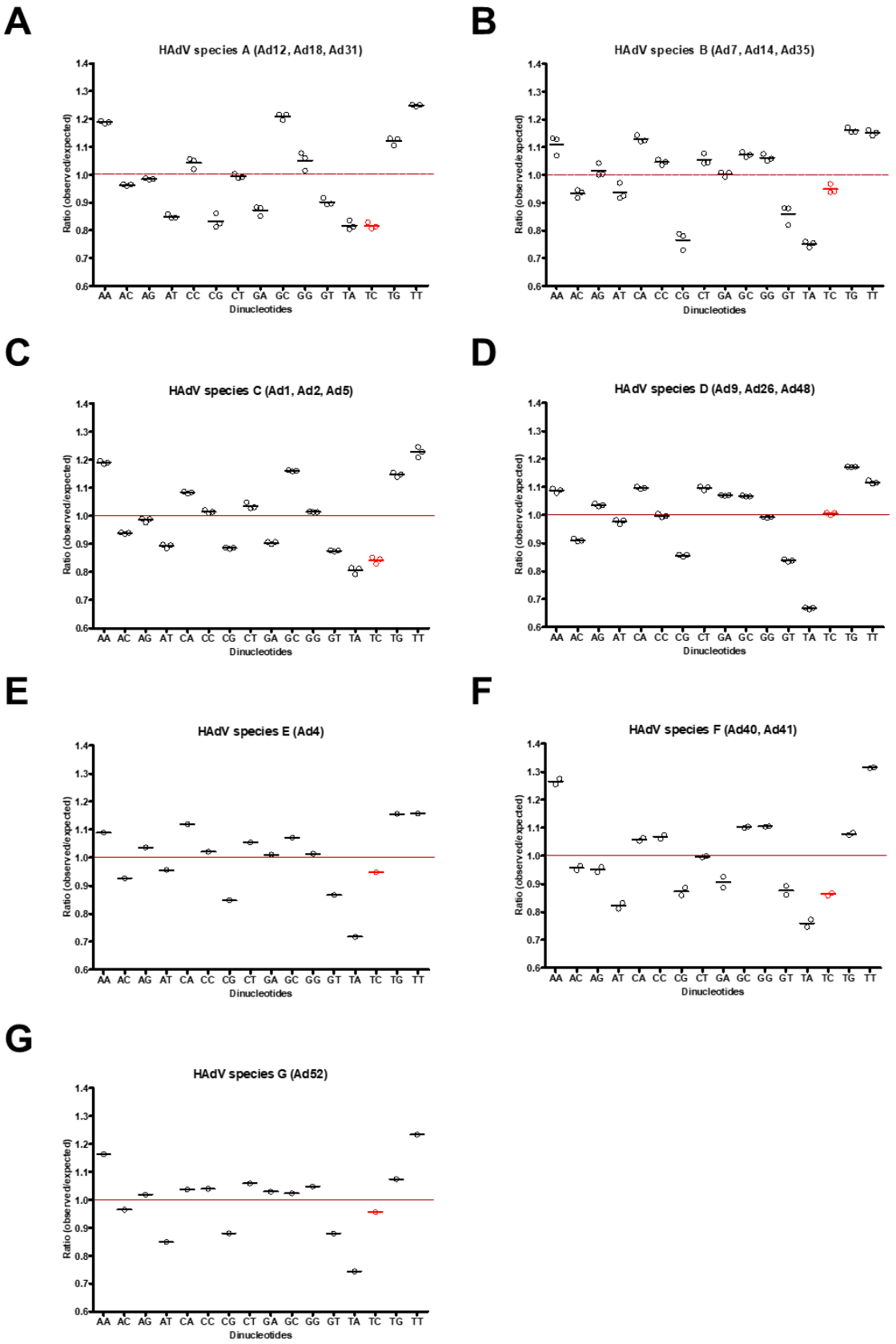

Figure 32: TC depletion is not conserved among different HAdV species.
The online tool *compseq* (Emboss) was used to investigate the dinucleotide frequencies of members of the (A) HAdV species A, (B) HAdV species B, (C) HAdV species C, (D) HAdV species D, (E) HAdV species E, (F) HAdV species F and (G) HAdV species G. The sequences were obtained from the nucleotide database of NCBI. The red line indicates, where the observed frequency is exactly like the expected one. Results for the TC dinucleotide, the preferred target of Apobec3A, are labelled in red.

4.3.3. TC depletion is specific for HAdV biology and does not represent a general viral defense mechanism

HPV genomes as well as HAdV genomes are depleted for TC dinucleotides [109] (4.3.1). Hence, a general mechanism of TC dinucleotide depletion among all different kinds of eukaryotic and viral genomes was assumed to prevent harmful deamination processes. Nevertheless, TC dinucleotide depletion was not observed in the reference genome for *homo sapiens* (GRCh38.p12) (Figure 33A). Furthermore, the HBV genome was also observed to exhibit an expected frequency of TC dinucleotides (Figure 33B). Taken together, TC dinucleotide depletion neither represents a general mechanism nor is conserved among different viruses for defense purposes.

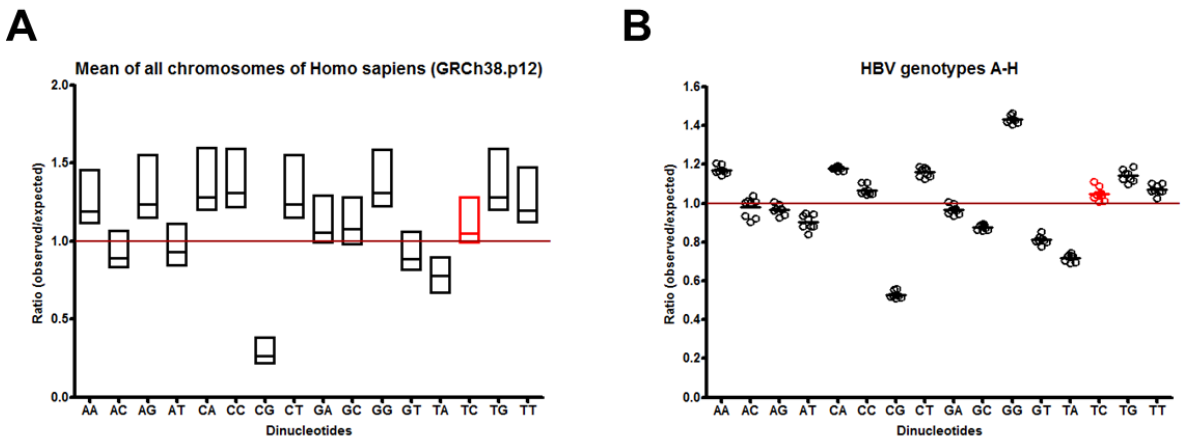

Figure 33: TC dinucleotides exhibit normal frequencies in other sequences.
The online tool *compseq* (Emboss) was used to analyze dinucleotide frequencies in other sequences. The sequences were obtained from the nucleotide database of NCBI. (A) The mean of all chromosomes of the reference genome for homo sapiens (GRCh38.p12) was studied concerning dinucleotide distributions. (B) The HBV genome was investigated for its dinucleotide distributions. The red line indicates, where the observed frequency is exactly like the expected one. Results for the TC dinucleotide, the preferred target of Apobec3A, are labelled in red.

4.4. Role of Apobec3A post-translational modifications during infection

Posttranslational modifications (PTMs) are known to play crucial roles in a variety of different cellular processes including gene transcription, DNA repair, replication and many more [126]. Many studies on PTMs revealed the existence of hundreds of different PTM versions, including ubiquitinylation and SUMOylation, which are frequently observed [128]. There is only limited data on PTMs, which are involved in the regulation of Apobec protein functions. For example, Apobec3G was shown to be ubiquitinylated by the HIV Vif protein, leading to its proteasomal degradation, thereby counteracting its restrictive function on virus replication [96]. Also, phosphorylation plays a crucial role for Apobec activity, as it was shown for Apobec1 deamination [205]. SUMOylation was shown to be crucial for the nuclear exclusion of Apobec2 to avoid genomic DNA editing, which was shown to depend on the SUMO

modification of its N-terminus [206]. Furthermore, the ubiquitin-conjugating enzyme E2 L3 (UBE2L3) promotes Apobec3A ubiquitinylation and proteasome-dependent degradation, which facilitates HBV infection by maintaining cccDNA stability [207]. Apobec3A is known to be ubiquitinylated at position K137 [170]. However, there is a lack of knowledge concerning Apobec3A SUMOylation as well as the potential effects of HAdV infection on Apobec3A PTMs, which could demonstrate another possible mechanism of adenoviral counteraction of Apobec3A restriction.

4.4.1. Higher migrating band pattern of Apobec3A is increased during HAdV infection

PTM refers to the covalent attachment of a modifying group to one or two amino acids of a certain protein following ribosomal translation and thereby can be observed using western blot analysis, represented by higher migrating bands above the unmodified protein band due to changes in the molecular weight [127]. To visualize potential PTMs of Apobec3A, HepaRG cells were transfected with pLenti6.3-Apobec3A-V5 and infected with HAdV wt (MOI 50). Following harvesting of the cells, one part of the lysates was prepared according to standard protocols, whereas another part was treated differently. To stabilize PTMs or oligomeric structures, neither β-mercaptoethanol was added to the lysate, nor was it boiled to 95°C which is normally used for protein denaturation. These samples, present in a more “native” state, were then applied for Apobec3A staining during western blot analysis and revealed a strong increase of Apobec3A PTM or oligomeric structures upon adenoviral infection (Figure 34, lanes 4 and 5).

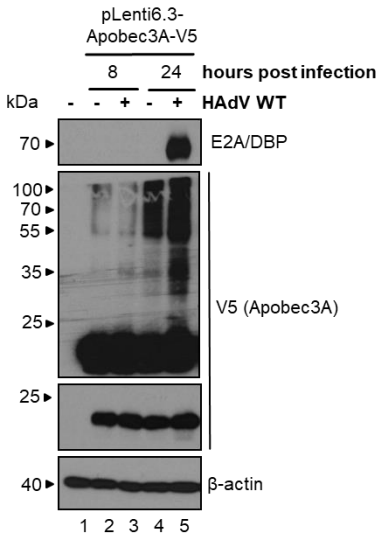

Figure 34: Upcoming bands for Apobec3A are increased during HAdV infection.
HepaRG cells were transfected with 5 µg pLenti6.3-Apobec3A-V5 and infected with HAdV wild type using a MOI of 50. 8 h and 24 h post infection, the cells were harvested, and cell lysates were performed according to standard protocols. For one part of the lysates, neither ß-mercaptoethanol was added nor it was boiled to 95°C, which was then applied for V5 (Apobec3A) staining. Normal lysates were stained with E2A, which served as an infection control, and β-actin, which was used as a loading control during western blot analysis. Stained proteins are indicated on the right, molecular weights in kDa on the left. The depicted blots represent the result of several repetitions.

4.4.2. Apobec3A SUMOylation is increased during HAdV infection

Until now, it was unknown if Apobec3A represents a target for SUMOylation. To address this question, HepaRG-SUMO2 cells were transfected with pLenti6.3-Apobec3A-V5 and infected with HAdV wild type (MOI 50), to additionally investigate the influence of adenoviral infection on the potential SUMOylation of Apobec3A. Ni-NTA assays were performed to pull down the His tagged, SUMO modified proteins, which were visualized by western blot analysis. The band indicating mono-SUMOylation of Apobec3A was only detected in the HepaRG-SUMO2 cells, stably expressing His tagged SUMO2, whereas no corresponding band was observed for the control cell line HepaRG, expressing only the His tag (Figure 35A, lanes 10 and 12). Hence, SUMOylation of Apobec3A was detected for the first time in the present study. Interestingly, Apobec3A SUMOylation was upregulated during HAdV infection. Confirming earlier obtained data, E2A SUMOylation was decreased upon Apobec3A expression (4.2.6) (Figure 35A, lanes 11 and 12). Since earlier experiments already showed an increase of Apobec3A input levels upon HAdV infection, the *ImageJ* program was used to analyze if the increased SUMOylation level of Apobec3A during adenoviral infection is only due to upregulated Apobec3A input levels. However, normalizing the IP results on the corresponding input levels still depicted an increase of Apobec3A SUMOylation during HAdV infection (Figure 35B). Taken together, adenoviral infection leads to the upregulation of the SUMO2 modification of Apobec3A (Figure 35C), which is in accordance with results from earlier experiments, showing increasing upcoming bands for Apobec3A during adenoviral infection (4.4.1).

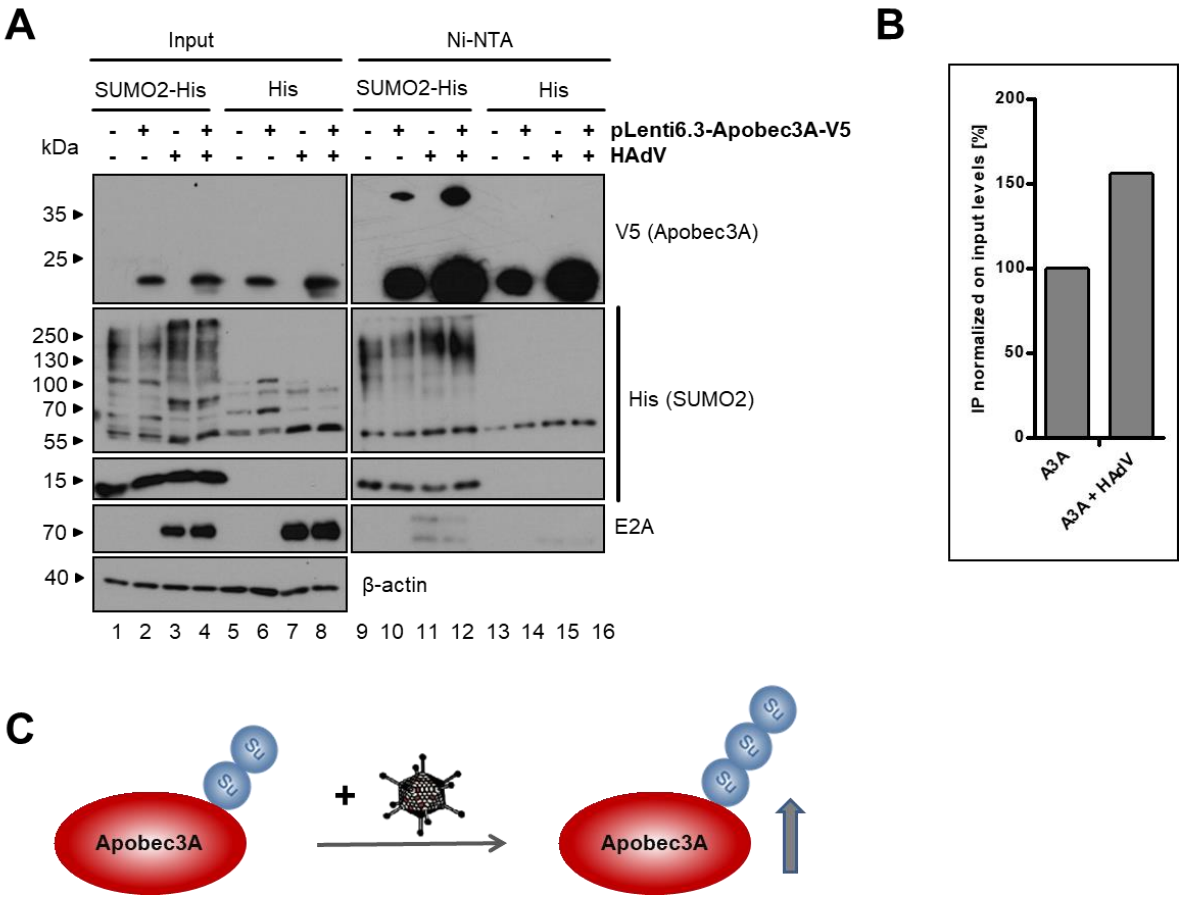

Figure 35: Apobec3A is SUMO modified, which is increased during HAdV infection.
(A) HepaRG-His and HepaRG-His-SUMO2 cells were transfected with 5 µg pLenti6.3-Apobec3A-V5 and infected with HAdV wild type using a MOI of 50. 48 h post infection, the cells were harvested and lysates as well as a Ni-NTA assay were carried out. The proteins were separated by SDS-PAGE and subjected to western blot analysis, using antibodies for V5 (Apobec3A), 6xHis (SUMO2) as a cellular control, E2A as an infection control and β-actin as a loading control. Stained proteins are indicated on the right, molecular weights in kDa on the left. The depicted blots represent the result of several repetitions. (B) The *ImageJ* program was used to calculate signal intensities. Thereby, Apobec3A IP signals were normalized to His IP signals, whereas Apobec3A input levels were normalized on β-actin levels. The normalized IP results were then normalized again on the normalized input results. (C) Schematic representation of adenoviral influence on Apobec3A SUMO modification.

To investigate, if the upregulation of Apobec3A SUMOylation is conserved among human DNA viruses to counteract its restrictive function, the effect of HBV infection on Apobec3A SUMOylation was investigated. Therefore, HepaRG-SUMO2 cells were co-transfected with pLenti6.3-Apobec3A-V5 and the pHBV1.1 plasmid, which expresses the HBV pgRNA, thereby establishing HBV infection. The Ni-NTA assay showed that the SUMOylation of Apobec3A is not affected by HBV (Figure 36, lanes 3 and 4). In conclusion, HBV infection does not influence Apobec3A SUMOylation, meaning that the upregulation of Apobec3A SUMOylation is not conserved among human DNA viruses. It is rather specific for HAdV infection.

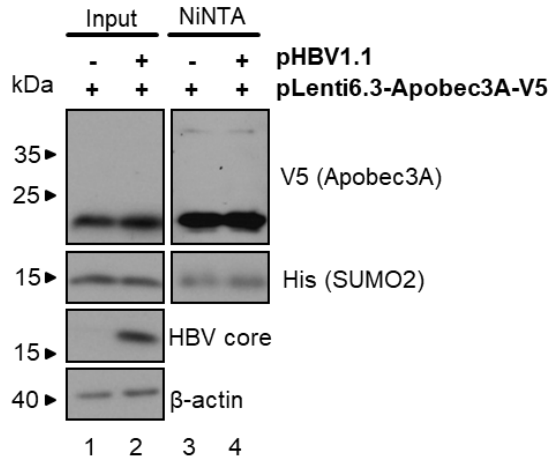

Figure 36: Apobec3A SUMOylation is not affected by HBV.
HepaRG-SUMO2 cells were co-transfected with 5 µg pLenti6.3-Apobec3A-V5 and 10 µg pHBV1.1 plasmid, which establishes HBV infection. 72 h post transfection, the cells were harvested and lysates as well as a Ni-NTA assay were performed. Proteins were separated via SDS-PAGE and subjected to western blot analysis, using antibodies for V5 (Apobec3A), 6xHis as a cellular control, HBV core as an infection control as well as β-actin as a loading control. Stained proteins are indicated on the right, molecular weights in kDa on the left. The depicted blots represent the result of several repetitions.

4.4.3. Generation and phenotypic characterization of potential Apobec3A SUMO mutants

To identify potential consequences and functions of Apobec3A SUMOylation, it was desirable to clone a mutant for Apobec3A, which cannot be SUMOylated anymore. The program *GPS SUMO (*The CUCKOO Workgroup), which predicts potential SUMOylation sites as well as SUMO-interacting motifs (SIMs) was used to analyze the Apobec3A amino acid sequence. The *in silico* prediction revealed five different potential SUMOylation sites within the Apobec3A sequence. The lysines at position 30, 47, 60, 137 as well as 159 within the depicted motifs are potential SUMO targets, with K47 having the highest probability for SUMOylation (Figure 37A). Inverse PCR was performed using adequate primers containing mutations (Table 5) to mutate the wild type pLenti6.3-Apobec3A-V5 plasmid at the corresponding lysine (K) residues to arginine (R) residues. Following re-ligation of the PCR product, the correct vector assembly was confirmed by a restriction digest with NcoI (Table 10), which was analyzed on an agarose gel. Digestion of the plasmids with NcoI was expected to yield three visible bands at 5.241, 1.419, and 0.994 kb, as well as two bands at 0.404 and 0.220 kb (Figure 37B). The presence of the mutations at the target lysine residues in the sequence of Apobec3A was confirmed by sequencing. In the next steps, these Apobec3A mutants were investigated for their SUMO modification, by performing a Ni-NTA assay. Therefore, HeLa-SUMO2 cells were transfected with the five different Apobec3A mutants, harvested after 24 h and subjected to lysate and Ni-NTA assay preparation. However, western blot analysis revealed no reduction or abolishment of SUMO conjugation to any of the Apobec3A mutants (Figure 37C, lanes 9-14). In conclusion, cloning of different

Apobec3A mutants did not result in the discovery of an Apobec3A SUMO mutant, which is less or not SUMOylated. A possible explanation therefore is that Apobec3A SUMOylation might occur at several lysine residues simultaneously. Consequently, further cloning steps are necessary to discover an Apobec3A SUMO mutant, to further reveal the function of Apobec3A SUMOylation.

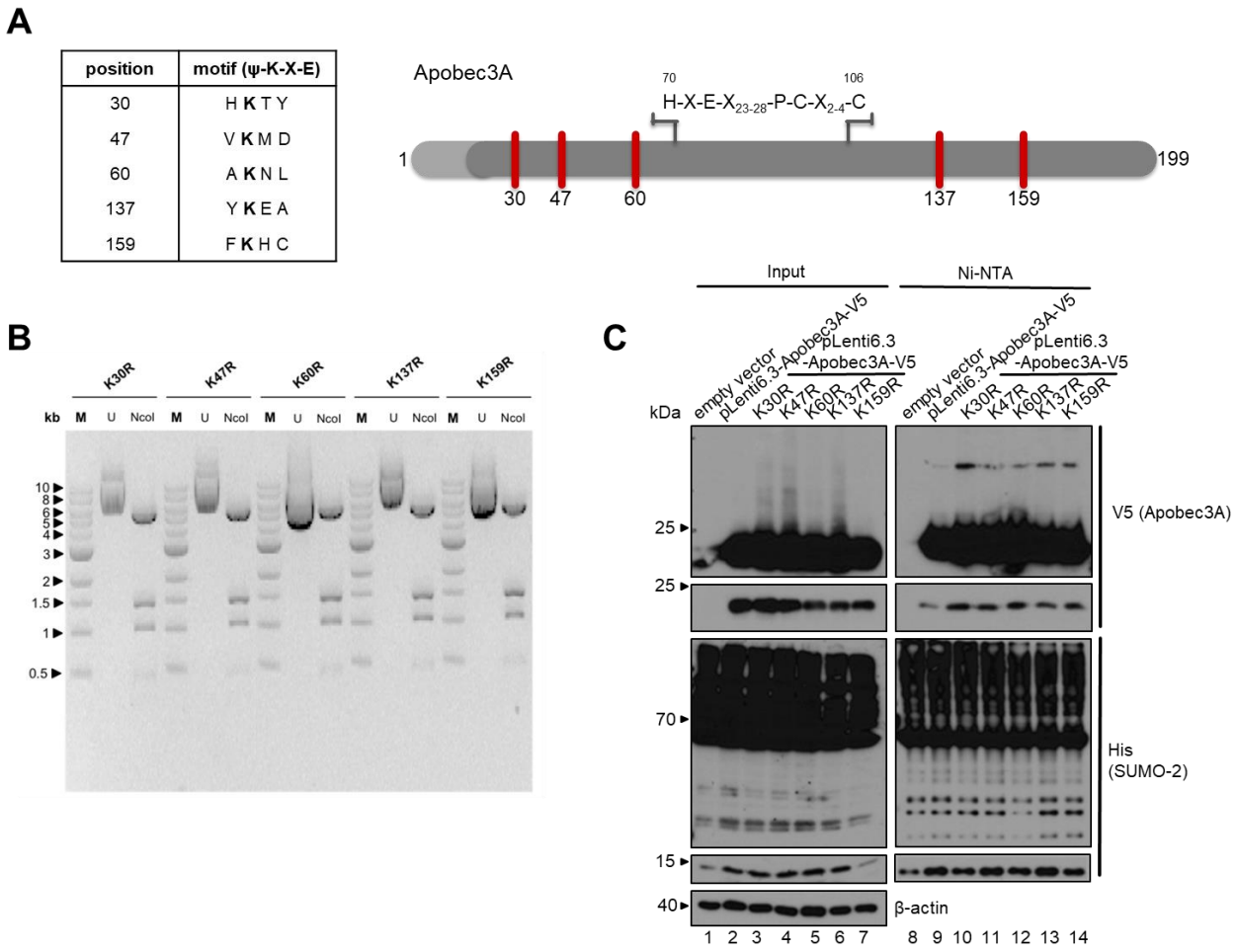

Figure 37: Cloning and investigation of potential Apobec3A SUMO mutants.
(A) The *GPS SUMO* (The CUCKOO Workgroup) program was used to predict potential SUMOylation sites in the Apobec3A amino acid sequence. Five potential SUMOylation sites were found at the indicated positions within the indicated motifs, which are presented schematically in the Apobec3A sequence. (B) Inverse PCR reactions were performed using adequate primers to mutate the potentially SUMO modified lysine (K) residues to arginine (R) residues. Proper religation of the vector was assessed by a restriction digest with NcoI, which was analyzed on an agarose gel (M = marker, U = undigested) and the correct mutations were confirmed by sequencing. (C) HeLa-S2 cells were transfected with 5 µg pLenti6.3-Apobec3A-V5 wild type or mutant versions. After 24 h, the cells were harvested and lysates as well as a Ni-NTA assay were conducted. The proteins were separated via SDS-PAGE and subjected to western blot analysis, using antibodies for V5 (Apobec3A), 6xHis (SUMO2) as well as β-actin as a loading control. Stained proteins are indicated on the right, molecular weights in kDa on the left. The depicted blots represent the result of several repetitions.

4.4.4. HAdV decreases Apobec3A ubiquitinylation

Since Apobec3A SUMOylation was affected by HAdV infection, the question arose, if the known ubiquitinylation at position K137 of Apobec3A is also influenced by adenoviral infection [170]. To address this, H1299 cells were transfected with pLenti6.3-Apobec3A-V5 as well as 6xHis-ubiquitin and infected with HAdV wt (MOI 50) and a Ni-NTA assay performed. Several higher migrating bands were detected, indicating Apobec3A ubiquitinylation and confirming the known ubiquitinylation of Apobec3A at lysine 137 (Figure 38A, lane 8). Including adenoviral infection in the experiment revealed a decrease of Apobec3A ubiquitinylation during HAdV infection (Figure 38B, lanes 9 and 10). Normalization of the Apobec3A IP signals on the input levels still confirmed the downregulation of Apobec3A ubiquitinylation during HAdV infection (Figure 38C). In conclusion, HAdV decreases Apobec3A ubiquitin modification, which might contribute to the increase of Apobec3A during adenoviral infection (Figure 38D).

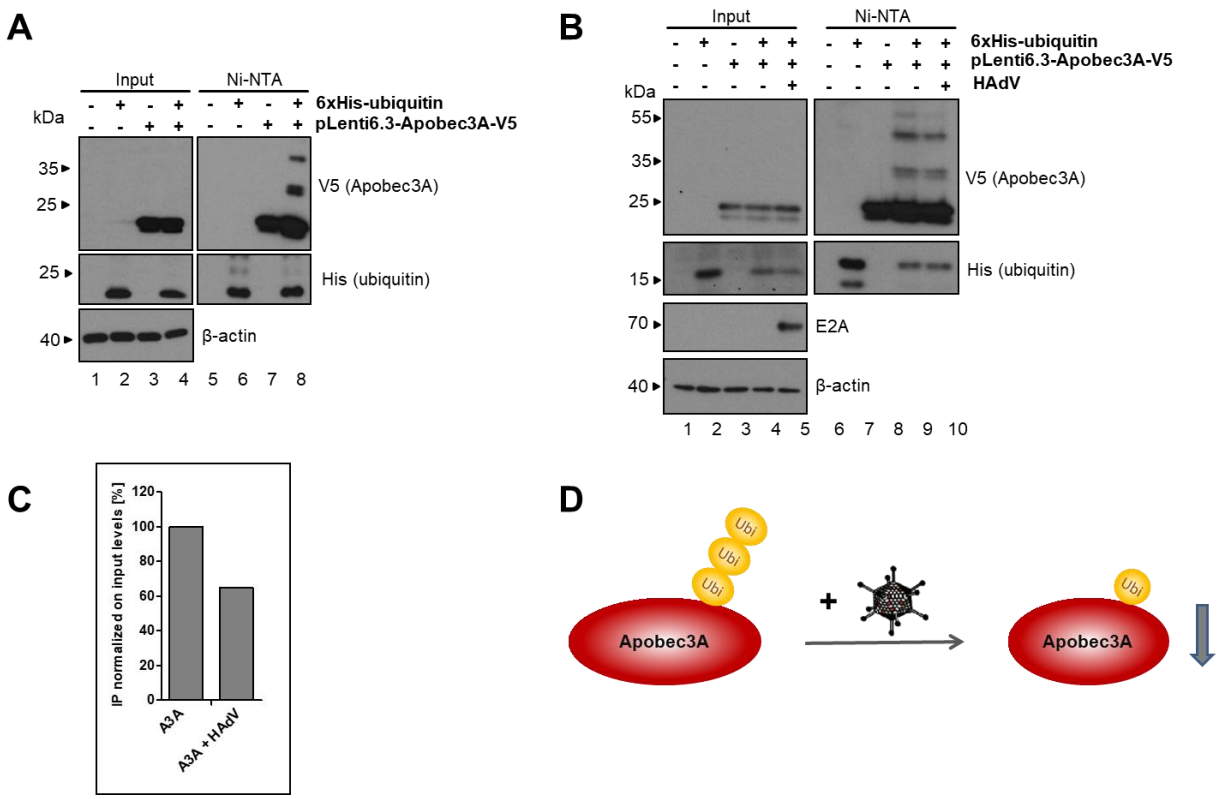

Figure 38: Apobec3A ubiquitinylation is decreased during HAdV infection.
(A) H1299 cells were transfected with 5 µg pLenti6.3-Apobec3A-V5 as well as 10 µg 6xHis-ubiquitin. 24 h post transfection, the cells were harvested and cell lysates as well as a Ni-NTA assay were performed. Proteins were separated via SDS-PAGE and visualized by immunoblotting, using antibodies for V5 (Apobec3A), 6xHis (ubiquitin) and β-actin as a loading control. Stained proteins are indicated on the right, molecular weights in kDa on the left. (B) H1299 cells were transfected with 5 µg pLenti6.3-Apobec3A-V5 as well as 10 µg 6xHis-ubiquitin and infected with HAdV wt (MOI 50). 24 h post infection, the cells were harvested and cell lysates as well as a Ni-NTA assay were performed. Proteins were separated via SDS-PAGE and visualized by immunoblotting, using antibodies for V5 (Apobec3A), 6xHis (ubiquitin), E2A as an infection control and β-actin as a loading control. Stained proteins are indicated on the right, molecular weights in kDa on the left. The depicted blots represent the result of several repetitions. (C) The program *ImageJ* was used to determine signal intensities, which were normalized on input levels. (D) Schematic representation of adenoviral influence on Apobec3A ubiquitin modification.

4.4.5. RNF4 promotes Apobec3A ubiquitinylation and degradation

SUMO targeted ubiquitin ligases (STUBLs) were shown to link SUMOylation to the ubiquitin-proteasome pathway [208]. Up to date, RNF4 and RNF111 (Arkadia) are the only two human STUBLs identified [146, 147]. A potential role of STUBLs for Apobec3A SUMO- and ubiquitinylation was assumed, since both modifications of Apobec3A were observed during earlier experiments (4.4.2, 4.4.4). To investigate the influence of the STUBL RNF4 on Apobec3A expression levels, HepaRG-SUMO2 cells were chosen, which ensure sufficient SUMO modification of Apobec3A due to high SUMO levels in these cells. Co-transfection of pLenti6.3-Apobec3A-V5 as well as RNF4-Flag followed by western blot revealed a decrease of Apobec3A protein levels upon RNF4 expression (Figure 39A, lane 3). Since RNF4 ubiquitinylates SUMOylated proteins, a Ni-NTA assay was conducted, to study the influence of RNF4 on Apobec3A ubiquitin modification [146]. Therefore, H1299 cells were transfected with the plasmids pLenti6.3-Apobec3A-V5, 6xHis-ubiquitin and RNF4-Flag. Following harvesting, cell lysates as well as a Ni-NTA assay were performed and the results were investigated via SDS-PAGE and following immunoblotting. Interestingly, Apobec3A ubiquitinylation was increased by RNF4 (Figure 39B, lanes 12 and 14). In contrast to what was expected, Apobec3A input levels were not decreased upon RNF4 expression, which might be due to the usage of a different cell line not containing factors necessary for Apobec3A degradation, such as p53 (Figure 39B, lane 7). In conclusion, RNF4 increases Apobec3A ubiquitin modification, leading to its proteasomal degradation, which is summarized in Figure 39C.

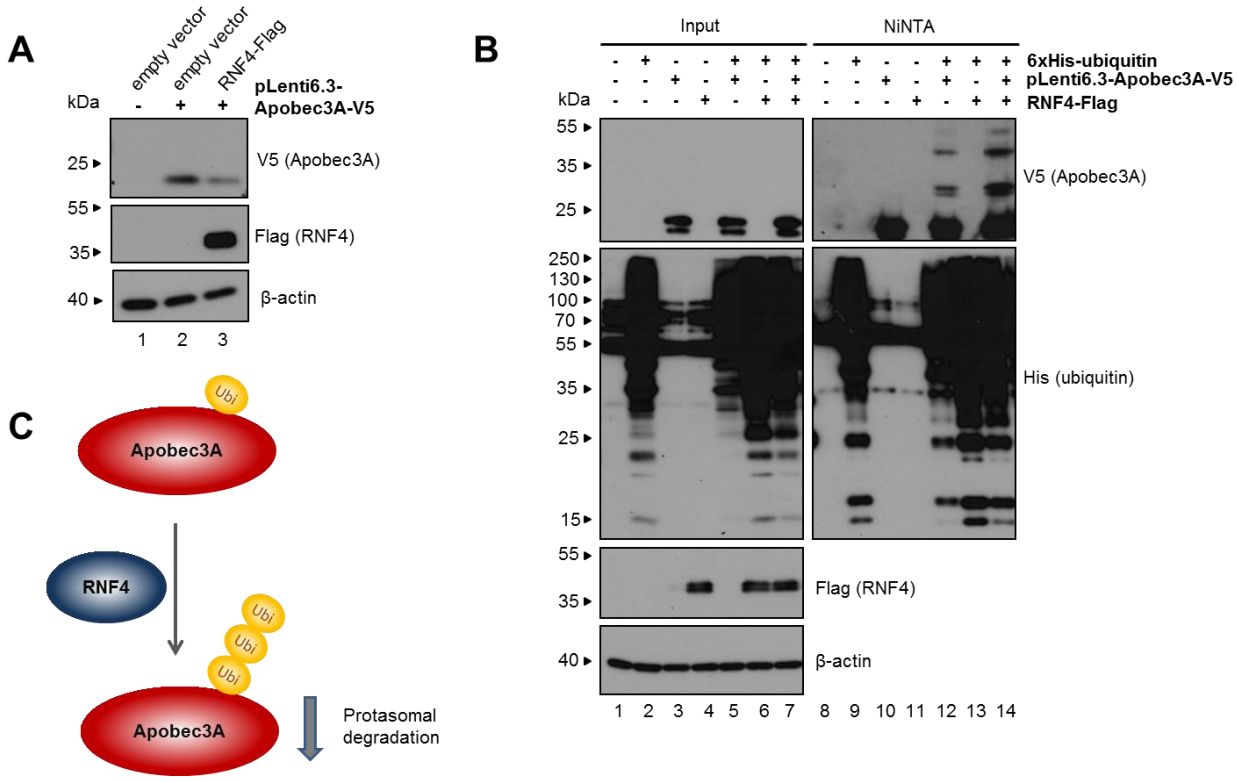

Figure 39: Apobec3A protein levels are decreased by RNF4 due to increased ubiquitin modification.
(A) HepaRG-SUMO2 cells were transfected with 5 µg pLenti6.3-Apobec3A-V5 and RNF4-Flag. Cells were harvested 24 h later and cell lysates conducted which were analyzed via SDS-PAGE and immunoblotting using the antibodies V5 (Apobec3A), Flag (RNF4) and β-actin as a loading control. Stained proteins are indicated on the right, molecular weights in kDa on the left. (B) H1299 cells were transfected with 5 µg pLenti6.3-Apobec3A-V5 and RNF4-Flag as well as 10 µg 6xHis-ubiquitin. The cells were harvested 24 h later and cell lysates as well as a Ni-NTA assay conducted, which were analyzed via SDS-PAGE and immunoblotting using the antibodies V5 (Apobec3A), 6xHis (ubiquitin), Flag (RNF4) and β-actin as a loading control. Stained proteins are indicated on the right, molecular weights in kDa on the left. The depicted blots represent the result of several repetitions. (C) Schematic representation of RNF4 influence on Apobec3A ubiquitin modification.

4.4.6. RNF4 is not forming a complex with Apobec3A in the host cell

RNF4 can directly bind to its substrate, for example Daxx, which is subsequently targeted for ubiquitin modification. HAdV infection promotes the interaction of RNF4 and Daxx, leading to increased Daxx ubiquitinylation and proteasomal degradation, which facilitates viral replication [165]. Consequently, an interaction of RNF4 with Apobec3A, which showed increased ubiquitin modification upon RNF4 expression in earlier experiments (4.4.5), was assumed. Immunoprecipitation assays should reveal the potential interaction of RNF4 with Apobec3A. Therefore, HepaRG-SUMO2 cells were transfected with pLenti6.3-Apobec3A-V5 and RNF4. Following harvesting of the cells, protein lysates were prepared, an IP was conducted, and the results investigated by western blot analysis. As depicted in Figure 40, neither a signal for RNF4-Flag was detected after V5 antibody pull down nor a signal for Apobec3A-V5 after Flag antibody pull down (Figure 40, lanes 8 and 12). Due to unknown reasons, RNF4 input signals were reduced in lane 4. Hence, RNF4 was not able to decrease Apobec3A expression levels (Figure 40, lane 4), which was observed in earlier experiments

(4.4.5). In conclusion, RNF4 did not interact with its target Apobec3A, which was contradictive to expected findings.

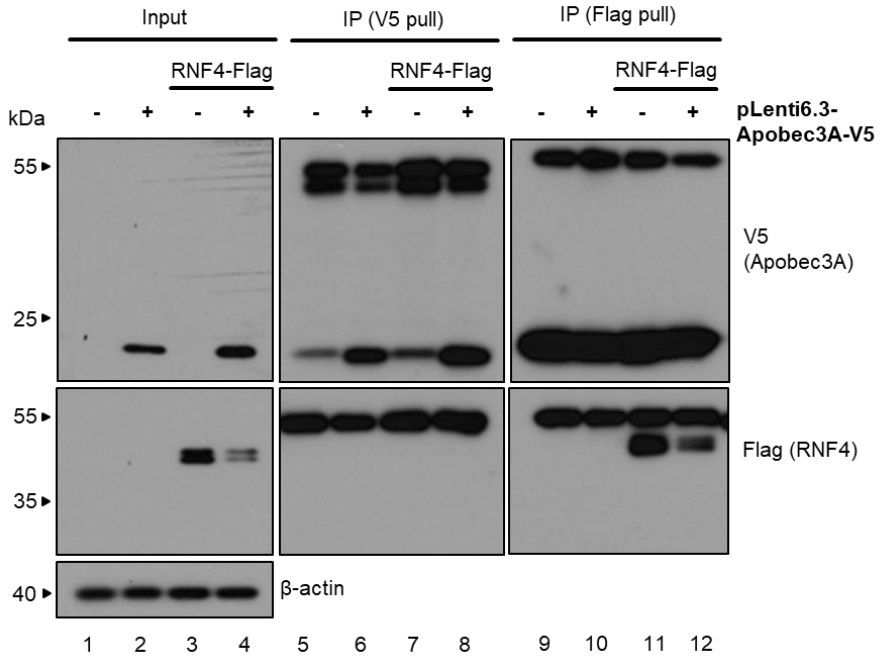

Figure 40: RNF4 does not interact with Apobec3A.
HepaRG-SUMO2 cells were transfected with 5 µg pLenti6.3-Apobec3A-V5 and RNF4-Flag and harvested after 24 h. Cell lysates as well as an IP were performed, proteins separated by SDS-PAGE and the results analyzed by immunoblotting using the antibodies for V5 (Apobec3A), Flag (RNF4) and β-actin as a loading control. Stained proteins are indicated on the right, molecular weights in kDa on the left. The depicted blots represent the result of several repetitions.

4.4.7. RNF4-mediated Apobec3A ubiquitinylation is decreased during HAdV infection

Since Apobec3A ubiquitinylation was increased by RNF4 (4.4.5), but adenoviral infection led to decreased ubiquitin modification of Apobec3A (4.4.4), we analyzed the RNF4-mediated ubiquitinylation of Apobec3A during HAdV infection. Hence, H1299 cells were transfected with pLenti6.3-Apobec3A-V5, RNF4-Flag and 6xHis-ubiquitin, followed by infection with HAdV wt (MOI 50). After harvesting, cell lysates as well as a Ni-NTA assay were performed and the results analyzed via SDS-PAGE, which were followed by immunoblotting. Confirming earlier performed experiments (4.4.5), RNF4 increased Apobec3A ubiquitin modification, which was not the case, if adenoviral infection was present (Figure 41, lanes 17 and 20). Concluding, RNF4-mediated increase of Apobec3A ubiquitinylation is counteracted by HAdV infection, which is in accordance with already published data, showing that adenoviral infection leads to a relocalization of RNF4 to the nuclear matrix fraction [165].

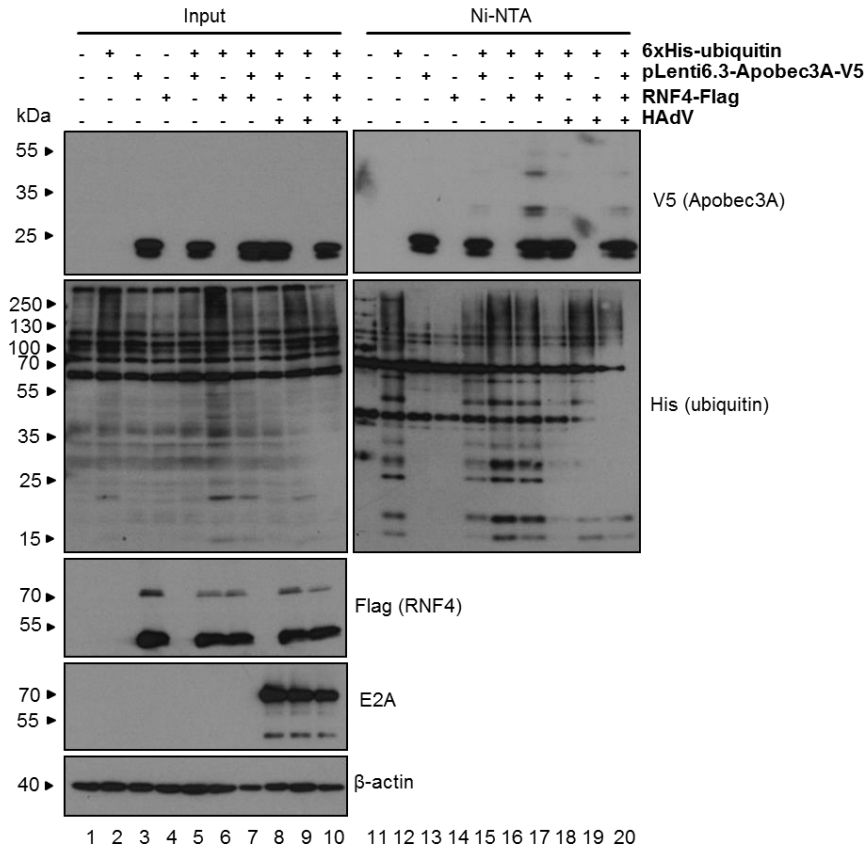

Figure 41: RNF4 increased Apobec3A ubiquitin modification is counteracted during HAdV infection.
(A) H1299 cells were transfected with 5 µg pLenti6.3-Apobec3A-V5 and RNF4-Flag, as well as 10 µg 6xHis-ubiquitin, followed by infection with HAdV wt using a MOI of 50. 24 h post infection, the cells were harvested and cell lysates as well as a Ni-NTA assay performed. Proteins were separated via SDS-PAGE and subjected to western blot analysis using the antibodies for V5 (Apobec3A), 6xHis (ubiquitin), Flag (RNF4), E2A as an infection control and β-actin as a loading control. Stained proteins are indicated on the right, molecular weights in kDa on the left. The depicted blots represent the result of several repetitions.

4.5. HAdV infection affects Apobec3A dimer formation

4.5.1. Confirmation of Apobec3A dimer formation

Recently, Bohn and colleagues found that Apobec3A forms a homodimer via a symmetric swap of its N-terminal residues, which is believed to regulate Apobec3A activity [120]. The homodimer interface connects the active sites of both monomers and thereby forms a positively charged groove, which is crucial for substrate recognition and specificity [120]. To investigate the Apobec3A dimer formation, H1299 cells were transfected with pLenti6.3-Apobec3A-V5 and pEYFP-Apobec3A. Following harvesting, cell lysates as well as an IP assay were performed, the proteins separated via SDS-PAGE and subjected to western blot analysis. Pulling down the V5 tag of Apobec3A resulted in the detection of a signal for GFP (Apobec3A), confirming Apobec3A homodimer formation (Figure 42, lane 8).

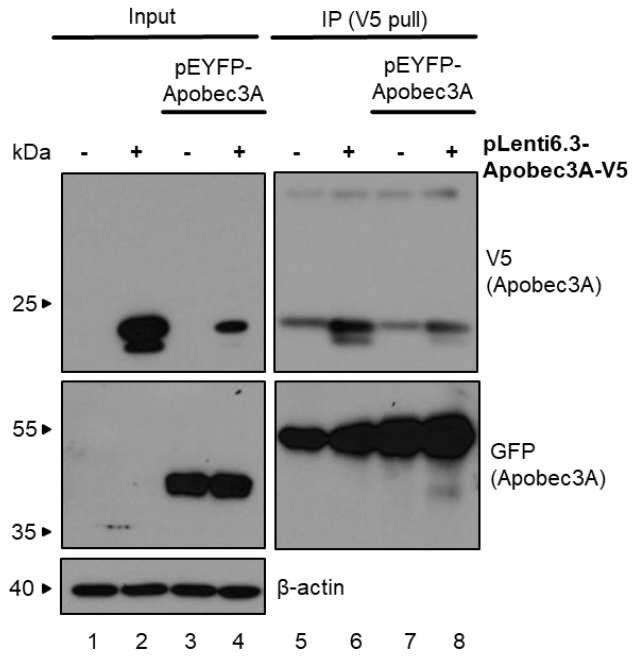

Figure 42: Apobec3A forms a homodimer.
H1299 cells were transfected with 5 µg pLenti6.3-Apobec3A-V5 as well as 5 µg pEYFP-Apobec3A. 24 h post transfection, the cells were harvested, followed by preparation of whole-cell lysates as well as a Co-IP. The proteins were separated by SDS-PAGE and subjected to immunoblotting using the antibodies for V5 (Apobec3A), GFP (Apobec3A) and β-actin as a loading control. Stained proteins are indicated on the right, molecular weights in kDa on the left.

4.5.2. Apobec3A dimer formation is increased during HAdV infection

The initial hypothesis was, that Apobec3A dimer formation is decreased by adenoviral infection, since the homodimer is the active form of Apobec3A and HAdV were assumed to counteract Apobec3A functions [120]. To study this issue, HepaRG cells were transfected with pLenti6.3-Apobec3A-V5 and pEYFP-Apobec3A, followed by infection with HAdV wt (MOI 50). A Co-IP was performed and the results analyzed by western blot. Interestingly, a strong signal was detected for Apobec3A-V5 after pulling down the YFP tagged Apobec3A via the GFP antibody 48 h post HAdV infection (Figure 43A, lane 14). However, to make sure, that this is not only due to increased Apobec3A input levels upon adenoviral infection, the signal intensities were determined with the *ImageJ* program and normalized on the input levels. Apobec3A IP levels were increased during HAdV infection compared to the non-infected control, concluding that HAdV infection promotes Apobec3A dimer formation (Figure 43B, C). Thus, the infected host cell might increase the active dimer form of Apobec3A to improve antiviral defense.

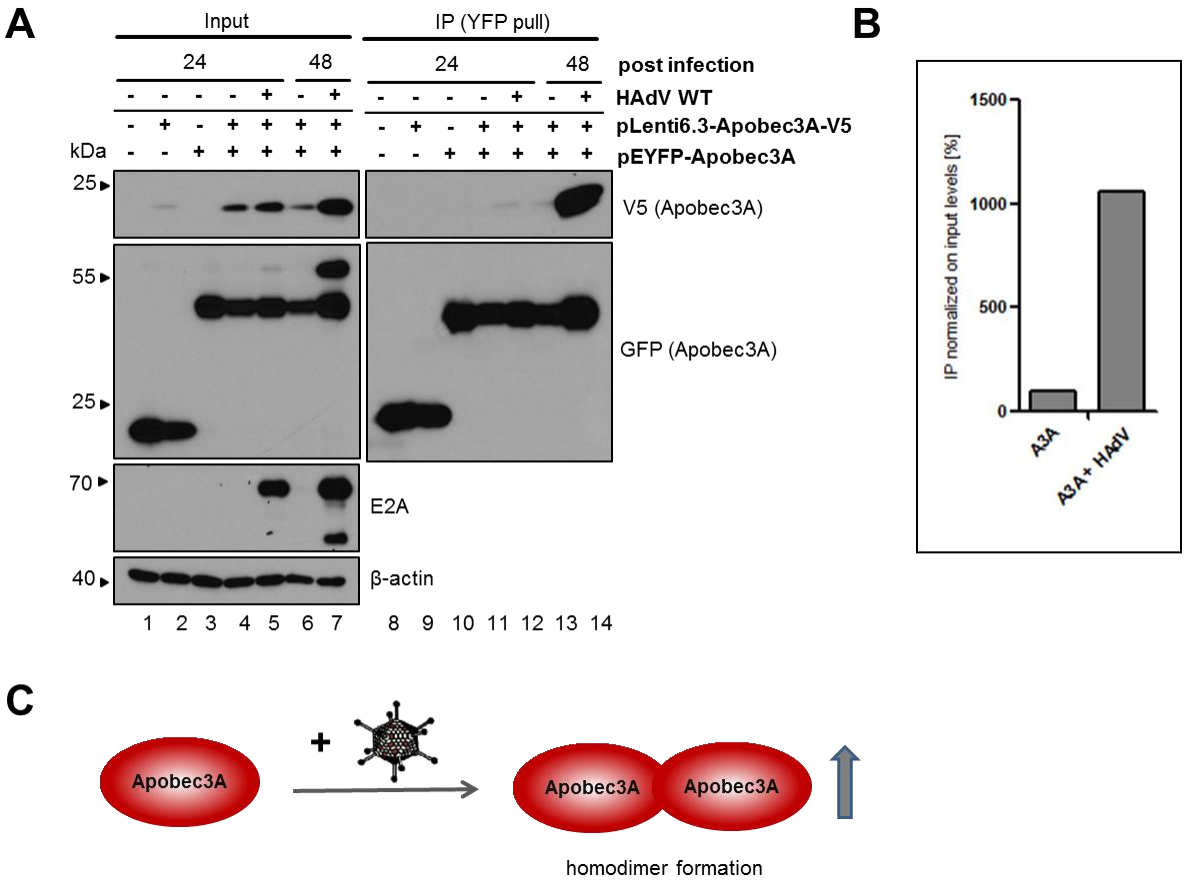

Figure 43: Apobec3A dimer formation is increased during HAdV infection.
(A) HepaRG cells were transfected with 5 µg pLenti6.3-Apobec3A-V5 and pEYFP-Apobec3A and infected with HAdV wt using a MOI of 50. Following harvesting after 24 h or 48 h, cell lysates as well as a Co-IP using the *ChromoTek GFP-Trap® beads* were performed. The proteins were separated by SDS-PAGE and subjected to western blot and immunostaining, using the antibodies for V5 (Apobec3A), GFP (Apobec3A), E2A as an infection control as well as β-actin as a loading control. Stained proteins are indicated on the right, molecular weights in kDa on the left. The depicted blots represent the result of several repetitions. (B) The *ImageJ* program was used to determine the signal intensities, and the signals for the Apobec3A IP were normalized on Apobec3A input levels. (C) Schematic representation of the adenoviral impact on Apobec3A homodimer formation.

5. Discussion

Apobec proteins are cytidine deaminases, which promote antiviral activity against many different viruses including HIV or HPV [75, 94, 108]. However, data on HAdV restriction by Apobec proteins was very limited until now. One study demonstrated Apobec3B upregulation during adenoviral infection and another suggested, without showing verifying data, HAdV to be not targeted by any Apobec protein due to the double stranded DNA genome [104, 192]. Nevertheless, more recent publications could show that also double stranded DNA viruses are targeted by Apobec proteins [108]. Consequently, the present study was conducted to investigate the reciprocal impact of HAdV infection on Apobec expression and vice versa. Since the strongest effect of adenoviral infection was detected for Apobec3A mRNA levels in an initial experiment comparing all different Apobec mRNA levels during HAdV infection (Figure 10), the focus was set on Apobec3A in the following experiments. In contrast to initial expectations, Apobec3A mRNA and protein levels were increased upon HAdV infection and were not degraded via the viral E3 ubiquitin ligase complex (Figure 11 and 12). Several factors were found to be important for the increase of Apobec3A during adenoviral infection.

5.1. Apobec3A upregulation during HAdV infection

Figure 44 shows a schematic representation, which sums up the current findings for Apobec3A upregulation during HAdV infection, involving the viral factors E1B-55K and E4orf6 as well as the cellular factors p53 and RNF4. E1B-55K and E4orf6 build up the viral E3 ubiquitin ligase complex and lead to the efficient degradation of p53 [66]. Furthermore, E1B-55K is known to promote p53 SUMO modification, which is another way to suppress p53 [163]. Thus, inhibited p53 cannot reduce Apobec3A, which is also stabilized by E4orf6 expression via a so far unknown mechanism, leading to a drastic upregulation of Apobec3A expression during HAdV infection. Furthermore, RNF4 was shown to increase Apobec3A ubiquitin modification, which was not the case, if adenoviral infection was present (Figure 41). Concluding, RNF4-mediated increase of Apobec3A ubiquitinylation is counteracted by HAdV infection, which is in accordance with already published data, showing that adenoviral infection leads to a relocalization of RNF4 to the nuclear matrix fraction [165]. This might result in cellular separation of the two proteins, thereby inhibiting increased Apobec3A ubiquitinylation by RNF4 expression. Consequently, RNF4 might be one important factor, which is involved in the observed decrease of Apobec3A ubiquitinylation during HAdV infection (4.4.4), thereby contributing to Apobec3A stabilization during adenoviral infection (Figure 44).

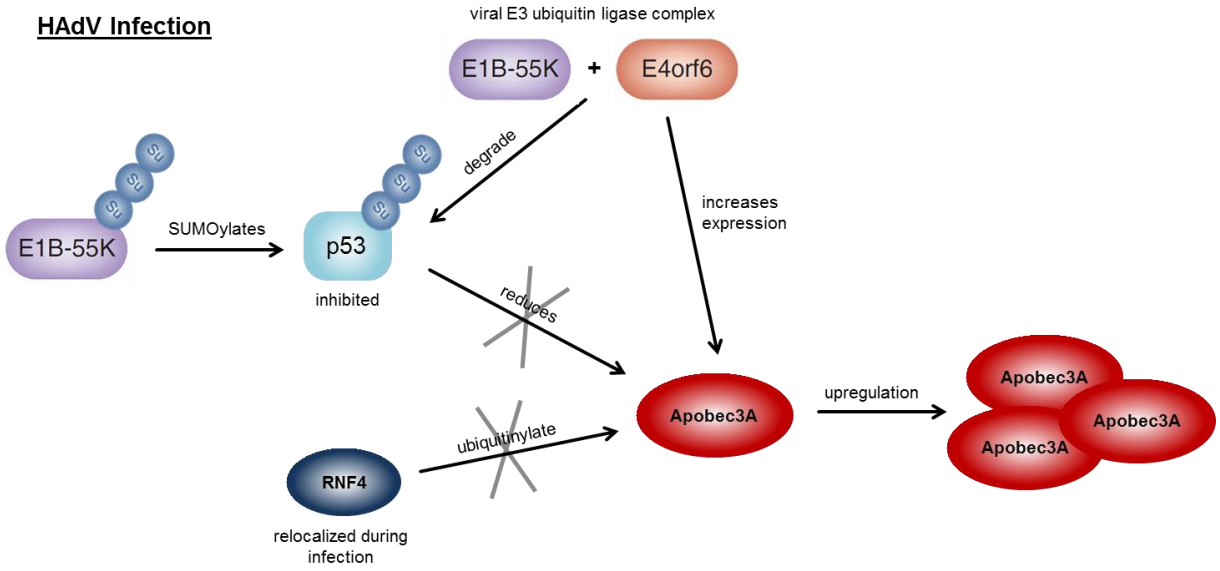

Figure 44: Schematic overview of Apobec3A upregulation during HAdV infection.
The current hypothesis is that Apobec3A stabilization during HAdV infection does not depend on one single factor. It rather seems to depend on several factors including E1B-55K, E4orf6, p53 and RNF4, functioning together in a network, which is depicted schematically for a better overview.

Interestingly, p53 downregulates Apobec3A protein levels (Figure 15), which is counteracted during adenoviral infection, thereby contributing to Apobec3A upregulation. This finding was unexpected, since p53 was recently found to regulate Apobec activity on a transcriptional level by binding to p53 response elements (p53RE), thereby leading to an increase of mRNA levels in the case of Apobec3A [195, 209]. Nevertheless, it is not unlikely, that mRNA levels are differentially regulated than protein levels, like it was found for c-myc expression, which showed decreased mRNA levels during HAdV infection, while being increased in protein levels [210]. Moreover, it should be favorable for the tumor suppressor p53, the “guardian of the genome”, to decrease harmful Apobec3 editing processes, like it was observed for Apobec3B [211]. Overexpression of Apobec3B in different cancer types correlates with the loss of p53, since p53 was shown to repress Apobec3B [211]. This is achieved by p53 induction of p21 and the recruitment of repressive DREAM (dimerization partner, RB-like, E2F and MuvB) complexes to the promoter region of Apobec3B [211]. Since Apobec3A protein expression was also decreased by p53, further experiments should be performed to elucidate the role of p21 and repressive DREAM complexes in the regulation of Apobec3A activation. Additionally, it was interesting, if Apobec3A is involved in HAdV-mediated cell transformation, which was shown to depend on the viral oncogenes E1A, E1B, E4orf3 and E4orf6 [212-214]. Inhibition of the cellular p53 protein was identified as a prerequisite for adenoviral transformation processes, which is mostly achieved by the two early viral proteins E1B-55K and E4orf6 [215, 216]. Besides p53 degradation by the adenoviral E3 ubiquitin ligase complex as well as the E1B-55K induced SUMOylation and inhibition of p53, it is furthermore known, that E4orf6 alone can block p53-induced apoptosis [66, 68, 163, 217].

Moreover, E1B-55K, E4orf6 and p53 influence Apobec3A protein levels during adenoviral infection (Figure 44). Apobec3A expression levels are elevated in different human cancer types, leading to a widespread mutagenesis pattern [218]. Based on this, it would be highly interesting to investigate the potential impact of Apobec3A on HAdV-mediated cell transformation processes in prospective experiments.

Recently, a cellular protein was found to decrease Apobec3A expression levels, named ubiquitin conjugating enzyme E2 L3 (UBE2L3) [207]. UBE2L3 was shown to interact with Apobec3A, leading to increased Apobec3A ubiquitinylation and proteasomal degradation, thereby contributing to efficient HBV infection [207]. It was assumed, that UBE2L3 expression levels are decreased during HAdV infection, thereby contributing to the Apobec3A upregulation. In contrast to what was expected, first experiments revealed a potential increase of UBE2L3 expression during adenoviral infection (data not shown). However, an increase of UBE2L3 does not mandatorily correlate with decreasing Apobec3A expression levels, suggesting that the interaction of UBE2L3 and Apobec3A might be affected during HAdV infection due to possible protein relocalization for example, but this remains to be elucidated.

In conclusion, the Apobec3A upregulation during HAdV infection was demonstrated to involve a variety of different proteins, including E1B-55K, E4orf6 and p53 as well as further proteins, which are currently being determined.

5.2. HAdV restriction by Apobec3A and counteraction by the virus

A variety of other viruses was already shown to be restricted by Apobec3A, including HIV, HPV, HBV, HTLV and Parvoviruses [98, 103, 105, 108, 114]. By contrast, the observed upregulation of Apobec3A expression levels during HAdV infection, led to the hypothesis, that Apobec3A might be a positive factor for adenoviral replication. Yet, the opposite was proven in this study: Apobec3A is a novel restriction factor antagonizing efficient HAdV replication (0). The obtained results are contradictory to a single publication, suggesting HAdV to be not targeted by any Apobec protein due to their double stranded genome [104]. More recent work, demonstrating double stranded DNA viruses like HPV to be restricted by Apobec proteins, refuted the assumption made before, that single stranded DNA genomes are required for Apobec deamination [108]. Taken together, here we found that Apobec3A decreases adenoviral DNA-, RNA- and protein levels as well as progeny production (Figure 21-25).

Viral restriction by Apobec3A is known to depend on its deaminase activity in most cases, except for parvoviruses, which are inhibited via a so far unknown, deaminase-independent mechanism [98, 103, 105, 108, 114]. Consequently, the importance of the Apobec3A deaminase activity for HAdV restriction was assessed in follow-up experiments. 3D-PCR analysis was performed to investigate potential deamination processes and confirmed the

already published Apobec3A-mediated editing of the HBV cccDNA, indicating appropriate functionality of the assay (Figure 29) [103]. Sequencing results revealed G to A as well as C to T transitions in the deaminated cccDNA, which is contradictory to already published work, demonstrating only G to A transitions, thereby concluding preferential minus strand editing of the HBV cccDNA [103]. However, another study found that both HBV strands are targeted for Apobec3 deamination [102]. Since the specific detection of HBV cccDNA is known to be very difficult, it might be possible that the results of the 3D-PCR in this study also reveal total HBV DNA editing, which would explain the editing of both strands [219]. In the following, investigating a favored Apobec3A target region in the Hexon amplicon, containing a high amount of TC dinucleotides, suggested a crucial dependency on the Apobec3A deaminase activity for HAdV restriction (Figure 28). Subsequent isolation and sequencing of several amplification products of the 3D-PCR revealed many G to A transitions, indicating preferential minus strand deamination of the adenoviral Hexon amplicon (Figure 28). Minus strand specificity was already observed for Apobec3G editing of the HIV genome [220]. Furthermore, Apobec3A editing of the HBV cccDNA as well as the HTLV-1 genome preferentially occurs on the minus strand, observed by a high amount of G to A mutations [98, 103]. In summary, preferential minus strand deamination might be a conserved mechanism for Apobec restriction of different viruses.

Interestingly, Apobec3A was recently found to inhibit HIV reactivation in latently infected T cells, which does not depend on its deaminase activity [221]. Apobec3A was shown to bind the HIV long terminal repeat (LTR) and to recruit KRAB-associated protein 1 (KAP1) and heterochromatin protein 1 (HP1), leading to epigenetic silencing of the LTR, thereby maintaining HIV latency [221]. KAP1 is known to recruit histone repressing complexes, like SETDB1, which coordinate histone methylation, leading to gene silencing [222]. Furthermore, KAP1 was recently identified as a novel restriction factor for HAdV. It is deSUMOylated during adenoviral infection, which minimizes epigenetic silencing [161]. Consequently, through its recruitment by Apobec3A, KAP1 might play an important role during potential deaminase-independent restriction of HAdV by Apobec3A. Additionally, KAP1 was demonstrated to increase E1B-55K SUMOylation via a so far unknown mechanism [161]. This is in accordance with the obtained results in the present study, which showed that increased SUMOylation of E1B-55K correlates with increased Apobec3A expression levels (Figure 16B). Thereby, upregulated SUMO modification of E1B-55K leads to increased SUMOylation and inhibition of p53, which is not able to decrease Apobec3A protein levels anymore (Figure 15A and 16C). Thus, recruitment of KAP1 by Apobec3A, might upregulate Apobec3A expression as well as increase adenoviral gene silencing, thereby contributing to HAdV restriction. Here, further experiments must be performed to reveal the impact of KAP1 expression on the interplay of Apobec3A and HAdV.

In the present work, HAdV species C was found to counteract Apobec3A restrictive functions by depleting the TC dinucleotide, the preferred target of Apobec3A, in the genome [119] (Figure 31). This is in accordance with Apobec3A counteraction by HPV, which also evolved towards TC dinucleotide depletion [109]. For HAdV as well as HPV, the observed versus expected ratio of TC dinucleotides was reduced to 70-80% in the respective sequence [109] (Figure 31). Furthermore, the strongest reduction of TC dinucleotides was detected for alpha HPVs, which are known to primarily infect mucosal tissue [109]. Basal expression levels of Apobec3 family members are elevated in mucosal tissues compared with cutaneous skin, indicating a crucial role for Apobec3 on papillomavirus evolution [109]. However, TC dinucleotide depletion neither represented a general mechanism nor was conserved among different viruses, since TC dinucleotides were represented to an expected amount in the reference genome for *Homo sapiens* as well as the HBV genome (Figure 33). In addition, TC dinucleotide depletion was also conserved among different HAdV species. For HAdV species A, C and F, TC dinucleotide depletion was detected in their genomes, while the TC dinucleotide was represented to an expected extent in the sequences of HAdV species B, D, E and G (Figure 32). Interestingly, HAdV species A and C, which exhibit TC dinucleotide depletion in their genomes, were revealed not to be closely related in a recent phylogenetic analysis which was based on 115 human and simian adenovirus genomes [223]. This suggests that the TC dinucleotide depletion developed at least two times independently in the evolution of adenoviruses and might represent an example for a convergent adaption of HAdVs to counteract Apobec3A. Furthermore, the TC dinucleotide depletion correlated with the species seroprevalence. For HAdV species A and C, exhibiting a high seroprevalence, a depletion of the TC dinucleotide was observed, while for rarely occurring HAdV species, such as B and D, the TC dinucleotide was not depleted [224, 225]. It is assumed that HAdV species with a high prevalence were more frequently exposed to Apobec3A restriction during evolution, which led to Apobec3A counteraction via TC dinucleotide depletion. By contrast, less prevalent HAdV species are suggested to evolve more slowly towards TC dinucleotide depletion, which might not be detected yet. Nevertheless, TC dinucleotide depletion could also depend on the different cell tropisms of the HAdV species. Most HAdV species, like species C, are known to bind the cellular receptor CAR, thereby infecting mainly airway epithelial cells [28, 226]. However, HAdV of species B primarily bind the cellular receptor CD46, leading to the infection of other cell types, including hematopoietic cells [30, 227]. Furthermore, members of HAdV species D were shown to bind to sialic acid instead of CAR, resulting in preferential binding and infection of conjunctival cells [228, 229]. Since Apobec3A expression levels differ in these cells, it is reasonable to assume that cellular tropism might have influenced TC dinucleotide frequencies in the genomes of different HAdV species.

Additionally, it should be considered that the TC dinucleotide depletion might come at unknown costs, which would be highly interesting to investigate.
Taken together, the present study revealed Apobec3A as a novel restriction factor for HAdV, which requires its deaminase activity and is counteracted by TC dinucleotide depletion in the adenoviral genome during evolution.

5.3. Role of Apobec3A PTMs

Apobec3A was identified as a novel target for SUMO2 modification in the present work. Furthermore, SUMOylation of Apobec3A was increased during HAdV infection (Figure 35). Interestingly, Apobec3A SUMOylation was not affected by HBV infection, indicating a HAdV specific increase of Apobec3A SUMO modification, which is not conserved among different viruses (Figure 36). As already mentioned in the beginning, the SUMOylation pathway plays an important role in different processes of the adenoviral infection cycle. One well-studied example therefore is p53 SUMOylation by the early viral protein E1B-55K, which leads to p53 repression to ensure efficient viral replication [162, 163]. Hence, HAdV-mediated increase of Apobec3A SUMO modification was suggested to inhibit and thereby counteract Apobec3A restrictive functions. By contrast, Apobec3A expression levels were elevated 48 h after HAdV infection, so it was excluded that increased Apobec3A SUMO modification leads to protein instability and degradation. Nevertheless, upregulated Apobec3A SUMOylation could still affect Apobec3A localization and thereby its function in the cell. One example is the small GTPase activating protein RanGAP, playing an important role for nuclear import, which localizes at the nuclear pore complex in a SUMO-dependent manner [230]. However, immunofluorescence analysis did not reveal HAdV-mediated relocalization of overexpressed Apobec3A due to its distribution throughout the whole cell (Figure 26). Therefore, it is urgently recommended to study endogenous Apobec3A localization in future experiments.
Additionally, a fractionation assay as described recently by Günther et al. could be performed to investigate the potential impact of HAdV infection on Apobec3A localization [231]. Furthermore, increased Apobec3A SUMOylation could also influence Apobec3A interaction with other proteins and thereby negatively modulate its functions. Several protein interactions are known to depend on SUMOylation, among them the interaction of the SUMO modified helicase Senataxin with the exosome, playing a crucial role during DNA damage responses [232]. In conclusion, there are many more possibilities, how upregulation of Apobec3A SUMO modification could lead to its functional repression, but this remains to be elucidated in further studies. An oppositional explanation for the increase of Apobec3A SUMOylation might be an antiviral mechanism of the cell in response to HAdV infection. Hereby, elevated SUMO modification of Apobec3A is suggested to enhance its restrictive function to counteract HAdV infection. The function of some proteins was already shown to require SUMO modification, like it was demonstrated for the cellular PML protein. Hereby,

SUMOylation of PML is crucial for the accumulation of cellular proteins like Daxx and Sp100 at PML-NB, enabling the proper establishment of these cellular complexes [233]. In conclusion, the exact function and consequences of upregulated Apobec3A SUMO modification during adenoviral infection still need to be determined. Strikingly, the increase of Apobec3A expression was only detected for HAdV wt infection, whereas HAdV mutant viruses lacking functional E1B-55K or E4orf6 were not observed to increase Apobec3A expression (Figure 17). Consequently, the impact of these mutant viruses on Apobec3A SUMOylation would be very interesting to investigate in prospective experiments. Since E1B-55K as well as E4orf6 influence Apobec3A expression levels in the present work, it is assumed that both proteins affect Apobec3A SUMOylation, contributing to the increased Apobec3A SUMOylation during HAdV infection.

To determine the function of Apobec3A SUMOylation, potential SUMO mutants of Apobec3A were identified using the program *GPS SUMO (*The CUCKOO Workgroup). The five predicted SUMOylation sites at position 30, 47, 60, 137 and 159 in the Apobec3A sequence were cloned. Despite confirming the correct clones by agarose gels and sequencing, none of the Apobec3A mutations resulted in reduction or complete abolishment of Apobec3A SUMOylation in the Ni-NTA assay (Figure 37). This finding indicates that Apobec3A SUMOylation occurs at more than one lysine residue simultaneously. However, cloning and investigation of different Apobec3A double mutants (K30R/K47R, K30R/K60R, K47R/K60R, and K47R/K159R) also did not reveal a mutant of Apobec3A, which exhibits reduced or completely abolished SUMOylation. Consequently, a more detailed investigation of the present Apobec3A mutants is needed as well as further cloning steps combining more than two lysine mutations. Additionally, it should be considered, that only SUMO2 modification was analyzed in the present study, which emphasizes the urgent need of investigating SUMO1 and -3 as well. Taken together, the discovery of an Apobec3A SUMO mutant is desirable, as it could be included in prospective studies to reveal the function of Apobec3A SUMOylation.

In following experiments of the present work, the known ubiquitinylation of Apobec3A at lysine 137 could be confirmed [170]. Moreover, Apobec3A ubiquitin modification was decreased during HAdV infection (Figure 38), which probably contributes to the increased Apobec3A expression levels observed during adenoviral infection. A possible explanation therefore would be reduced interaction of Apobec3A with known binding partners that are targeting Apobec3A for ubiquitinylation and subsequent proteasomal degradation. As already discussed, UBE2L3 represents such a protein, thereby contributing to HBV replication [207]. In contrast to what was expected, UBE2L3 expression levels were elevated upon HAdV infection in initial experiments (data not shown). Thus, the localization of UBE2L3 or any interaction with Apobec3A might be affected by adenoviral infection.

Other proteins, so called STUBLs, were predicted to play an important role for Apobec3A ubiquitin modification, since they are known to target SUMOylated proteins for subsequent ubiquitinylation [208]. Indeed, investigation of the human STUBL RNF4 resulted in a decrease of Apobec3A ubiquitinylation during co-transfection experiments, which led to downregulated Apobec3A protein levels (Figure 39). However, RNF4-mediated increase of Apobec3A ubiquitin modification was counteracted during adenoviral infection (Figure 41). This was not surprising, since a relocalization of RNF4 during HAdV infection was recently published [165]. Thereby, the adenoviral early protein E1B-55K recruits RNF4 to the nuclear matrix fraction to promote RNF4-dependent ubiquitinylation of Daxx, which inhibits this antiviral factor [165]. Consequently, RNF4 is beneficial for HAdV infection on the one hand. On the other hand, it is assumed that RNF4 is not able to increase Apobec3A ubiquitinylation during HAdV infection, which might be due to the local separation of both proteins. This would represent a negative function of RNF4 for HAdV infection, since Apobec3A is not degraded and therefore able to restrict HAdV infection. However, further experiments are required to investigate this issue. Interestingly, no direct interaction could be detected for RNF4 and Apobec3A (Figure 40). Therefore, several explanations are plausible. First, the protocol of the performed IP experiment might need to be modified to detect the interaction of RNF4 and Apobec3A. Second, RNF4 and Apobec3A do not interact with each other and the increase of Apobec3A ubiquitinylation is the consequence of a signaling cascade involving several proteins. And third, RNF4 and Apobec3A interaction involves a third unknown factor, which interacts with both proteins in a complex. For instance, the HPV16 E7 protein also does not directly interact with Apobec3A. Hereby, cullin 2 is the factor, which interacts with both proteins, leading to a stabilization of Apobec3A by HPV16 E7 [234]. In conclusion, RNF4 seems to contribute to Apobec3A upregulation during HAdV infection due to its relocalization to the nuclear matrix fraction, which inhibits the RNF4-mediated increase of Apobec3A ubiquitinylation.

5.4. Apobec3A homodimer formation

Recently, Apobec3A was found to build homodimers, which is suggested to be its functional form [120]. After confirming the homodimer formation of Apobec3A in the present study (Figure 42), the question arose, how it is influenced by HAdV infection. Therefore, immunoprecipitation experiments were performed, pulling down YFP tagged Apobec3A and staining for V5 tagged Apobec3A during HAdV infection. Western blot analysis revealed an increased interaction of YFP and V5 tagged Apobec3A during HAdV infection in comparison to the mock control, indicating an upregulation of Apobec3A dimer formation during adenoviral infection (Figure 43). This is contradictive to the initial hypothesis, which suggested a repression of Apobec3A dimer formation during adenoviral infection to counteract Apobec3A restrictive functions. However, it matches the hypothesis of an antiviral

defense mechanism of the host cell, which increases Apobec3A expression levels, as well as its SUMOylation and dimerization to ensure efficient counteraction of HAdV infection. Thereby, Apobec3A SUMOylation is suggested to be required for its homodimerization. Interestingly, some of the residues predicted to be SUMOylated by the *GPS SUMO (*The CUCKOO Workgroup) program are known to be crucial for the dimer interface of Apobec3A, underlining the present assumption [120] (Figure 37). Among other residues, lysine 30 and 60 bridge the dimer interface and contribute to the positive charge and shape of the putative DNA-binding groove, thereby affecting substrate affinity and deamination [120]. K30 and K60 are conserved among Apobec3A orthologues of different primates, emphasizing their crucial role for Apobec3A functions [235]. However, these lysine residues are not conserved among different members of the Apobec3 family, since Apobec3G exhibits different amino acids at these positions [235]. Intriguingly, transferring lysines to the corresponding residues in the sequence of Apobec3G could confer restriction of LINE1 to Apobec3G, albeit to a less extent than Apobec3A inhibition of LINE1 [235, 236]. This demonstrates the importance of K30 and K60 for Apobec3A restrictive functions. Furthermore, SUMOylation is suggested to play an important role for Apobec3A functions, since K30 and K60 were predicted to be SUMOylated in the present study. However, despite performing different Apobec3A mutational analysis, it is still unclear, how many and which lysine residues are SUMO modified in the Apobec3A sequence. Hopefully, prospective studies will reveal an Apobec3A SUMO mutant, which can be used to further analyze the function of Apobec3A SUMOylation for homodimerization. Nevertheless, it is still believed that upregulated Apobec3A SUMOylation is required for the increasing formation of Apobec3A homodimers during adenoviral infection, representing an antiviral defense of the host cell. Since it was demonstrated that the increase of Apobec3A expression and SUMOylation is not conserved among different viruses, it would be interesting to examine if the upregulation of Apobec3A dimer formation is specific for HAdV or conserved among different viruses.

5.5. Concluding remarks

This work demonstrates HAdV restriction by Apobec3A, which requires the deaminase activity of Apobec3A. E2A SUMOylation was reduced upon Apobec3A expression, promoting impaired formation of adenoviral replication centers and indicating an additional mechanism how Apobec3A restricts HAdV. To counteract Apobec3A restrictive functions, its preferred target sequence, the TC dinucleotide, is underrepresented in the adenoviral genome, suggesting TC dinucleotide depletion during adenoviral evolution [119]. In contrast to what was expected, Apobec3A expression was increased during HAdV infection, which might be due to its reduced ubiquitinylation. Beyond that, we suggest that a protein network is involved in Apobec3A upregulation during HAdV infection, including the viral proteins E1B-55K and E4orf6 as well as the cellular proteins p53 and RNF4 (Figure 44). Thereby, the influence of

further proteins, such as UBE2L3 and/or KAP1 is currently discussed and under investigation. Finally, Apobec3A SUMOylation as well as homodimer formation were upregulated during HAdV infection. Since the same residues predicted to be SUMO modified are involved in Apobec3A dimerization [120], we hypothesized that Apobec3A SUMOylation might be required for the dimer formation. The increase of Apobec3A expression levels, as well as its SUMOylation and dimerization is currently believed to represent a cellular antiviral defense mechanism, ensuring an adequate amount of Apobec3A in its active form to counteract HAdV infection. A schematic overview of the observed findings in the present work is depicted in Figure 45.

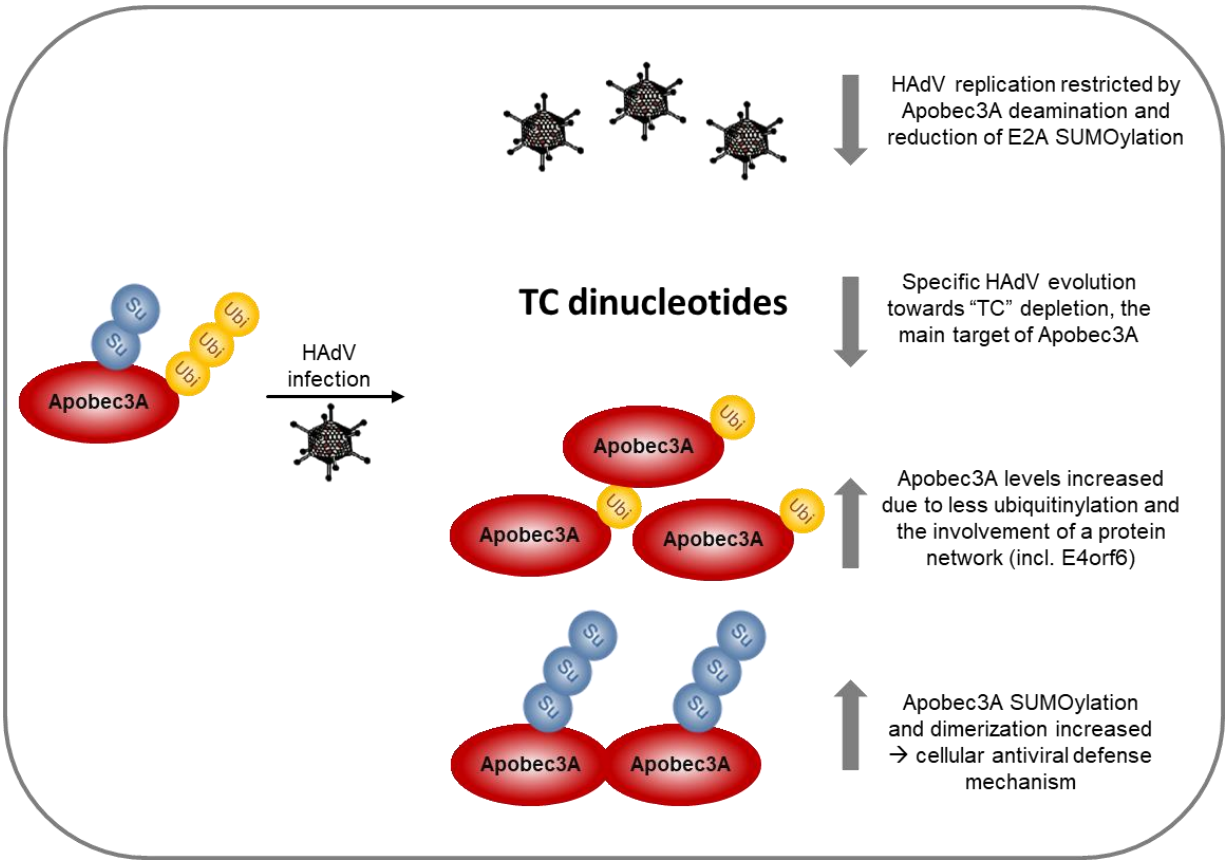

Figure 45: Schematic representation of the observed findings in this work.
Apobec3A inhibits HAdV infection, which counteracts Apobec3A restrictive functions by evolving towards TC dinucleotide depletion. Nevertheless, HAdV infection was shown to drastically increase Apobec3A expression levels, as well as its SUMOylation and dimer formation, which is thought to be an antiviral effect of the host cell.

5.6. Clinical relevance of the study

The outcome of the present study provides novel insights into HAdV-host interplay and evolved strategies, which will improve future HAdV treatment options and HAdV vector application and safety in clinical approaches.

HAdV infections are mild and self-limiting in healthy patients, whereas they can cause severe outcome with high morbidity and mortality in immunocompromised patients, like AIDS or transplant patients [18, 237]. So far, there is no specific treatment for adenoviral infections and therapy is only limited to common anti-viral drugs, like cidofovir or ribavirin, which can lead to severe, potential life-threatening side effects, especially in pediatric patients [22, 23]. Consequently, new therapeutic approaches are necessary to minimize fatal outcomes of HAdV infections in immunocompromised patients, which requires basic research in the field of HAdV-host interplay. In the present work, it was shown that HAdV infection is severely restricted by Apobec3A (Figure 21-25). Due to a lack of functional antibodies for endogenous Apobec3A, the findings of this study were only observed for Apobec3A overexpression. Therefore, it is required to confirm these results investigating endogenous Apobec3A. The problem is currently dealt in the Schreiner lab by establishing an endogenous Apobec3A knockdown cell line using small hairpin RNA (shRNA). Thereby, the cell line is assumed to increase HAdV infection, which would prove efficient HAdV restriction by endogenous Apobec3A. During adenoviral infection, Apobec3A expression levels were increased in several different cell lines (Figure 13), suggesting an antiviral response mechanism of the host cell to diminish HAdV infection. Thus, Apobec3A upregulation occurs quite late during HAdV infection and it would be interesting to study the effect of upregulated Apobec3A expression levels already before initial adenoviral infection. Apobec3 expression is induced by interferon alpha [238]. As a consequence, HBV infection was treated with interferon alpha, leading to the inhibition of HBV replication by the upregulation of Apobec3A expression levels [103]. In accordance with that, it was demonstrated that the E1A protein of HAdV counteracts interferon alpha responses of the host cell for efficient virus replication [239]. Furthermore, interferon beta was already shown to be effective against adenovirus-induced epidemic keratoconjunctivitis [240]. Consequently, it is recommended to study the effect of interferon alpha treatment of cells before adenoviral infection. However, dosing of interferon alpha treatment requires careful assignment, since elevated Apobec3A levels come at a cost of genomic DNA deamination, thereby threatening genomic integrity. If the desired effect would be observed, the next step would be to analyze interferon-alpha-induced upregulation of Apobec3A and its impact on HAdV infection in animal models as well as clinical trials, which could finally lead to improved therapeutic strategies for adenoviral infections.

Furthermore, HAdV have been extensively investigated concerning their application as vaccine vectors, including new clinical trials to establish vaccines for Ebola or HIV [241-243].

Thereby, the adenoviral vectors are constructed to express a viral immunogenic protein, like the glycoprotein of the Zaire Ebolavirus, to elicit high T and B cell responses in the vaccinated individuum [242]. To apply the newly obtained information from the present study, it might be valuable to increase Apobec3A expression to elicit higher immune responses during HAdV-based vaccine development. This would be in accordance with a recent publication, showing an increase of Apobec3G expression in CD4+ T cells after mucosal immunization in macaques, suggesting a memory-like function for Apobec3G [244]. Additionally, adenoviral vectors are the most used vectors in the field of gene therapy, which could be another approach that might benefit from the observed findings in the present work [245, 246]. Hereby, the adenoviral vector is used as a delivery vehicle, to transfer therapeutic genes for the treatment of genetic or acquired diseases, for example the HAdV-based transfer of exogenous p53 into patients suffering from glioma [246, 247]. Silencing Apobec3A gene expression in target cells might therefore be beneficial for improved adenovirus vector gene transfer, due to reduced antiviral defenses of the cell. Moreover, oncolytic adenoviruses were identified as a new class of anticancer agents, which have been extensively examined in recent studies [248]. One example therefore is the oncolytic adenovirus Onyx-015, with an E1B-55K gene deletion, leading to its exclusive replication and lysis of cancer cells lacking functional p53 variants [249]. Also in this case, suppression of Apobec3A expression would be advantageous to enable efficient tumor cell elimination by the modified adenoviruses without Apobec3A restriction. Taken together, the present study substantially extended the current knowledge concerning HAdV-host interplay and provides a solid basis for further basic research and future clinical trials.

6. Addendum

6.1. Abbreviations

µg	Microgram
µl	Microliter
AAV	Adeno-associated virus
Apobec	Apolipoprotein B mRNA editing catalytic polypeptide-like
bp	Base pair
BSA	Bovine serum albumin
CAR	Coxsackievirus-adenovirus receptor
CMV	Cytomegalovirus
DAPI	4′,6-diamidino-2-phenylindole
DBP	DNA-binding protein
DDR	DNA damage response
DMEM	Dulbecco's Modified Eagle Medium
DMSO	Dimethyl sulfoxide
DNA	Desoxyribonucleic acid
ds	Double-stranded
DSB	Double-strand breaks
E.coli	*Escherichia coli*
FBS	Fecal bovine serum
ffu	Fluorescent forming units
fwd	Forward
h	Hours
H1299	Human non-small cell lung carcinoma cell line
HAdV	Human Adenovirus
HBV	Hepatitis B virus
HeLa	Human cervical carcinoma cell line
HepaRG	Human hepatic progenitor cell line
His	Histidine
HIV	human immunodeficiency virus
HIV-1	Human immunodeficiency virus type 1
HP1	Heterochromatin protein 1
HPV	Human papillomavirus
HRP	Horseradish peroxidase
IF	Immunofluorescence
IP	Immunoprecipitation

ITR	Inverted terminal repeats
K	Lysine
KAP1	KRAB-associated protein 1
kb	Kilobase
kbp	Kilobase pairs
kDa	Kilodalton
LB	Luria-bertani
mA	Milliampere
mg	Milligram
ml	Milliliter
MLTU	Major late transcription unit
MOI	Multiplicity of infection
MRN	Mre11-Rad50-Nbs1
Ni-NTA	Nickel-nitrilotriacetic acid
nm	Nanometer
OD	Optical density
ORF	Open reading frame
PAGE	Polyacrylamide gel electrophoresis
PBS	Phosphate buffered saline
PCR	Polymerase chain reaction
PEI	Polyethylenimine
PFA	Paraformaldehyde
PML	Promyelocytic leukemia protein
PML-NB	PML nuclear body
PMSF	Phenylmethylsulfonyl fluoride
PTM	Posttranslational modification
PVDF	Polyvinylidene fluoride
rev	Reverse
RGD	Arg-Gly-Asp
RING	Really interesting new gene
RIPA	Radioimmunoprecipitation assay
RNA	Ribonucleic acid
rpm	Rotations per minute
RT	Room temperature
SDS	Sodium dodecyl sulphate
SDS-PAGE	SDS-polyacrylamid gel electrophoresis
shRNA	Small hairpin RNA

SIM	SUMO interacting motif
ss	Single-stranded
STUbL	SUMO-targeted ubiquitin ligases
SUMO	Small ubiquitin-related modifier
TBE	Tris/Borate/EDTA buffer
TBS-BG	Tris-buffered saline with BSA and glycine
TGS	Tris, glycine, SDS
TP	Terminal protein
TRIB3	Human tribbles 3
UBE2L3	Ubiquitin conjugating enzyme E2 L3
UNG2	Uracil-N-glycosylase 2
UV	Ultraviolet
V	Volt
v/v	Volume per volume
w/v	Weight per volume
wt	Wild type
YFP	Yellow fluorescent protein

6.2. List of Figures

6.3. Acknowledgments

First, I would like to express my sincere gratitude to my first supervisor PD Dr. Sabrina Schreiner for giving me the opportunity to work on that very interesting project in her group. I am very grateful for her exceptional supervision and patience, never giving up in supporting me scientifically and personally. Starting with not using the word “somehow” in scientific presentations, I learned so much from her during my whole PhD time and I am really grateful for that. We also had such a great time together, spending so many funny as well as emotional moments, which I will never forget!

I also want to thank my second supervisor Prof. Dr. Percy Knolle and my mentor Prof. Dr. Andreas Pichlmair for their great support with helpful suggestions and nice discussions of results and hypotheses.

Additionally, I want to acknowledge Prof. Dr. Ulrike Protzer and Dr. Daniela Stadler for their support and constructive discussions and suggestions for my project.

Special thanks go to all the lovely people of our group: Peter Groitl, Miona Stubbe, Verena Plank, Sawinee Masser, Samuel Hofmann, Julia Mai, Lilian Göttig, Maryam Karimi, Johanna Markert, Nathalie Skvorc, Ute Finkel. Without their great support, my PhD would not have been possible. I will always remember great scientific discussions, really interesting conferences together, as well as having a nice time at the beer garden, barbecuing or going to the Oktoberfest.

Furthermore, I also want to thank all the current and former members of the institute of Virology for supporting me during my PhD time and having such a great time together.

I am deeply thankful to Lilian Göttig and Frédéric Schedel for proofreading of the thesis and giving many helpful advices.

Finally, I like to thank my parents and whole family, as well as my friends and especially Freddy for always being there for me during the time of my PhD thesis. Without them, I would not have been able to reach that point where am I now, so I am deeply grateful for all their support, inspiration, motivation and faith in me!

6.4. Publications and Conferences

6.4.1. Articles in peer-reviewed journals

Müncheberg S, Hay RT, Ip WH, Meyer T, **Weiß C**, Brenke J, Masser S, Hadian K, Dobner T, Schreiner S. 2018: *E1B-55K-Mediated Regulation of RNF4 SUMO-Targeted Ubiquitin Ligase Promotes Human Adenovirus Gene Expression.* J Virol. 2018 Jun 13;92(13).

Weiß et al. (manuscript in preparation, this work)

6.4.2. Presentations at scientific conferences

2017 - 1st annual IRTG PhD and Post-Doc Retreat (DFG TRR 179)

February 6 – 8, 2017, Bad Herrenalb, Germany

Oral presentation: Apobec3A is a novel restriction factor antagonizing efficient HAdV replication

2017 - Retreat of the Institute of Virology 2017

May 31 – June 1, 2017, Tutzing, Germany

Oral presentation: Apobec3A is a novel restriction factor antagonizing efficient HAdV replication

2017 - DNA Tumour Virus Conference 2017

July 17 – 22, 2017, University of Birmingham, England, UK

Oral presentation: Apobec3A is a novel restriction factor antagonizing efficient HAdV replication

Financial support: travel grant of GlaxoSmithKline

2017 - 4th ASM Conference on viral manipulation of nuclear processes

December 3 – 6, 2017, Charleston, South Carolina, USA

Poster presentation: Apobec3A is a novel restriction factor antagonizing efficient HAdV replication

2018 - 28th annual Meeting of the Society of Virology

March 14 – 17, 2018, Julius-Maximilians-Universität, Würzburg, Germany

Oral presentation: Apobec3A is a novel restriction factor antagonizing efficient HAdV replication

Financial support: travel grant of the Society of Virology

2018 - Retreat of the Institute of Virology 2018

June 18 – 19, 2018, Herrsching, Germany

Oral presentation: Apobec3A is a novel restriction factor antagonizing efficient HAdV replication

2019 - 29th annual Meeting of the Society of Virology

March, 20 – 23, 2019, Heinrich-Heine-Universität, Düsseldorf, Germany

Poster presentation: Apobec3A is a novel restriction factor antagonizing efficient HAdV replication

2019 - Retreat of the Institute of Virology 2019

June 18 – 19, 2019, Herrsching, Germany

Oral presentation: Apobec3A is a novel restriction factor antagonizing efficient HAdV replication

7. References

1. Hllleman, M. and J.H. Werner, *Recovery of new agent from patients with acute respiratory illness.* Proceedings of the Society for Experimental Biology and Medicine, 1954. **85**(1): p. 183-188.
2. Rowe, W.P., et al., *Isolation of a cytopathogenic agent from human adenoids undergoing spontaneous degeneration in tissue culture.* Proceedings of the Society for Experimental Biology and Medicine, 1953. **84**(3): p. 570-573.
3. Enders, J.F., et al., *" Adenoviruses": Group name proposed for new respiratory-tract viruses.* Science (Washington), 1956. **124**: p. 119-20.
4. Benkö, M. and B. Harrach, *A proposal for a new (third) genus within the family Adenoviridae.* Archives of virology, 1998. **143**(4): p. 829-837.
5. Bailey, A. and V. Mautner, *Phylogenetic relationships among adenovirus serotypes.* Virology, 1994. **205**(2): p. 438-452.
6. Wadell, G., *Molecular epidemiology of human adenoviruses*, in *The Molecular Biology of Adenoviruses 2*. 1984, Springer. p. 191-220.
7. Dhingra, A., et al., *Molecular evolution of Human Adenovirus (HAdV) species C.* Scientific reports, 2019. **9**(1): p. 1039.
8. Hashimoto, S., et al., *Recombinant type Human mastadenovirus D85 associated with epidemic keratoconjunctivitis since 2015 in Japan.* Journal of medical virology, 2018. **90**(5): p. 881-889.
9. Jones, M.S., et al., *New adenovirus species found in a patient presenting with gastroenteritis.* Journal of virology, 2007. **81**(11): p. 5978-5984.
10. Berk, A., *Adenoviridae: the viruses and their replication.* Fields virology, 2007. **2**: p. 2355-2394.
11. Chen, S. and X. Tian, *Vaccine development for human mastadenovirus.* Journal of thoracic disease, 2018. **10**(Suppl 19): p. S2280.
12. Shenk, T.E., *Adenoviridae: the viruses and their replication.* Fundamental virology, 2001: p. 1053-1088.
13. Roberts, R.J., K.E. O'Neill, and C.T. Yen, *DNA sequences from the adenovirus 2 genome.* Journal of Biological Chemistry, 1984. **259**(22): p. 13968-13975.
14. Yabe, Y., J.J. Trentin, and G. Taylor, *Cancer induction in hamsters by human type 12 adenovirus. Effect of age and of virus dose.* Proceedings of the Society for Experimental Biology and Medicine, 1962. **111**(2): p. 343-344.
15. Jawetz, E., et al., *A Laboratory Infection with Adenovirus Type 8. Laboratory and Epidemiologic Observations.* American journal of hygiene, 1959. **69**(1): p. 13-20.
16. Albert, M., *Enteric adenoviruses.* Archives of Virology, 1986. **88**(1-2): p. 1-17.
17. Yolken, R.H., et al., *Gastroenteritis associated with enteric type adenovirus in hospitalized infants.* The Journal of pediatrics, 1982. **101**(1): p. 21-26.
18. Echavarría, M., *Adenoviruses in immunocompromised hosts.* Clinical microbiology reviews, 2008. **21**(4): p. 704-715.
19. Carrigan, D.R., *Adenovirus infections in immunocompromised patients.* The American journal of medicine, 1997. **102**(3): p. 71-74.
20. Louie, J.K., et al., *Severe pneumonia due to adenovirus serotype 14: a new respiratory threat?* Clinical infectious diseases, 2008. **46**(3): p. 421-425.
21. Lenaerts, L., E. De Clercq, and L. Naesens, *Clinical features and treatment of adenovirus infections.* Reviews in medical virology, 2008. **18**(6): p. 357-374.
22. Gavin, P.J. and B.Z. Katz, *Intravenous ribavirin treatment for severe adenovirus disease in immunocompromised children.* Pediatrics, 2002. **110**(1): p. e9-e9.
23. Ganapathi, L., et al., *Use of cidofovir in pediatric patients with adenovirus infection.* F1000Research, 2016. **5**.
24. Rux, J.J. and R.M. Burnett, *Adenovirus structure.* Human gene therapy, 2004. **15**(12): p. 1167-1176.
25. Davison, A.J., M. Benkő, and B. Harrach, *Genetic content and evolution of adenoviruses.* Journal of General Virology, 2003. **84**(11): p. 2895-2908.

26. Nemerow, G., et al., *Insights into adenovirus host cell interactions from structural studies.* Virology, 2009. **384**(2): p. 380-388.
27. Russell, W., *Adenoviruses: update on structure and function.* Journal of General Virology, 2009. **90**(1): p. 1-20.
28. Bergelson, J.M., et al., *Isolation of a common receptor for Coxsackie B viruses and adenoviruses 2 and 5.* Science, 1997. **275**(5304): p. 1320-1323.
29. Wu, E., et al., *Flexibility of the adenovirus fiber is required for efficient receptor interaction.* Journal of virology, 2003. **77**(13): p. 7225-7235.
30. Gaggar, A., D.M. Shayakhmetov, and A. Lieber, *CD46 is a cellular receptor for group B adenoviruses.* Nature medicine, 2003. **9**(11): p. 1408.
31. Mathias, P., et al., *Multiple adenovirus serotypes use alpha v integrins for infection.* Journal of virology, 1994. **68**(10): p. 6811-6814.
32. Vellinga, J., S. Van der Heijdt, and R.C. Hoeben, *The adenovirus capsid: major progress in minor proteins.* Journal of General Virology, 2005. **86**(6): p. 1581-1588.
33. Wiethoff, C.M., et al., *Adenovirus protein VI mediates membrane disruption following capsid disassembly.* Journal of virology, 2005. **79**(4): p. 1992-2000.
34. Schreiner, S., et al., *Transcriptional activation of the adenoviral genome is mediated by capsid protein VI.* PLoS pathogens, 2012. **8**(2): p. e1002549.
35. Harpst, J., J. Ennever, and W. Russell, *Physical properties of nucleoprotein cores from adenovirus type 5.* Nucleic acids research, 1977. **4**(2): p. 477-490.
36. Russell, W. and B. Precious, *Nucleic acid-binding properties of adenovirus structural polypeptides.* Journal of General Virology, 1982. **63**(1): p. 69-79.
37. Everitt, E., L. Lutter, and L. Philipson, *Structural proteins of adenoviruses: XII. Location and neighbor relationship among proteins of adenovirion type 2 as revealed by enzymatic lodination, immunoprecipitation and chemical cross-linking.* Virology, 1975. **67**(1): p. 197-208.
38. Zhang, W., et al., *Role for the adenovirus IVa2 protein in packaging of viral DNA.* Journal of virology, 2001. **75**(21): p. 10446-10454.
39. Webster, A., et al., *Characterization of the adenovirus proteinase: substrate specificity.* Journal of General Virology, 1989. **70**(12): p. 3225-3234.
40. Wadell, G., *Mastadenovirus*, in *The Springer Index of Viruses*, C.A. Tidona, G. Darai, and C. Büchen-Osmond, Editors. 2001, Springer Berlin Heidelberg: Berlin, Heidelberg. p. 19-28.
41. Weinmann, R., H.J. Raskas, and R.G. Roeder, *Role of DNA-dependent RNA polymerases II and III in transcription of the adenovirus genome late in productive infection.* Proceedings of the National Academy of Sciences, 1974. **71**(9): p. 3426-3430.
42. Ahi, Y.S. and S.K. Mittal, *Components of adenovirus genome packaging.* Frontiers in microbiology, 2016. **7**: p. 1503.
43. Wold, W. and M. Horwitz, *Adenoviruses.* Fields Virology, 5th edition, 2007.
44. Varga, M.J., C. Weibull, and E. Everitt, *Infectious entry pathway of adenovirus type 2.* Journal of virology, 1991. **65**(11): p. 6061-6070.
45. Blumenthal, R., et al., *pH-dependent lysis of liposomes by adenovirus.* Biochemistry, 1986. **25**(8): p. 2231-2237.
46. Wickham, T.J., et al., *Integrin alpha v beta 5 selectively promotes adenovirus mediated cell membrane permeabilization.* The Journal of cell biology, 1994. **127**(1): p. 257-264.
47. Leopold, P.L., et al., *Dynein-and microtubule-mediated translocation of adenovirus serotype 5 occurs after endosomal lysis.* Human gene therapy, 2000. **11**(1): p. 151-165.
48. Greber, U.F., et al., *The role of the nuclear pore complex in adenovirus DNA entry.* The EMBO journal, 1997. **16**(19): p. 5998-6007.
49. Harlow, E., et al., *Association of adenovirus early-region 1A proteins with cellular polypeptides.* Molecular and cellular biology, 1986. **6**(5): p. 1579-1589.
50. Berk, A.J., *Adenovirus promoters and E1A transactivation.* Annual review of genetics, 1986. **20**(1): p. 45-77.

51. Nevins, J.R., *Mechanism of activation of early viral transcription by the adenovirus E1A gene product.* Cell, 1981. **26**(2): p. 213-220.
52. Berk, A., *Functions of adenovirus E1A.* Cancer surveys, 1986. **5**(2): p. 367-387.
53. Windheim, M., A. Hilgendorf, and H.-G. Burgert, *Immune evasion by adenovirus E3 proteins: exploitation of intracellular trafficking pathways*, in *Adenoviruses: Model and Vectors in Virus-Host Interactions*. 2004, Springer. p. 29-85.
54. de Jong, R.N., P.C. van der Vliet, and A.B. Brenkman, *Adenovirus DNA replication: protein priming, jumping back and the role of the DNA binding protein DBP*, in *Adenoviruses: Model and Vectors in Virus-Host Interactions*. 2003, Springer. p. 187-211.
55. Debbas, M. and E. White, *Wild-type p53 mediates apoptosis by E1A, which is inhibited by E1B.* Genes & development, 1993. **7**(4): p. 546-554.
56. Waye, M.M.Y. and C.W. Sing, *Anti-viral drugs for human adenoviruses.* Pharmaceuticals, 2010. **3**(10): p. 3343-3354.
57. Nevins, J. and J. Darnell, *Groups of adenovirus type 2 mRNA's derived from a large primary transcript: probable nuclear origin and possible common 3'ends.* Journal of virology, 1978. **25**(3): p. 811-823.
58. Beltz, G.A. and S. Flint, *Inhibition of HeLa cell protein synthesis during adenovirus infection: restriction of cellular messenger RNA sequences to the nucleus.* Journal of molecular biology, 1979. **131**(2): p. 353-373.
59. Horwitz, M.S., M.D. Scharff, and J.V. Maizel Jr, *Synthesis and assembly of adenovirus 2: I. Polypeptide synthesis, assembly of capsomeres, and morphogenesis of the virion.* Virology, 1969. **39**(4): p. 682-694.
60. Hong, S.S., et al., *The 100K-chaperone protein from adenovirus serotype 2 (Subgroup C) assists in trimerization and nuclear localization of hexons from subgroups C and B adenoviruses.* Journal of molecular biology, 2005. **352**(1): p. 125-138.
61. Fessler, S.P. and C. Young, *The role of the L4 33K gene in adenovirus infection.* Virology, 1999. **263**(2): p. 507-516.
62. Velicer, L.F. and H. Ginsberg, *Synthesis, transport, and morphogenesis of type 5 adenovirus capsid proteins.* Journal of virology, 1970. **5**(3): p. 338-352.
63. Hearing, P., et al., *Identification of a repeated sequence element required for efficient encapsidation of the adenovirus type 5 chromosome.* Journal of virology, 1987. **61**(8): p. 2555-2558.
64. Tollefson, A.E., et al., *The adenovirus death protein (E3-11.6 K) is required at very late stages of infection for efficient cell lysis and release of adenovirus from infected cells.* Journal of virology, 1996. **70**(4): p. 2296-2306.
65. Weiden, M.D. and H.S. Ginsberg, *Deletion of the E4 region of the genome produces adenovirus DNA concatemers.* Proceedings of the National Academy of Sciences, 1994. **91**(1): p. 153-157.
66. Schreiner, S., P. Wimmer, and T. Dobner, *Adenovirus degradation of cellular proteins.* Future microbiology, 2012. **7**(2): p. 211-225.
67. Blanchette, P., et al., *Both BC-box motifs of adenovirus protein E4orf6 are required to efficiently assemble an E3 ligase complex that degrades p53.* Molecular and cellular biology, 2004. **24**(21): p. 9619-9629.
68. Querido, E., et al., *Degradation of p53 by adenovirus E4orf6 and E1B55K proteins occurs via a novel mechanism involving a Cullin-containing complex.* Genes & development, 2001. **15**(23): p. 3104-3117.
69. Schreiner, S., et al., *Proteasome-dependent degradation of Daxx by the viral E1B-55K protein in human adenovirus-infected cells.* Journal of virology, 2010. **84**(14): p. 7029-7038.
70. Schreiner, S., et al., *SPOC1-mediated antiviral host cell response is antagonized early in human adenovirus type 5 infection.* PLoS pathogens, 2013. **9**(11): p. e1003775.

71. Cheng, C.Y., et al., *Role of E1B55K in E4orf6/E1B55K E3 ligase complexes formed by different human adenovirus serotypes.* Journal of virology, 2013. **87**(11): p. 6232-6245.
72. Stracker, T.H., C.T. Carson, and M.D. Weitzman, *Adenovirus oncoproteins inactivate the Mre11–Rad50–NBS1 DNA repair complex.* Nature, 2002. **418**(6895): p. 348.
73. Evans, J.D. and P. Hearing, *Relocalization of the Mre11-Rad50-Nbs1 complex by the adenovirus E4 ORF3 protein is required for viral replication.* Journal of virology, 2005. **79**(10): p. 6207-6215.
74. Evans, J.D. and P. Hearing, *Distinct roles of the adenovirus E4 ORF3 protein in viral DNA replication and inhibition of genome concatenation.* Journal of virology, 2003. **77**(9): p. 5295-5304.
75. Salter, J.D., R.P. Bennett, and H.C. Smith, *The APOBEC protein family: united by structure, divergent in function.* Trends in biochemical sciences, 2016. **41**(7): p. 578-594.
76. Jarmuz, A., et al., *An anthropoid-specific locus of orphan C to U RNA-editing enzymes on chromosome 22.* Genomics, 2002. **79**(3): p. 285-296.
77. Petersen-Mahrt, S.K., R.S. Harris, and M.S. Neuberger, *AID mutates E. coli suggesting a DNA deamination mechanism for antibody diversification.* Nature, 2002. **418**(6893): p. 99.
78. Koning, F.A., et al., *Defining APOBEC3 expression patterns in human tissues and hematopoietic cell subsets.* Journal of virology, 2009. **83**(18): p. 9474-9485.
79. Stenglein, M.D., et al., *APOBEC3 proteins mediate the clearance of foreign DNA from human cells.* Nature structural & molecular biology, 2010. **17**(2): p. 222.
80. Bross, L., et al., *DNA double-strand breaks: prior to but not sufficient in targeting hypermutation.* Journal of Experimental Medicine, 2002. **195**(9): p. 1187-1192.
81. Landry, S., et al., *APOBEC3A can activate the DNA damage response and cause cell-cycle arrest.* EMBO reports, 2011. **12**(5): p. 444-450.
82. Holmes, R.K., M.H. Malim, and K.N. Bishop, *APOBEC-mediated viral restriction: not simply editing?* Trends in biochemical sciences, 2007. **32**(3): p. 118-128.
83. Sowden, M.P., et al., *The editosome for cytidine to uridine mRNA editing has a native complexity of 27S: identification of intracellular domains containing active and inactive editing factors.* Journal of cell science, 2002. **115**(5): p. 1027-1039.
84. Methot, S.P., et al., *Consecutive interactions with HSP90 and eEF1A underlie a functional maturation and storage pathway of AID in the cytoplasm.* Journal of Experimental Medicine, 2015. **212**(4): p. 581-596.
85. Bennett, R.P., et al., *Nuclear Exclusion of the HIV-1 host defense factor APOBEC3G requires a novel cytoplasmic retention signal and is not dependent on RNA binding.* Journal of Biological Chemistry, 2008. **283**(12): p. 7320-7327.
86. Smith, H.C., et al. *Functions and regulation of the APOBEC family of proteins*. in *Seminars in cell & developmental biology*. 2012. Elsevier.
87. Alexandrov, L.B., et al., *Signatures of mutational processes in human cancer.* Nature, 2013. **500**(7463): p. 415.
88. Yamanaka, S., et al., *A novel translational repressor mRNA is edited extensively in livers containing tumors caused by the transgene expression of the apoB mRNA-editing enzyme.* Genes & development, 1997. **11**(3): p. 321-333.
89. Burns, M.B., et al., *APOBEC3B is an enzymatic source of mutation in breast cancer.* Nature, 2013. **494**(7437): p. 366.
90. Harris, R.S. and J.P. Dudley, *APOBECs and virus restriction.* Virology, 2015. **479**: p. 131-145.
91. Madani, N. and D. Kabat, *An endogenous inhibitor of human immunodeficiency virus in human lymphocytes is overcome by the viral Vif protein.* Journal of virology, 1998. **72**(12): p. 10251-10255.
92. Apolonia, L., et al., *Promiscuous RNA binding ensures effective encapsidation of APOBEC3 proteins by HIV-1.* PLoS pathogens, 2015. **11**(1): p. e1004609.
93. Mangeat, B., et al., *Broad antiretroviral defence by human APOBEC3G through lethal editing of nascent reverse transcripts.* Nature, 2003. **424**(6944): p. 99.

94. Iwatani, Y., et al., *Deaminase-independent inhibition of HIV-1 reverse transcription by APOBEC3G.* Nucleic Acids Res, 2007. **35**(21): p. 7096-108.
95. Holmes, R.K., et al., *APOBEC3F can inhibit the accumulation of HIV-1 reverse transcription products in the absence of hypermutation. Comparisons with APOBEC3G.* J Biol Chem, 2007. **282**(4): p. 2587-95.
96. Yu, X., et al., *Induction of APOBEC3G ubiquitination and degradation by an HIV-1 Vif-Cul5-SCF complex.* Science, 2003. **302**(5647): p. 1056-60.
97. Mahieux, R., et al., *Extensive editing of a small fraction of human T-cell leukemia virus type 1 genomes by four APOBEC3 cytidine deaminases.* Journal of General Virology, 2005. **86**(9): p. 2489-2494.
98. Ooms, M., et al., *APOBEC3A, APOBEC3B and APOBEC3H haplotype 2 restrict human T-lymphotropic virus type I (HTLV-1).* Journal of virology, 2012: p. JVI. 06570-11.
99. Navarro, F., et al., *Complementary function of the two catalytic domains of APOBEC3G.* Virology, 2005. **333**(2): p. 374-386.
100. Strebel, K., *APOBEC3G & HTLV-1: inhibition without deamination.* Retrovirology, 2005. **2**: p. 37.
101. Beggel, B., et al., *Full genome ultra-deep pyrosequencing associates G-to-A hypermutation of the hepatitis B virus genome with the natural progression of hepatitis B.* Journal of viral hepatitis, 2013. **20**(12): p. 882-889.
102. Suspene, R., et al., *Extensive editing of both hepatitis B virus DNA strands by APOBEC3 cytidine deaminases in vitro and in vivo.* Proceedings of the National Academy of Sciences, 2005. **102**(23): p. 8321-8326.
103. Lucifora, J., et al., *Specific and nonhepatotoxic degradation of nuclear hepatitis B virus cccDNA.* Science, 2014. **343**(6176): p. 1221-1228.
104. Chen, H., et al., *APOBEC3A is a potent inhibitor of adeno-associated virus and retrotransposons.* Current Biology, 2006. **16**(5): p. 480-485.
105. Narvaiza, I., et al., *Deaminase-independent inhibition of parvoviruses by the APOBEC3A cytidine deaminase.* PLoS pathogens, 2009. **5**(5): p. e1000439.
106. Vartanian, J.-P., et al., *Evidence for editing of human papillomavirus DNA by APOBEC3 in benign and precancerous lesions.* Science, 2008. **320**(5873): p. 230-233.
107. Westrich, J.A., et al., *Human papillomavirus 16 E7 stabilizes APOBEC3A protein by inhibiting cullin 2-dependent protein degradation.* Journal of virology, 2018: p. JVI. 01318-17.
108. Warren, C.J., et al., *APOBEC3A functions as a restriction factor of human papillomavirus.* Journal of virology, 2014: p. JVI. 02383-14.
109. Warren, C.J., et al., *Role of the host restriction factor APOBEC3 on papillomavirus evolution.* Virus evolution, 2015. **1**(1).
110. Muramatsu, M., et al., *Specific expression of activation-induced cytidine deaminase (AID), a novel member of the RNA-editing deaminase family in germinal center B cells.* Journal of Biological Chemistry, 1999. **274**(26): p. 18470-18476.
111. Tobollik, S., et al., *Epstein-Barr virus nuclear antigen 2 inhibits AID expression during EBV-driven B-cell growth.* Blood, 2006. **108**(12): p. 3859-3864.
112. Bekerman, E., et al., *A role for host activation-induced cytidine deaminase in innate immune defense against KSHV.* PLoS pathogens, 2013. **9**(11): p. e1003748.
113. Kremer, M., et al., *Vaccinia virus replication is not affected by APOBEC3 family members.* Virology journal, 2006. **3**(1): p. 86.
114. Berger, G., et al., *APOBEC3A is a specific inhibitor of the early phases of HIV-1 infection in myeloid cells.* PLoS pathogens, 2011. **7**(9): p. e1002221.
115. Carpenter, M.A., et al., *Methylcytosine and normal cytosine deamination by the foreign DNA restriction enzyme APOBEC3A.* Journal of Biological Chemistry, 2012. **287**(41): p. 34801-34808.
116. Thielen, B.K., et al., *Innate immune signaling induces high levels of TC-specific deaminase activity in primary monocyte-derived cells through expression of*

APOBEC3A isoforms. Journal of Biological Chemistry, 2010. **285**(36): p. 27753-27766.
117. Refsland, E.W., et al., *Quantitative profiling of the full APOBEC3 mRNA repertoire in lymphocytes and tissues: implications for HIV-1 restriction.* Nucleic acids research, 2010. **38**(13): p. 4274-4284.
118. Land, A.M., et al., *Endogenous APOBEC3A DNA cytosine deaminase is cytoplasmic and nongenotoxic.* Journal of Biological Chemistry, 2013. **288**(24): p. 17253-17260.
119. Logue, E.C., et al., *A DNA sequence recognition loop on APOBEC3A controls substrate specificity.* PLoS One, 2014. **9**(5): p. e97062.
120. Bohn, M.-F., et al., *The ssDNA mutator APOBEC3A is regulated by cooperative dimerization.* Structure, 2015. **23**(5): p. 903-911.
121. Kouno, T., et al., *Crystal structure of APOBEC3A bound to single-stranded DNA reveals structural basis for cytidine deamination and specificity.* Nature communications, 2017. **8**: p. 15024.
122. Mitra, M., et al., *Structural determinants of human APOBEC3A enzymatic and nucleic acid binding properties.* Nucleic acids research, 2013. **42**(2): p. 1095-1110.
123. Sharma, S., et al., *APOBEC3A cytidine deaminase induces RNA editing in monocytes and macrophages.* Nature communications, 2015. **6**: p. 6881.
124. Ciechanover, A., *The ubiquitin–proteasome pathway: on protein death and cell life.* The EMBO journal, 1998. **17**(24): p. 7151-7160.
125. Andreou, A.M. and N. Tavernarakis, *SUMOylation and cell signalling.* Biotechnology Journal: Healthcare Nutrition Technology, 2009. **4**(12): p. 1740-1752.
126. Haglund, K. and I. Dikic, *Ubiquitylation and cell signaling.* The EMBO journal, 2005. **24**(19): p. 3353-3359.
127. Mann, M. and O.N. Jensen, *Proteomic analysis of post-translational modifications.* Nature biotechnology, 2003. **21**(3): p. 255.
128. Khoury, G.A., R.C. Baliban, and C.A. Floudas, *Proteome-wide post-translational modification statistics: frequency analysis and curation of the swiss-prot database.* Scientific reports, 2011. **1**: p. 90.
129. Johnson, E.S., *Protein modification by SUMO.* Annual review of biochemistry, 2004. **73**(1): p. 355-382.
130. Dohmen, R.J., *SUMO protein modification.* Biochimica et Biophysica Acta (BBA)-Molecular Cell Research, 2004. **1695**(1-3): p. 113-131.
131. Schulman, B.A. and J.W. Harper, *Ubiquitin-like protein activation by E1 enzymes: the apex for downstream signalling pathways.* Nature reviews Molecular cell biology, 2009. **10**(5): p. 319.
132. Olsen, S.K., et al., *Active site remodelling accompanies thioester bond formation in the SUMO E1.* Nature, 2010. **463**(7283): p. 906.
133. Tatham, M.H., Y. Chen, and R.T. Hay, *Role of Two Residues Proximal to the Active Site of Ubc9 in Substrate Recognition by the Ubc9⊙ SUMO-1 Thiolester Complex.* Biochemistry, 2003. **42**(11): p. 3168-3179.
134. Jentsch, S., et al., *Ubiquitin-conjugating enzymes: novel regulators of eukaryotic cells.* Trends in biochemical sciences, 1990. **15**(5): p. 195-198.
135. Desterro, J.M., J. Thomson, and R.T. Hay, *Ubch9 conjugates SUMO but not ubiquitin.* FEBS letters, 1997. **417**(3): p. 297-300.
136. Hershko, A. and A. Ciechanover, *The ubiquitin system*. 1998, Annual Reviews 4139 El Camino Way, PO Box 10139, Palo Alto, CA 94303-0139, USA.
137. Schwartz, D.C. and M. Hochstrasser, *A superfamily of protein tags: ubiquitin, SUMO and related modifiers.* Trends in biochemical sciences, 2003. **28**(6): p. 321-328.
138. Knipscheer, P., et al., *Ubc9 sumoylation regulates SUMO target discrimination.* Molecular cell, 2008. **31**(3): p. 371-382.
139. Rodriguez, M.S., C. Dargemont, and R.T. Hay, *SUMO-1 conjugation in vivo requires both a consensus modification motif and nuclear targeting.* Journal of Biological Chemistry, 2001. **276**(16): p. 12654-12659.

140. Saitoh, H. and J. Hinchey, *Functional heterogeneity of small ubiquitin-related protein modifiers SUMO-1 versus SUMO-2/3.* Journal of Biological Chemistry, 2000. **275**(9): p. 6252-6258.
141. Tatham, M.H., et al., *Polymeric chains of SUMO-2 and SUMO-3 are conjugated to protein substrates by SAE1/SAE2 and Ubc9.* Journal of Biological Chemistry, 2001. **276**(38): p. 35368-35374.
142. Vertegaal, A.C., *SUMO chains: polymeric signals*. 2010, Portland Press Limited.
143. Chen, Z. and C.M. Pickart, *A 25-kilodalton ubiquitin carrier protein (E2) catalyzes multi-ubiquitin chain synthesis via lysine 48 of ubiquitin.* Journal of Biological Chemistry, 1990. **265**(35): p. 21835-21842.
144. Chau, V., et al., *A multiubiquitin chain is confined to specific lysine in a targeted short-lived protein.* Science, 1989. **243**(4898): p. 1576-1583.
145. Miteva, M., et al., *Sumoylation as a signal for polyubiquitylation and proteasomal degradation*, in *Conjugation and deconjugation of ubiquitin family modifiers*. 2010, Springer. p. 195-214.
146. Sun, H., J.D. Leverson, and T. Hunter, *Conserved function of RNF4 family proteins in eukaryotes: targeting a ubiquitin ligase to SUMOylated proteins.* The EMBO journal, 2007. **26**(18): p. 4102-4112.
147. Erker, Y., et al., *Arkadia, a novel SUMO-targeted ubiquitin ligase involved in PML degradation.* Molecular and cellular biology, 2013. **33**(11): p. 2163-2177.
148. Liew, C.W., et al., *RING domain dimerization is essential for RNF4 function.* Biochemical Journal, 2010. **431**(1): p. 23-29.
149. Prudden, J., et al., *SUMO-targeted ubiquitin ligases in genome stability.* The EMBO journal, 2007. **26**(18): p. 4089-4101.
150. Salinas, S. and E.J. Kremer, *Virus induced and associated post-translational modifications.* Biology of the Cell, 2012. **104**(3): p. 119-120.
151. Tsai, W.-H., et al., *Streptococcal pyrogenic exotoxin B-induced apoptosis in A549 cells is mediated through αvβ3 integrin and Fas.* Infection and immunity, 2008. **76**(4): p. 1349-1357.
152. Zhang, N.-H., et al., *Proteasome inhibitor MG-132 modifies coxsackie and adenovirus receptor expression in colon cancer cell line lovo.* Cell Cycle, 2008. **7**(7): p. 925-933.
153. Wodrich, H., et al., *A capsid-encoded PPxY-motif facilitates adenovirus entry.* PLoS pathogens, 2010. **6**(3): p. e1000808.
154. Horwitz, G.A., et al., *Adenovirus small e1a alters global patterns of histone modification.* Science, 2008. **321**(5892): p. 1084-1085.
155. Balakirev, M.Y., et al., *Deubiquitinating function of adenovirus proteinase.* Journal of virology, 2002. **76**(12): p. 6323-6331.
156. Sohn, S.-Y. and P. Hearing, *Adenovirus early proteins and host SUMOylation.* MBio, 2016. **7**(5): p. e01154-16.
157. Yousef, A., et al., *Identification of a molecular recognition feature in the E1A oncoprotein that binds the SUMO conjugase UBC9 and likely interferes with polySUMOylation.* Oncogene, 2010. **29**(33): p. 4693.
158. Ledl, A., D. Schmidt, and S. Müller, *Viral oncoproteins E1A and E7 and cellular LxCxE proteins repress SUMO modification of the retinoblastoma tumor suppressor.* Oncogene, 2005. **24**(23): p. 3810.
159. Endter, C., et al., *SUMO-1 modification required for transformation by adenovirus type 5 early region 1B 55-kDa oncoprotein.* Proceedings of the National Academy of Sciences, 2001. **98**(20): p. 11312-11317.
160. Wimmer, P., et al., *Cross-talk between phosphorylation and SUMOylation regulates transforming activities of an adenoviral oncoprotein.* Oncogene, 2013. **32**(13): p. 1626.
161. Burck, C., et al., *KAP1 Is a Host Restriction Factor That Promotes Human Adenovirus E1B-55K SUMO Modification.* J Virol, 2016. **90**(2): p. 930-46.
162. Pennella, M.A., et al., *Adenovirus E1B 55-kilodalton protein is a p53-SUMO1 E3 ligase that represses p53 and stimulates its nuclear export through interactions with*

promyelocytic leukemia nuclear bodies. Journal of virology, 2010. **84**(23): p. 12210-12225.
163. Muller, S. and T. Dobner, *The adenovirus E1B-55K oncoprotein induces SUMO modification of p53.* Cell Cycle, 2008. **7**(6): p. 754-758.
164. Schreiner, S., et al., *Adenovirus type 5 early region 1B 55K oncoprotein-dependent degradation of cellular factor Daxx is required for efficient transformation of primary rodent cells.* J Virol, 2011. **85**(17): p. 8752-65.
165. Muncheberg, S., et al., *E1B-55K-Mediated Regulation of RNF4 SUMO-Targeted Ubiquitin Ligase Promotes Human Adenovirus Gene Expression.* J Virol, 2018. **92**(13).
166. Sohn, S.Y. and P. Hearing, *Adenovirus regulates sumoylation of Mre11-Rad50-Nbs1 components through a paralog-specific mechanism.* J Virol, 2012. **86**(18): p. 9656-65.
167. Sohn, S.Y. and P. Hearing, *The adenovirus E4-ORF3 protein functions as a SUMO E3 ligase for TIF-1gamma sumoylation and poly-SUMO chain elongation.* Proc Natl Acad Sci U S A, 2016. **113**(24): p. 6725-30.
168. Forrester, N.A., et al., *Adenovirus E4orf3 targets transcriptional intermediary factor 1gamma for proteasome-dependent degradation during infection.* J Virol, 2012. **86**(6): p. 3167-79.
169. Bridges, R.G., et al., *The Adenovirus E4-ORF3 Protein Stimulates SUMOylation of General Transcription Factor TFII-I to Direct Proteasomal Degradation.* MBio, 2016. **7**(1): p. e02184-15.
170. Kim, W., et al., *Systematic and quantitative assessment of the ubiquitin-modified proteome.* Molecular cell, 2011. **44**(2): p. 325-340.
171. Hanahan, D., *Studies on transformation of Escherichia coli with plasmids.* Journal of molecular biology, 1983. **166**(4): p. 557-580.
172. Marion, M.-J., O. Hantz, and D. Durantel, *The HepaRG cell line: biological properties and relevance as a tool for cell biology, drug metabolism, and virology studies*, in *Hepatocytes*. 2010, Springer. p. 261-272.
173. Lucey, B.P., W.A. Nelson-Rees, and G.M. Hutchins, *Henrietta Lacks, HeLa cells, and cell culture contamination.* Archives of pathology & laboratory medicine, 2009. **133**(9): p. 1463-1467.
174. Vertegaal, A.C., et al., *A proteomic study of SUMO-2 target proteins.* Journal of Biological Chemistry, 2004. **279**(32): p. 33791-33798.
175. Sloan, E., et al., *Analysis of the SUMO2 proteome during HSV-1 infection.* PLoS pathogens, 2015. **11**(7): p. e1005059.
176. Mitsudomi, T., et al., *p53 gene mutations in non-small-cell lung cancer cell lines and their correlation with the presence of ras mutations and clinical features.* Oncogene, 1992. **7**(1): p. 171-180.
177. Graham, F.L., et al., *Characteristics of a human cell line transformed by DNA from human adenovirus type 5.* Journal of general virology, 1977. **36**(1): p. 59-72.
178. Stadler, D., *Mechanism of the Elimination of Hepatitis B Viral (HBV) DNA through Interferons (IFN)*, in *Faculty of Medicine*. 2013, TECHNICAL UNIVERSITY OF MUNICH. p. 89.
179. Lucifora, J., et al., *Hepatitis B virus X protein is essential to initiate and maintain virus replication after infection.* Journal of hepatology, 2011. **55**(5): p. 996-1003.
180. Banning, C., et al., *A flow cytometry-based FRET assay to identify and analyse protein-protein interactions in living cells.* PloS one, 2010. **5**(2): p. e9344.
181. Nassal, M., *The arginine-rich domain of the hepatitis B virus core protein is required for pregenome encapsidation and productive viral positive-strand DNA synthesis but not for virus assembly.* Journal of virology, 1992. **66**(7): p. 4107-4116.
182. Kindsmüller, K., et al., *Intranuclear targeting and nuclear export of the adenovirus E1B-55K protein are regulated by SUMO1 conjugation.* Proceedings of the National Academy of Sciences, 2007. **104**(16): p. 6684-6689.
183. Vojtěšek, B., et al., *An immunochemical analysis of the human nuclear phosphoprotein p53: new monoclonal antibodies and epitope mapping using recombinant p53.* Journal of immunological methods, 1992. **151**(1-2): p. 237-244.

184. Li, H., et al., *Soluble amyloid precursor protein (APP) regulates transthyretin and Klotho gene expression without rescuing the essential function of APP.* Proceedings of the National Academy of Sciences, 2010. **107**(40): p. 17362-17367.
185. Marton, M.J., et al., *The adenovirus E4 17-kilodalton protein complexes with the cellular transcription factor E2F, altering its DNA-binding properties and stimulating E1A-independent accumulation of E2 mRNA.* Journal of virology, 1990. **64**(5): p. 2345-2359.
186. Harlow, E., B. Franza, and C. Schley, *Monoclonal antibodies specific for adenovirus early region 1A proteins: extensive heterogeneity in early region 1A products.* Journal of Virology, 1985. **55**(3): p. 533-546.
187. Reich, N.C., et al., *Monoclonal antibodies which recognize native and denatured forms of the adenovirus DNA-binding protein.* Virology, 1983. **128**(2): p. 480-484.
188. Siu, P.M., et al., *Proteasome inhibition alleviates prolonged moderate compression-induced muscle pathology.* BMC musculoskeletal disorders, 2011. **12**(1): p. 58.
189. Sarnow, P., C.A. Sullivan, and A.J. Levine, *A monoclonal antibody detecting the adenovirus type 5 E 1 b-58Kd tumor antigen: Characterization of the E 1 b-58Kd tumor antigen in adenovirus-infected and-transformed cells.* Virology, 1982. **120**(2): p. 510-517.
190. Bradford, M.M., *A rapid and sensitive method for the quantitation of microgram quantities of protein utilizing the principle of protein-dye binding.* Analytical biochemistry, 1976. **72**(1-2): p. 248-254.
191. Gronenborn, A.M., et al., *Deaminase-independent inhibition of HIV-1 reverse transcription by APOBEC3G.* Nucleic Acids Research, 2007. **35**(21): p. 7096-7108.
192. Lejeune, N., *L'expression de la désaminase de cytosine de l'ADN Apobec3B est induite par les adénovirus.* 2017.
193. Schneider-Poetsch, T., et al., *Inhibition of eukaryotic translation elongation by cycloheximide and lactimidomycin.* Nature chemical biology, 2010. **6**(3): p. 209.
194. Dyson, N., et al., *Homologous sequences in adenovirus E1A and human papillomavirus E7 proteins mediate interaction with the same set of cellular proteins.* Journal of virology, 1992. **66**(12): p. 6893-6902.
195. Menendez, D., et al., *The cytidine deaminase APOBEC3 family is subject to transcriptional regulation by p53.* Molecular Cancer Research, 2017.
196. Gabler, S., et al., *E1B 55-kilodalton-associated protein: a cellular protein with RNA-binding activity implicated in nucleocytoplasmic transport of adenovirus and cellular mRNAs.* Journal of virology, 1998. **72**(10): p. 7960-7971.
197. Blackford, A.N., et al., *A role for E1B-AP5 in ATR signaling pathways during adenovirus infection.* Journal of virology, 2008. **82**(15): p. 7640-7652.
198. Higashino, F., J.M. Pipas, and T. Shenk, *Adenovirus E4orf6 oncoprotein modulates the function of the p53-related protein, p73.* Proceedings of the National Academy of Sciences, 1998. **95**(26): p. 15683-15687.
199. Blackford, A.N., et al., *Adenovirus 12 E4orf6 inhibits ATR activation by promoting TOPBP1 degradation.* Proceedings of the National Academy of Sciences, 2010. **107**(27): p. 12251-12256.
200. Jost, C.A., M.C. Marin, and W.G. Kaelin Jr, *p73 is a human p53-related protein that can induce apoptosis.* Nature, 1997. **389**(6647): p. 191.
201. Hoopes, J.I., et al., *APOBEC3A and APOBEC3B preferentially deaminate the lagging strand template during DNA replication.* Cell reports, 2016. **14**(6): p. 1273-1282.
202. Stubbe, M., et al., *Viral DBP SUMOylation promotes PML-NB localization juxtaposed to viral replication centers* 2019. Manuscript submitted.
203. Suspene, R., et al., *Recovery of APOBEC3-edited human immunodeficiency virus G→ A hypermutants by differential DNA denaturation PCR.* Journal of General Virology, 2005. **86**(1): p. 125-129.
204. Derse, D., et al., *Resistance of human T cell leukemia virus type 1 to APOBEC3G restriction is mediated by elements in nucleocapsid.* Proceedings of the National Academy of Sciences, 2007. **104**(8): p. 2915-2920.

205. Zhigang, C., T.L. EGGERMAN, and A.P. PATTERSON, *Phosphorylation is a regulatory mechanism in apolipoprotein B mRNA editing.* Biochemical Journal, 2001. **357**(3): p. 661-672.
206. Powell, C., E. Cornblath, and D. Goldman, *Zinc-binding domain-dependent, deaminase-independent actions of apolipoprotein B mRNA-editing enzyme, catalytic polypeptide 2 (Apobec2), mediate its effect on zebrafish retina regeneration.* Journal of Biological Chemistry, 2014. **289**(42): p. 28924-28941.
207. Zhou, L., et al., *A functional variant in UBE 2L3 contributes to HBV infection and maintains ccc DNA stability by inducing degradation of APOBEC 3A protein.* Hepatology, 2019.
208. Sriramachandran, A.M. and R.J. Dohmen, *SUMO-targeted ubiquitin ligases.* Biochimica et Biophysica Acta (BBA)-Molecular Cell Research, 2014. **1843**(1): p. 75-85.
209. Ashur-Fabian, O., et al., *apoB and apobec1, two genes key to lipid metabolism, are transcriptionally regulated by p53.* Cell Cycle, 2010. **9**(18): p. 3785-3794.
210. Löhr, K., et al., *Mutual interference of adenovirus infection and myc expression.* Journal of virology, 2003. **77**(14): p. 7936-7944.
211. Periyasamy, M., et al., *p53 controls expression of the DNA deaminase APOBEC3B to limit its potential mutagenic activity in cancer cells.* Nucleic acids research, 2017. **45**(19): p. 11056-11069.
212. Endter, C. and T. Dobner, *Cell transformation by human adenoviruses*, in *Adenoviruses: Model and Vectors in Virus-Host Interactions*. 2004, Springer. p. 163-214.
213. Täuber, B. and T. Dobner, *Adenovirus early E4 genes in viral oncogenesis.* Oncogene, 2001. **20**(54): p. 7847.
214. McLorie, W., et al., *Individual adenovirus E1B proteins induce transformation independently but by additive pathways.* Journal of general virology, 1991. **72**(6): p. 1467-1471.
215. Yew, P.R. and A.J. Berk, *Inhibition of p53 transactivation required for transformation by adenovirus early 1B protein.* Nature, 1992. **357**(6373): p. 82.
216. Nevels, M., et al., *The adenovirus E4orf6 protein contributes to malignant transformation by antagonizing E1A-induced accumulation of the tumor suppressor protein p53.* Oncogene, 1999. **18**(1): p. 9.
217. Moore, M., N. Horikoshi, and T. Shenk, *Oncogenic potential of the adenovirus E4orf6 protein.* Proceedings of the National Academy of Sciences, 1996. **93**(21): p. 11295-11301.
218. Roberts, S.A., et al., *An APOBEC cytidine deaminase mutagenesis pattern is widespread in human cancers.* Nature genetics, 2013. **45**(9): p. 970.
219. Li, X., et al., *Detection of HBV covalently closed circular DNA.* Viruses, 2017. **9**(6): p. 139.
220. Yu, Q., et al., *Single-strand specificity of APOBEC3G accounts for minus-strand deamination of the HIV genome.* Nature structural & molecular biology, 2004. **11**(5): p. 435.
221. Taura, M., et al., *Apobec3A maintains HIV-1 latency through recruitment of epigenetic silencing machinery to the long terminal repeat.* Proceedings of the National Academy of Sciences, 2019. **116**(6): p. 2282-2289.
222. Schultz, D.C., et al., *SETDB1: a novel KAP-1-associated histone H3, lysine 9-specific methyltransferase that contributes to HP1-mediated silencing of euchromatic genes by KRAB zinc-finger proteins.* Genes & development, 2002. **16**(8): p. 919-932.
223. Abbink, P., et al., *Construction and evaluation of novel rhesus monkey adenovirus vaccine vectors.* Journal of virology, 2015. **89**(3): p. 1512-1522.
224. Abbink, P., et al., *Comparative seroprevalence and immunogenicity of six rare serotype recombinant adenovirus vaccine vectors from subgroups B and D.* Journal of virology, 2007. **81**(9): p. 4654-4663.

225. Vogels, R., et al., *Replication-deficient human adenovirus type 35 vectors for gene transfer and vaccination: efficient human cell infection and bypass of preexisting adenovirus immunity.* Journal of virology, 2003. **77**(15): p. 8263-8271.
226. Walters, R.W., et al., *Basolateral localization of fiber receptors limits adenovirus infection from the apical surface of airway epithelia.* Journal of Biological Chemistry, 1999. **274**(15): p. 10219-10226.
227. Murakami, S., et al., *Interaction of penton base Arg-Gly-Asp motifs with integrins is crucial for adenovirus serotype 35 vector transduction in human hematopoietic cells.* Gene therapy, 2007. **14**(21): p. 1525.
228. Arnberg, N., et al., *Adenovirus type 37 uses sialic acid as a cellular receptor.* Journal of virology, 2000. **74**(1): p. 42-48.
229. Huang, S., et al., *A single amino acid in the adenovirus type 37 fiber confers binding to human conjunctival cells.* Journal of virology, 1999. **73**(4): p. 2798-2802.
230. Mahajan, R., et al., *A small ubiquitin-related polypeptide involved in targeting RanGAP1 to nuclear pore complex protein RanBP2.* Cell, 1997. **88**(1): p. 97-107.
231. Günther, T., et al., *Influence of ND10 components on epigenetic determinants of early KSHV latency establishment.* PLoS pathogens, 2014. **10**(7): p. e1004274.
232. Richard, P., S. Feng, and J.L. Manley, *A SUMO-dependent interaction between Senataxin and the exosome, disrupted in the neurodegenerative disease AOA2, targets the exosome to sites of transcription-induced DNA damage.* Genes & development, 2013. **27**(20): p. 2227-2232.
233. Zhong, S., et al., *Role of SUMO-1–modified PML in nuclear body formation.* Blood, 2000. **95**(9): p. 2748-2752.
234. Westrich, J.A., et al., *Human papillomavirus 16 E7 stabilizes APOBEC3A protein by inhibiting Cullin 2-dependent protein degradation.* Journal of virology, 2018. **92**(7): p. e01318-17.
235. Bulliard, Y., et al., *Structure-function analyses point to a polynucleotide-accommodating groove essential for APOBEC3A restriction activities.* Journal of virology, 2011. **85**(4): p. 1765-1776.
236. Muckenfuss, H., et al., *APOBEC3 proteins inhibit human LINE-1 retrotransposition.* Journal of Biological Chemistry, 2006. **281**(31): p. 22161-22172.
237. Ljungman, P., *Treatment of adenovirus infections in the immunocompromised host.* European Journal of Clinical Microbiology and Infectious Diseases, 2004. **23**(8): p. 583-588.
238. Bonvin, M., et al., *Interferon-inducible expression of APOBEC3 editing enzymes in human hepatocytes and inhibition of hepatitis B virus replication.* Hepatology, 2006. **43**(6): p. 1364-1374.
239. Kalvakolanu, D., et al., *Inhibition of interferon-inducible gene expression by adenovirus E1A proteins: block in transcriptional complex formation.* Proceedings of the National Academy of Sciences, 1991. **88**(17): p. 7459-7463.
240. Romano, A., et al., *Use of human fibroblast-derived (beta) interferon in the treatment of epidemic adenovirus keratoconjunctivitis.* Journal of interferon research, 1980. **1**(1): p. 95-100.
241. Tatsis, N. and H.C. Ertl, *Adenoviruses as vaccine vectors.* Molecular Therapy, 2004. **10**(4): p. 616-629.
242. Kobinger, G.P., et al., *Chimpanzee adenovirus vaccine protects against Zaire Ebola virus.* Virology, 2006. **346**(2): p. 394-401.
243. Catanzaro, A.T., et al., *Phase 1 safety and immunogenicity evaluation of a multiclade HIV-1 candidate vaccine delivered by a replication-defective recombinant adenovirus vector.* The Journal of infectious diseases, 2006. **194**(12): p. 1638-1649.
244. Wang, Y., et al., *Mucosal immunization in macaques upregulates the innate APOBEC 3G anti-viral factor in CD4+ memory T cells.* Vaccine, 2009. **27**(6): p. 870-881.
245. St George, J., *Gene therapy progress and prospects: adenoviral vectors.* Gene therapy, 2003. **10**(14): p. 1135.

246. Nash, L.A. and R.J. Parks, *Book Chapter 1. Adenovirus Biology and Development as a Gene Delivery Vector.* Exosomes: A novel biomarker and approach to gene therapy for spinal muscular atrophy, 2019: p. 172.
247. Lang, F.F., et al., *Phase I trial of adenovirus-mediated p53 gene therapy for recurrent glioma: biological and clinical results.* Journal of Clinical Oncology, 2003. **21**(13): p. 2508-2518.
248. Goradel, N.H., et al., *Oncolytic adenovirus: A tool for cancer therapy in combination with other therapeutic approaches.* Journal of cellular physiology, 2019. **234**(6): p. 8636-8646.
249. Ganly, I., et al., *A phase I study of Onyx-015, an E1B attenuated adenovirus, administered intratumorally to patients with recurrent head and neck cancer.* Clinical Cancer Research, 2000. **6**(3): p. 798-806.